SENSOR BASED MODELING OF CHEMICAL MECHANICAL PLANARIZATION (CMP) OF COPPER FOR SEMICONDUCTOR APPLICATIONS

By

UPENDRA MILIND PHATAK

Bachelor of Engineering (Mechanical)

Modern Education Society's College of Engineering,

University of Pune, Pune, Maharashtra, INDIA

2005

Submitted to the Faculty of the

Graduate College of the

Oklahoma State University

in partial fulfillment of

the requirements for

the Degree of

MASTER OF SCIENCE

May, 2008

SENSOR BASED MODELING OF CHEMICAL MECHANICAL PLANARIZATION (CMP) OF COPPER FOR SEMICONDUCTOR APPLICATIONS

Thesis Approved:

Dr. Ranga Komanduri

Thesis Adviser

Dr. Satish Bukkapatnam

Thesis Co-Adviser

Dr. Hongbing Lu

Committee member

Dr. Gordon Emslie

Dean of the Graduate College

Acknowledgements

I take this opportunity to thank my revered advisor Dr.Ranga Komanduri, Regents Professor and A. H. Nelson, Jr. Endowed Chair in Engineering, School of Mechanical and Aerospace Engineering. I am grateful for his continuous help and support. He has been like the *Kalpavriksha*, all my wishes have been granted so far royally.

I express my sincere gratitude towards my other mentors Dr. Satish Bukkapatnam and Dr. James Kong for their unending help in statistics and signal analyses. They have given me a new perspective at analysis of a process.

I am indebted to my parents Mr. Milind Yashwant Phatak and Mrs. Mugdha Milind Phatak for their unsurpassable love and timely words of wisdom. They have been a beacon in torrid times.

I thank NSF for their grant DMI 0428356, CMMI 0700680 for conducting this experimental investigation. I also thank the Micron Foundation (Drs Naga Chandrasekaran, Sony Varghese, and Gundu Sabde) for their interest and support of this study.

I sincerely thank my seniors Mr. Milind Malshe and Mr. Rutuparna Narulkar for their help and intriguing discussions. I am thankful to my

friend and colleague from the Mechanical and Aerospace Engineering department, Mr. Vijay Krishnan Subramanian for his suggestions and discussions. I thank my colleagues Ritesh, Pablo and Alicia for giving me the much needed helping hand in the conduct of numerous experiments.

Table of Contents

Chapter **Page**

CHAPTER 1: INTRODUCTION....1

CHAPTER 2: LITERATURE REVIEW....7

2.1 Effect of slurry pH on Cu-CMP process....7
2.2 Effect of oxidizing agent content....16
2.3 Effect of complexing agent content....23
2.3 Effect of corrosion inhibiting agent content....34

CHAPTER 3: SENSORS IN CMP....41

CHAPTER 4: PROBLEM STATEMENT....48

CHAPTER 5: EXPERIMENTAL SETUP....50

5.1 Experimental Setup:....50
5.2 Design of Experiments....56

CHAPTER 6: MAIN EFFECTS OF VARIOUS SLURRY CHEMISTRY PARAMETERS ON AVERAGE MRR....60

CHAPTER 7: SENSOR SIGNAL ANALYSIS AND FEATURE EXTRACTION....64

CHAPTER 8: PROCESS MODELING USING RESPONSE SURFACE ANALYSIS....69

8.1 Model 1: Modeling Average Material Removal Rate (MRR) with Process Parameters....72
8.2 Model 2: Modeling average MRR with Key Sensor Features....74
8.3 Model 3: Modeling the Variation in Machine Settings using the Sensor Data....75
8.3.1 Modeling variations in slurry pH using key sensor features....76
8.3.2 Modeling variations in complexing agent content using key sensor features....77
8.3.3 Modeling the BTA content using key sensor features....79
8.3.4 Modeling slurry flow rate variations using key sensor features....81

CHAPTER 9: ELECTROCHEMICAL POLISHING OF COPPER....83

9.1 Effects of slurry chemistry on copper electrochemical polishing....95
9.2 Experimental Apparatus and Design of Experiments....100

CHAPTER 10: SURFACE PROFILES AND MRR TRENDS OF COPPER ECP....105

CHAPTER 11: SENSOR DATA, FEATURE EXTRACTION AND, PROCESS MODELING....110

Chapter **Page**

11.1 Vibration sensor data acquisition and processing ... 110
11.2 Process Modeling ... 112
Modeling MRR with machine settings for phosphoric acid slurry chemistry ... 112
Modeling Ra with machine settings for phosphoric acid slurry chemistry ... 113
Modeling MRR with machine settings for acetic acid slurry chemistry ... 114
Modeling Ra with machine settings for acetic acid slurry chemistry ... 114
Modeling the MRR and Ra with sensor features ... 115
Modeling MRR with sensor features for the phosphoric acid slurry chemistry ... 115
Modeling Ra with sensor features for phosphoric acid based slurry chemistry ... 117
Modeling MRR with sensor features for acetic acid slurry chemistry ... 119
Modeling Ra with sensor features for acetic acid slurry chemistry ... 120
Modeling the variations in slurry chemistry in Copper electrochemical polishing. ... 121
Modeling the variation in phosphoric acid content of the slurry ... 121
Modeling the variations in the water content of the slurry ... 122
Modeling the variations in Ethylene Glycol content of the slurry ... 122
Multi stage optimization of slurry chemistry for copper ECP ... 123

CHAPTER 12: CONCLUSIONS AND FUTURE WORK ... 128

CHAPTER 13: REFERENCE ... 133

List of Figures

Figure **Page**

Fig. 1-1: Schematic representation of CMP process [3]. 1

Fig. 2-1: *In-situ* open circuit potential measurements of copper in polishing slurry comprising 3 wt % alumina abrasives, 5 wt % hydrogen peroxide, 1 wt % glycine and DI water as vehicle media [47]. 10

Fig. 2-2 : Microhardness of copper disk before and after 10 min exposure to a slurry containing 5 wt % hydrogen peroxide, 1 wt % glycine in DI water at pH 2,7, and 12 [47].. 12

Fig. 2-3 : Effect of polishing slurry pH on the settling rates and zeta potential of alumina slurry [53].. 13

Fig. 2-4 : Material removal rate of copper as a function of oxidizer content and polishing slurry pH [46]. 15

Fig. 2-5 : Concentration of dissolved copper ions and copper oxide film thickness as a function of hydrogen peroxide concentration [56].. 17

Fig. 2-6 : Potentiodynamic plots of copper in polishing slurries with varying amounts of hydrogen peroxide [56]. 18

Figure **Page**

Fig. 2-7 : XPS spectra of Cu 2p3/2 and 2p1/2 after immersion in (a): 1 wt % alumina abrasive, (b): (a) + 0.0078M citric acid, (c): (a) + 0.5M citric acid [60]. 21

Fig. 2-8 : XPS spectra of Cu $2p_{3/2}$ and $2p_{1/2}$ for Cu after immersion for 60 min in different slurries, (a): 1 wt % alumina + 9 vol. % H_2O_2; (b): (a)+0.0078M Citric acid: (c): (a) + 0.5 M Citric acid [60]. 22

Fig. 2-9 : Static etch rate of copper as a function of citric acid concentration at pH 4 with varying oxidizing agent content [56]. 26

Fig. 2-10 : Static etch rate of copper in pH 6 slurry as a function of citric acid content and oxidizing agent content [56]. 27

Fig. 2-11 : Potentiodynamic polarization curves for copper in Hydrogen peroxide and citric acid slurries at (a) pH 4, and (b) pH 6 [56]...28

Fig. 2-12 : Schematic of the Mechanism of material removal at different polishing conditions of oxidizer content, slurry pH and complexing agent content [56]. 29

Fig. 2-13 : Effect of pH on polarization of copper in aqueous solutions at various pH [61]. 31

Figure **Page**

Fig. 2-14 : The Effect of addition of 0.01 M of glycine to aqueous polishing solutions on polarization behavior of copper [61]....32

Fig. 2-15 : Polarization behavior of copper in aqueous solution at pH 12 (b) No Glycine and (b) 0.01 M Glycine : under no abrasion, polishing with pad and polishing with pad and 5 wt % abrasives [61]....33

Fig. 2-16 : Effect of BTA concentration on the zeta potential and slurry stability measured by the slurry settling rate [53]....36

Fig. 2-17 : Adsorption isotherms of BTA on alumina abrasive particles [53]....37

Fig. 2-18 : FTIR spectroscopy for (a) pure BTA, and (b) BTA adsorped on alumina abrasive particles [53]....37

Fig. 3-1 : Variation of signal skewness for two slurry pH values [52]....42

Fig. 3-2 : AE rms signal for a normal (unscratched) CMP run on an industrial grade machine [65]....45

Fig. 3-3 : AE rms data on laboratory polishing machine before pad conditioning [65]....45

Fig. 3-4 : AE rms data on laboratory machine after pad conditioning with 250 µm diamond wheel [65]....46

Figure **Page**

Fig. 3-5 : AE rms data taken on an industrial CMP machine after artificially adding hard and bigger alumina abrasives to the polishing slurry [65]. 46

Fig. 5-1: Experimental setup used for conducting sensor based Cu-CMP investigation. 51

Fig. 5-2: Unpatterned copper wafer used in the sensor based Cu-CMP investigation. 51

Fig. 5-3: Wired vibration sensor (Kistler 8728A500) used for sensor based Cu-CMP investigation. 52

Fig. 5-4: Wireless vibration sensor unit used in sensor based Cu-CMP investigation. 54

Fig. 5-5: Sartorius manufactured precision digital weighing scale used to measure wafer weight after each polishing cycle. 54

Fig. 5-6: ADE Phase Shift Technologies, MicroXAM, Laser interferometric microscope used for surface quality measurement during Cu-CMP experiments. 55

Fig. 6-1: Sensitivity of avg. MRR to various slurry chemistry parameters. 61

Figure **Page**

Fig. 7-1: Time series representation of wired sensor data for treatment condition R11 (pH = 5, down pressure = 1 psi, slurry flow rate = 50 ml/min, complexing agent content = 20 gms/lit. BTA content = 0 gm). Red: Polish start, Green: Polish end 65

Fig. 7-2: Frequency domain representation of wired vibration sensor signal for treatment condition R 11................................65

Fig. 7-3: Time series data from wireless vibration sensor signal for R 11 (Red: Polish start, Green: Polish end)............................66

Fig. 7-4: Frequency domain representation of the wireless vibration sensor signal for treatment condition R 11. 66

Fig. 8-1 : Normal probability plot of residuals for regression model of MRR against machine settings only namely, slurry pH, complexing agent content of slurry, BTA content and slurry flow rate..73

Fig. 9-1: Schematic of Copper overburden electropolishing [75].............88

Fig. 9-2: Schematic illustrating the analogy behind achieving planarity during copper electrochemical polishing [76].............88

Fig. 9-3: Various regions of copper electropolishing; the constant current plateau is the region of interest where actual surface improvement is taking place [77]........................90

Figure **Page**

Fig. 9-4: Salt film Mechanism for formation of limiting current density plateau in copper electropolishing [79]. 93

Fig. 9-5: Acceptor mechanism supporting the existence of limiting current density plateau during electropolishing [79]. 93

Fig. 9-6: End-point detection during copper ECP [81]. 95

Fig. 9-7: Variation in conductivity of polishing slurries with variation in the content of phosphoric acid and its effect on the surface generated post polishing [22]. 97

Fig. 9-8: Effect of addition of acetic acid and alcohol on copper electro chemical polishing [83]. 99

Fig. 9-9: Experimental apparatus used to conduct copper electro chemical polishing experiments. 101

Fig. 10-1: Average MRR for Runs R1 to R8. For Runs with High water content (R3, R4, R7, R8) MRR is higher than that with the corresponding low water content treatment conditions. 106

Fig. 10-2: Surface profile plots for treatment conditions R3, Red: As received profile, Green: surface profile after 1 min electropolish, Black: surface profile after 2 min electropolish, Blue: surface profile after 3 min electropolish. 106

Figure **Page**

Fig. 10-3: Surface profile plot for treatment conditions R7, Red: As received profile, Green: surface profile after 1 min electropolish, Black: surface profile after 2 min electropolish, Blue: surface profile after 3 min electropolish. 107

Fig. 10-4: Optical micrograph of 3 min polished copper surface in slurry with no acetic acid and ethylene glycol as additives for machine settings; Phosphoric acid = 10M, Water = 10M, Copper sulfate = 0.2M). 108

Fig. 10-5: Optical micrograph of copper surface after 3 min polishing in acetic acid and ethylene glycol added slurries with machine settings; Acetic acid = 90 ml, ethylene glycol = 300 ml. 109

Fig. 11-1: Time series of wireless sensor data for treatment condition R1 (Phosphoric acid = 10 M, Water = 10 M, Copper sulfate = 0 M). 111

Fig. 11-2: Model performance of sensor based model for MRR for phosphoric acid based slurries. 117

Fig. 11-4: Model performance of sensor based model for surface roughness of copper in phosphoric acid based slurries. 119

Fig. 11-5: Comparison of MRR for phosphoric acid based slurries (tall columns) and acetic acid based slurries (short columns). 124

Figure **Page**

Fig. 11-6: Comparison of surface roughness achieved using phosphoric acid (tall columns) and acetic acid (short columns) based slurry chemistries...125

Fig. 11-7: Flow chart for two-stage process proposed for copper ECP..127

List of Tables

Table **Page**

Table 5-1: Specifications of wired Kistler accelerometer used in the experimental investigation. 53

Table 5-2 : Taguchi L-12 Matrix implemented to study the slurry chemistry effects on MRR in Cu-CMP 57

Table 5-3 : High (H) and low (L) levels of machine settings given as per Experimental matrix defined in Table 5-1. 58

Table 7-1 : Candidate feature matrix for wired sensor signal for treatment condition R 11 67

Table 7-2 : Candidate feature matrix for wireless sensor signal for treatment condition R 1 67

Table 8-1 : Regression model of MRR with machine settings with two way interactions (R^2 = 94.2%, $R^2_{adjusted.}$ = 92.2%m $R^2_{predicted}$ = 88.47%) 72

Table 8-2 : Regression model of average MRR with key sensor features and two way interactions (R^2 = 97.7%, $R^2_{adjusted}$ = 92.66%, $R^2_{predicted}$ = 65.84%)....................74

Table **Page**

Table 8-3 : Regression model of pH of Polishing slurry with key sensor features and two way interactions (R^2 = 99.8%, $R^2_{adjusted}$. = 99.12%, $R^2_{predicted}$ = 72.81%) 76

Table 8-4 : Regression model of complexing agent in polishing slurry with key sensor features and two way interactions in between them (R^2 = 99.96%, $R^2_{adjusted}$ = 99.78%, $R^2_{predicted}$ = 92.73%) 78

Table 8-5 : Regression model of BTA against key sensor features and two way interactions in between them (R^2 = 90.21%, $R^2_{adjusted}$ = 81.97%, $R^2_{predicted}$ = 58.14%) 80

Table 8-6 : Regression model of variation in slurry flow rate with key sensor features and two way interactions between them (R^2 = 86.31%, $R^2_{adjusted}$ = 78.22%, $R2_{predicted}$ = 64.65%)...81

Table 9-1: Experimental matrix implemented in copper electropolishing experiments..102

Table 9-2: High and low levels of various factors investigated in Copper electrochemical polishing using phosphoric acid slurry chemistry. 103

Table 9-3: Experimental matrix implemented to study the effect of ethylene glycol and acetic acid content in polishing slurry on copper electrochemical polishing.............................104

Table	**Page**

Table 9-4: High and low levels of factors investigated in Copper electrochemical polishing using acetic acid slurry chemistry. 104

Table 11-1: Candidate feature matrix for R1 111

Table 11-2: Regression model of MRR with machine settings (R^2 = 69.3%, $R^2_{adj.}$ = 66.37%, $R^2_{predicted}$ = 59.9%) 112

Table 11-3: Regression model of average surface roughness with machine settings (R^2 = 29.23%, $R^2_{adj.}$ = 18.61%, $R^2_{predicted}$ = 0%) 113

Table 11-4: Regression model for avg. MRR with machine settings for acetic acid slurry chemistry (R^2 = 11.52%, $R^2_{adj.}$ = 0%, $R^2_{predicted}$ = 0%) 114

Table 11-5: Regression model for Ra with machine settings for the acetic acid slurry chemistry (R^2 = 4.06%, $R^2_{adj.}$ = 0%, $R^2_{predicted}$ = 0%) 115

Table 11-6: Regression model of MRR for phosphoric acid slurry chemistry with sensor data only (R^2 = 93.92%, $R^2_{adj.}$ = 84.45%). 116

Table 11-7: Regression model of average surface roughness with sensor data for phosphoric acid slurry chemistry (R^2 = 99.65%, $R^2_{adj.}$ = 98.40%) 118

Table **Page**

Table 11-8: Regression model for avg. MRR with sensor features for acetic acid slurry chemistry (R^2 = 98.64%, $R^2_{adj.}$ = 96.27%, $R^2_{predicted}$ = 73.59%) 120

Table 11-9: Regression model for Ra with sensor features for acetic acid slurry chemistry (R^2 = 96.45%, $R^2_{adj.}$ = 91.12%, $R^2_{predicted}$ = 62.39%) 120

Table 11-10: Regression model of variations in phosphoric acid content of slurry with sensor data.(R^2 = 96.17%, $R^2_{adj.}$ = 90.20%) 121

Table 11-11: Regression model of variations in the water content of the slurry with sensor data only. (R^2 = 85.38%, $R^2_{adj.}$ = 75.99%) 122

Table 11-12: Regression model for modeling variations in the Ethylene Glycol content of the slurry (R^2 = 95.08%, $R^2_{adj.}$ = 87.69%, $R^2_{predicted}$ = 69.91%) 123

Chapter 1: Introduction

Copper Chemical Mechanical Planarization (Cu-CMP) has evolved as a process of choice to achieve local as well as global planarity in VLSI and ULSI applications [1, 2]. The inherent nature of CMP process is that of fine abrasive polishing. The schematic of the CMP process is as shown in Fig. 1-1.

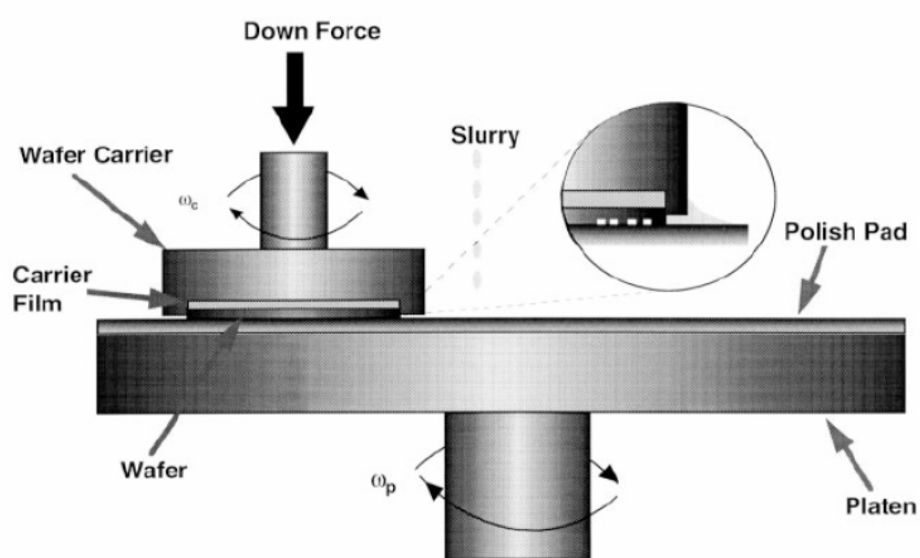

Fig. 1-1: Schematic representation of CMP process [3].

The wafer is pressed facedown on a rotating polishing pad. The slurry is dispensed over the rotating polishing pad and is circulated over

pad surface due to centrifugal force of the rotating platen. The simplistic nature of material removal is that of chemical modification of the surface and subsequent removal of material by abrasion. Judicious efforts have been put in getting a good insight on the mechanical aspects of the process [4-15]. Efforts have also been made to use various modeling techniques to achieve efficient process control [16-22].

The Tribological and thermal attributes of the process also play a critical role in determining the efficiency of the process. Rise of temperatures beyond a certain limiting value results in weakening of the novel low–k dielectric materials [23]. Overall process temperature also decides the rate of various chemical reactions which take place at the wafer-pad interface [24]. Hence, efforts also have been made to investigate the temperature rise associated with Cu-CMP process [14, 25, 26]. The main hindrance in estimating various tribological parameters at the wafer-pad interface is the complex nature of contact between the abrasives pad and the wafer [10, 26-29].

Polishing slurry chemistry also plays a crucial role in efficient operation of the entire process. It is critical in a way because copper being soft, can be scratched easily. These scratches can be sites for defect generations, which in turn could lead to electromigration defects in interconnects [30]. Numerous polishing slurry compositions are found in patent literature [29-42]. Fine tuning of various slurry parameters is

required by industry so as to maximize the throughput of the polishing process. Many of these slurry compositions are considered proprietary and tend to be one of the key actors in improving the throughput of the process. This directly reflects on the plethora of patents filed for application specific polishing slurry compositions [31-44].

The slurry contains numerous components, namely, de-ionized water, oxidizing agent, buffering agent, complexing agent, abrasives, acids, and corrosion inhibiting agent. The effect of various constituents and slurry characteristics will be discussed in detail in the literature review and the following slurry constituents will be briefly considered.

De-ionized water (DI water)

The primary purpose of using DI water is to facilitate easy flow of polishing compounds such as abrasives between the wafer-pad interface. It also functions as a diluting medium for concentrated acids which are used in the polishing slurry. Care needs to be taken to prevent organic as well as inorganic impurities reaching the wafer-pad interface. Chances of foreign particles getting into an otherwise “clean” wafer fabrication process are more through the slurry compounds, more so via DI water owing to the fact that it is used heavily not only in CMP but in the entire fabrication process.

Oxidizing agent

Various types of oxidizing agents, such as hydrogen peroxide, ferric nitrite, potassium iodate. Most commonly hydrogen peroxide is used as an oxidizing agent in conventional Cu-CMP slurries. The primary aim of an oxidizing agent is to facilitate formation of a native surface oxide film. This film prevents the removal of low areas of the surface while the high areas of the profile are removed by mechanical abrasion. This exposes the virgin surface for further oxidation and these cycles of abrasion and subsequent oxidation continue till the desired planarity is achieved [45].

Buffering agent

Various types of buffering agents, such as potassium hydroxide, sodium hydroxide are utilized small quantities in conventional Cu-CMP slurries. The function of these agents is to adjust the pH of polishing slurry and also aid in maintaining it at a certain standard during the polishing process. Other types of buffering agents such as, potassium acetate aid in foaming up the slurry there by reducing the chances of hard indentation on copper due to abrasion [34].

Complexing agent

Various types of complexing agents such as, citric acid, glycine, and ammonium hydroxide are used in conventional Cu-CMP slurries. In order to enhance the material removal capabilities of the slurry, and to prevent redeposition of abraded species on the wafer, a complexing agent

is added to the slurry. It forms complexes with the various abraded copper species [46]. Citric acid or glycine is a preferred complexing agent used normally in dissolution based industrial Cu-CMP slurries.

Abrasives

Nanometric size abrasives are incorporated in almost all CMP slurries. Addition of abrasives facilitates mechanical abrasion of high areas on the profile, thereby facilitating exposure of underlying virgin copper surface for further oxidation. The preferred abrasive used is alumina over silicon oxide, as alumina abrasive tend to be softer and tends to leave fewer deep indentations under overall CMP conditions.

Acids

Acidic pH slurries are preferred in Cu-CMP as it will be elucidated later [46, 47]. Various acids such as nitric acid, and acetic acid are used in conventional Cu-CMP slurries to achieve this required acidic pH value. Inclusion of these acids in the polishing slurry also facilitates easy dissolution of copper during polishing [1, 48]

Corrosion inhibiting agent

With the use of dissolution type slurries, it becomes imperative to protect the wafer surface from static etching [2]. These agents form non-native films over the copper surface preventing the low areas of the profile from active dissolution [1]. Benzotriazole (BTA) is the most common corrosion inhibiting agent used the conventional Cu-CMP

slurries. Improper selection of the quantity of BTA in the slurry can cause severe damage to the wafer being polished.

Each of the above listed slurry components along with the pH of the slurry has interplay with each other. These interactions determine the yield of the planarization process [2]. So, it becomes important not only to study the effect of each of the process parameter individually on the process output but also to study the interaction effects of each of the process parameters with the other. Then and only then a near complete estimation of effect of the slurry chemistry on the material removal rate can be obtained.

The drifts in the initial preset values of the above listed process parameters as polishing progresses are also a concern, as they affect the MRR as well as the surface characteristics produced after polishing. Hence process monitoring emerges as one of the key areas of interest to both industry and academia. Numerous approaches have been made for process monitoring [49-51] and modeling [52] using a variety of sensors including acoustic emission as well as vibration sensors.

Chapter 2: Literature Review

2.1 Effect of slurry pH on Cu-CMP process

Among the slurry related parameters, pH of the slurry has a direct effect on dissolution behavior of the metal to be polished. Nitric acid is used to achieve acidic pH in the polishing slurries while ammonium hydroxide is used to achieve alkaline pH in the polishing slurries. The pH of the polishing slurry drastically affects the chemical stability of the abrasive particles in the slurry [53]. Most abrasive particles dispersed in water have a hydroxide surface layer. This surface layer is amphoteric in nature and can react either as an acid or as a base. It can be charged either positively or negatively via the following mechanism [54].

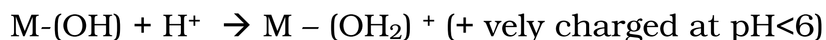

$$M\text{-}(OH) + H^{+} \rightarrow M - (OH_2)^{+} \text{ (+ vely charged at pH<6)}$$

$$M\text{-}(OH) + OH^{-} \rightarrow M\text{-} (O)^{-} + H_2O \text{ (- vely charged at pH>6)}$$

Alumina abrasive, which is preferred for copper-CMP, has distinct zeta potentials at different pH values. The Zeta potential refers to the electrostatic potential generated by the accumulation of ions at the surface of a colloidal particle. The particle is organized into an electrical double-layer, consisting of a stern layer and a diffuse layer. It has a

significant bearing on the stability of colloids, such as the CMP slurries. This potential for an alumina abrasive is near zero at a pH of ~ 6, positive for pH < 6, and negative at pH > 6. Consequently, slurry with alumina abrasive is very unstable at a pH of ~ 6 due to lack of electrostatic repulsion. Consequently the abrasives will quickly agglomerate. In contrast, the slurry is very stable at very low or very high pH values [53]. The role of pH and its effect on the mechanisms of material removal on Cu-CMP is discussed in Ref no. 47. Polishing with slurries containing hydrogen peroxide and glycine at varying pH values shows that a soft oxide/hydroxide layer is formed on bare copper surface. The rates of dissolution and abrasion of the above mentioned layers reduces with increase in pH [47].

Slurry pH value is crucial when considering selectivity issues. For example, the dissolution of silicon oxide is enhanced at alkaline pH. Hence, along with copper polishing, the slurry readily removes silicon oxide. Earlier studies [1, 48] have shown that removal rate of silicon oxide increases with increase in pH. This implies that in order to achieve a highly selective CMP of metal and oxide, dissolution type slurry with a low pH and an added corrosion inhibitor is preferred.

The use of low pH slurries, commonly realized using nitric acid, gives an appreciably high static etch rate. Nitric acid readily etches copper. The low pH and oxidizing nature of HNO_3 results in Cu^{2+} to be

the thermodynamically stable form of copper. This automatically provides a driving force for copper to readily dissolve in the solution. In order to have good planarity, a high ratio of polish to etch rate is desired. This ensures that the high areas or the peaks on the copper surface are polished away while the low areas or the valleys are protected from static etching [45]. Nitric acid does provide a wide range of ratios for selection, yet the overall higher etch rate causes material to be removed from the low areas on the surface. For acidic pH values ($pH < 6$), the rate is more dominated by chemical dissolution while for alkaline values ($pH > 9$) it is more mechanical in nature [1, 47, 48]. Although pH of polishing slurry is a key factor in Cu-CMP process, interactions with other slurry parameters, such as the oxidizing agent *(e.g. hydrogen peroxide)* and complexing agent *(e.g. citric acid, glycine)* are important determinants of MRR. Thus, it is seen that slurry pH has an impact on multiple process parameters and not just the MRR.

The effect of pH on the material removal mechanism of copper during CMP is elucidated by Jindal *et al.* [47]. Effect of the pH of polishing slurry is studied using open circuit potential studies during polishing and then subsequent measurement of surface microhardness. From the open circuit potential diagrams a useful insight can be gathered on the mechanisms of material removal at various pH values.

Fig. 2.1 shows the open circuit potential diagram for a period of 9 minutes.

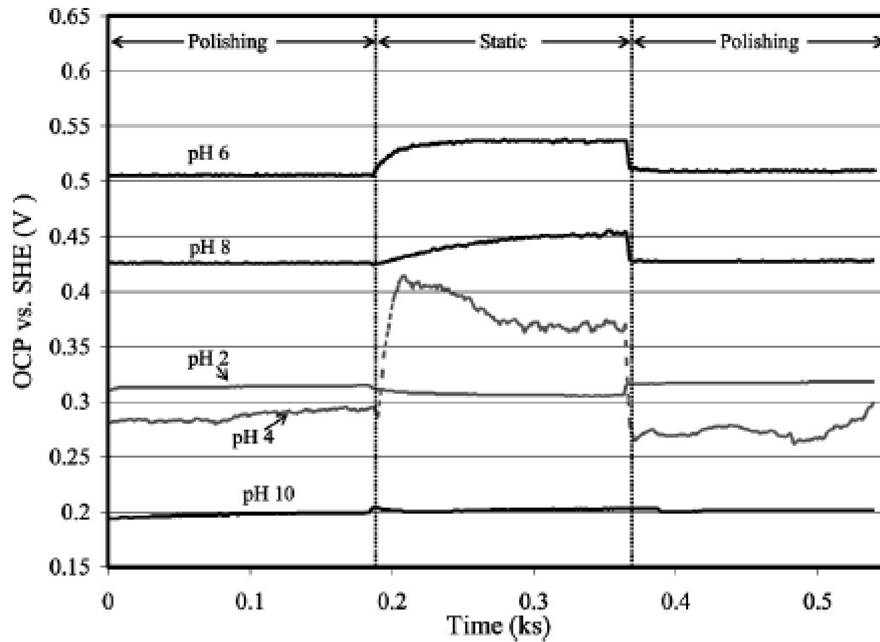

Fig. 2-1: *In-situ* open circuit potential measurements of copper in polishing slurry comprising 3 wt % alumina abrasives, 5 wt % hydrogen peroxide, 1 wt % glycine and DI water as vehicle media [47].

For the first 3 minutes the disk is polished, for the next 3 minutes it is stationary, and then polished again for the remaining 3 minutes. The slurry used during these experiments comprised of 3 wt % alumina abrasives, 5 wt % hydrogen peroxide, 1 wt % glycine and DI water remaining as vehicle media.

During polishing with slurry of pH 2, no change was observed in the open circuit potential. It drops somewhat during the static period and reverts back to the original value as soon as polishing is restarted

again. Since there is no significant jump in the potential during the static period, no passivation layer formation was found. Hence, the removal at this pH is a combination of mechanical abrasion and direct dissolution. Also from the potential value it can be seen that the potential is least anodic at pH value of 2. Hence, the tendency to dissolve actively is much more than that at any other pH value.

The mechanisms of material removal of copper at pH 4, 6, and 8 are found to be similar. The jump in potential during the static period symbolizes the growth of the passivation layer. But as soon as polishing is restarted the potentials drop back again. From the potential it can be seen that the passivity of the layers formed reduces in the order of pH 6, 8 and 4.

Microhardness testing was conducted on the copper disks before and after exposure for 10 minutes. The results indicate a drastic drop in the hardness value when the disk exposed to a solution of pH 2. This also supports the fact that passive film formation is not observed during polishing with slurry at pH 2. Fig. 2-2 shows the microhardness plots for copper disk before and after exposure to polishing slurries of varying pH. Comparing the drop in hardness at pH 2, the drop in hardness at pH of 7 and 12 is smaller.

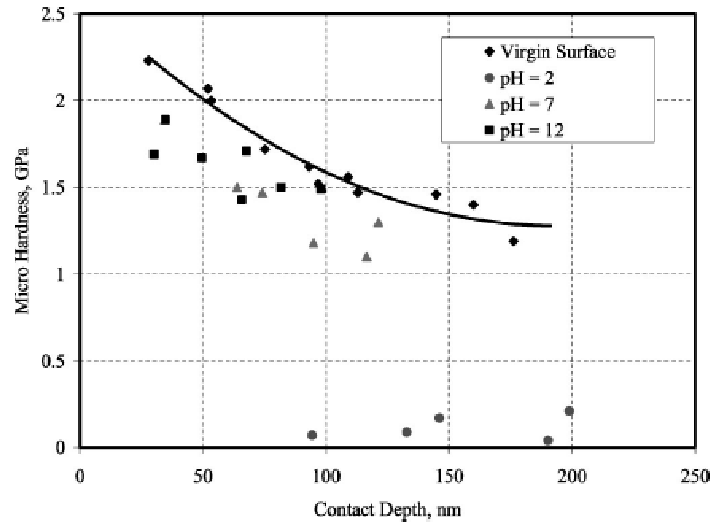

Fig. 2-2 : Microhardness of copper disk before and after 10 min exposure to a slurry containing 5 wt % hydrogen peroxide, 1 wt % glycine in DI water at pH 2,7, and 12 [47].

As discussed in the opening part of this section, polishing slurry pH has a significant affect on the zeta potential of the abrasive particles in the slurry. Hence, slurry pH would play a crucial role in slurry stability. The tendency of agglomeration is heavily dependant on the polishing slurry pH.

Luo *et al.* [53] elucidated the effect of pH on the slurry stability from the standpoint of abrasive agglomerate formation. A 50 ml vertical cylinder with stopper is used to determine the settling rates of alumina particles under various conditions. The zeta potentials of the abrasives in different slurries are measured. The particles were naturally dried and kept in desiccators for Fourier Transformed infrared Spectroscopy (FTIR) measurements.

The slurry is stable at both very high and very low pH, as the abrasives are positively charged at low pH and negatively charged at high pH. Electrostatic repulsion facilitates the slurry to be stable.

From Fig. 2-3, it can be seen that the settling rates of slurries at the extreme ends of the pH band are very low, while the slurry is extremely unstable or the settling rates at point of zero charge are very high. The zeta potential data also correlates well with the above observation.

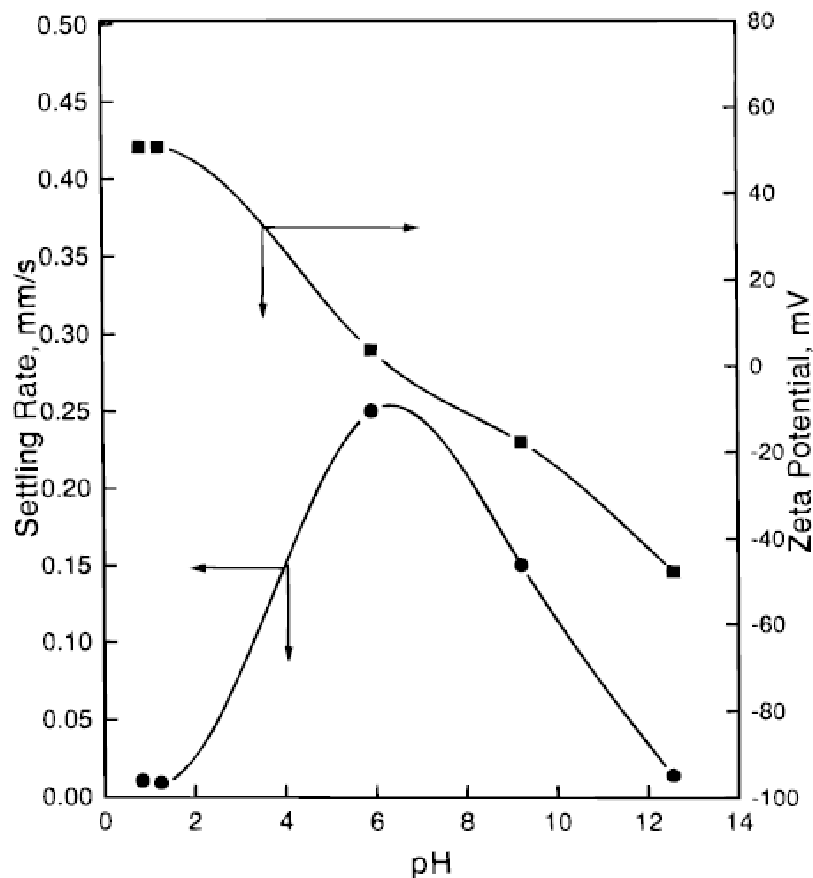

Fig. 2-3 : Effect of polishing slurry pH on the settling rates and zeta potential of alumina slurry [53].

Near the point of zero charge the zeta potential is almost zero, or rather it crosses from being positive at low pH to being negative at higher pH. This means that the electrostatic repulsion between individual abrasive particles is almost absent at a pH of ~6. Hence, the tendency of the abrasives to settle down and form agglomerates is very high in the pH value of ~6.

Hernandez *et al.* [46] elucidated the complex interactions between oxidizing agent content and the polishing slurry pH during the Cu-CMP process. Blanket copper wafer samples were polished with acidic alumina slurry containing an organic acid salt (phthalic acid salt) and an oxidizing agent (H_2O_2). They used X-ray photoelectron spectroscopy (XPS) to ascertain the nature of various oxide films formed on bare copper surface at varying slurry combinations.

Fig. 2-4 shows the combined effect of pH and oxidizer content on MRR in copper CMP. Variation of slurry pH has an effect on the solubility of various oxide films formed on bare Cu surface. At a lower pH value, the cupric slurries dissolve more easily. Again in this scenario, cupric oxide (CuO) is less soluble than cupric hydroxide ($Cu(OH)_2$). The removal rate at low oxidizing agent concentrations as a function of slurry pH is thus rate limited by the formation of these cupric oxide species, which in turn form cupric complexes. On the other hand, at high oxidizing agent

concentrations, the removal rate is determined by the solubility of the CuO film which is formed on the bare copper surface during CMP.

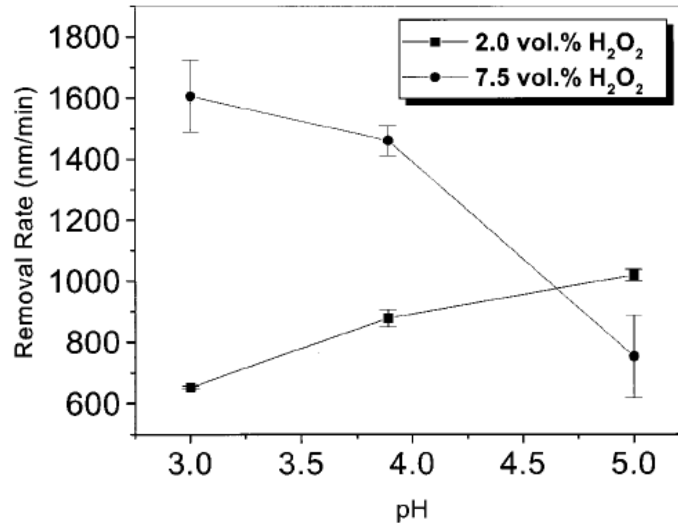

Fig. 2-4 : Material removal rate of copper as a function of oxidizer content and polishing slurry pH [46].

From Fig. 2-4 it can be seen that at higher oxidizer contents and high pH the MRR is low due to the fact that copper shows the tendency to passivate at higher pH. While at lower oxidizer contents, and higher pH, the MRR increases slightly. The reason attributed for this behavior is the increase in complexing ability of the phthalic salt with increasing pH [55]. This facet will be discussed in more detail when the effect of complexing agent content in the slurry is considered.

2.2 Effect of oxidizing agent content

The pH of polishing slurry combined with the oxidizing agent content of the slurry determines the nature of the film formed on the virgin copper surface [1, 46, 47]. Copper resists corrosion in near neutral or alkaline pH values, but, it is prone to chemical attack in strongly acidic slurries [47]. Formation of an oxide film over bare copper surface thus becomes a key factor in determining the throughput of the process [46]. Slurry pH along with the oxidizing agent content determines the nature of the film that is formed on the virgin copper surface. Higher content of the oxidizing agent in the slurry tends to passivate virgin copper surface by the formation of an oxide layer [46]. Under the conditions stated above, either cupric oxide (CuO) or hydroxide ($Cu(OH)_2$) films are formed on the bare copper surface. The dissolution of these films decreases with increase in pH. Cupric oxide (CuO) is less soluble than $Cu(OH)_2$ near a pH value of 4. Hence, the presence of CuO on the surface becomes a limiting factor in the removal rate of copper [46].

In a summary, polishing slurry pH and the oxidizing agent content of the slurry have a strong interaction with each other, which indeed is one of the very key factors determining the process yield.

Study of etching as well as removal behavior of copper as a function of slurry pH and oxidizer content in conventional citric acid

based polishing slurries is presented by Eom *et al.* [56]. Fig. 2-5 depicts the relation between concentration of dissolved copper ions in the slurry with copper oxide film thickness as a function of hydrogen peroxide concentration.

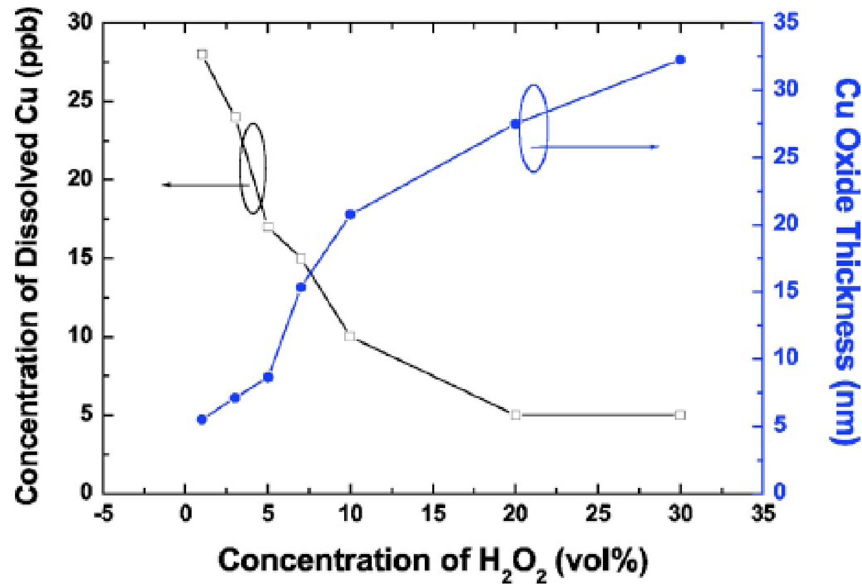

Fig. 2-5 : Concentration of dissolved copper ions and copper oxide film thickness as a function of hydrogen peroxide concentration [56].

Concentration of dissolved copper ions in the slurry decreases with increasing hydrogen peroxide content, while the thickness of the oxide film formed increases with increasing hydrogen peroxide content. This indicates that with increasing hydrogen peroxide content the copper surface passivates thereby preventing dissolution of bare copper. This inhibits active dissolution based removal of bare copper from the substrate.

Potentiodynamic curves for copper are plotted as a function of hydrogen peroxide content in the polishing slurry. Fig. 2-6 shows that with increasing hydrogen peroxide content at pH of 4 and 6, respectively the corrosion potential shifts towards more positive values, thereby suppressing the anodic dissolution of copper into the solution. This shows that with addition of more oxidizing agent to the slurry, the tendency to passivate the bare copper layer increases. This will inhibit active dissolution of copper into the slurry.

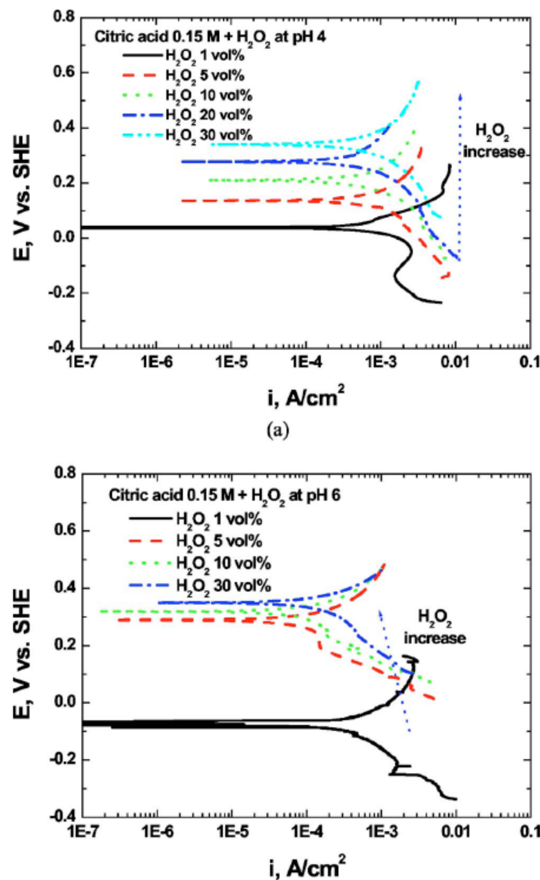

Fig. 2-6 : Potentiodynamic plots of copper in polishing slurries with varying amounts of hydrogen peroxide [56].

Lu *et al.* [57] have presented a detailed electrochemical study of certain chemical aspects of Cu-CMP in glycine–peroxide containing polishing slurry. *In-situ* potentiodynamic and open circuit potential measurements were used to ascertain the relative roles of Hydrogen Peroxide and Glycine in copper-CMP. At pH 4, the most common glycine species found is zwitterion, and this species is known to strongly chemisorb on bare Cu [58]. Recent study has also provided evidence that there is preferential formation of Cu-glycine complexes at surface sites of CuO [59]. Hence, it is likely that adsorption of glycine performs two tasks, namely, one of formation of *OH radical which would enhance the oxidation of bare Cu surface and the other of removing this oxide by formation of Cu-glycine complexes.

A three-step chemical cycle has also been proposed. First, *OH radical is catalytically produced from hydrogen peroxide by soluble Cu-Glycine complexes in the solution. Second, *OH thus produced enhances the oxidation of the copper surface. The predominant oxide specie on the surface is CuO. Third, this oxide layer becomes unstable due to its interaction with solvated glycine through formation of soluble Cu-glycine complexes. Regeneration of these complexes brings us back to step one.

A combined study of effect of alumina abrasive, citric acid, and hydrogen peroxide is presented by Chen *et al.* [60]. Surface analysis is performed using X-ray photoelectron spectroscopy and atomic force

microscopy (AFM). Several slurry combinations containing two concentrations of citric acid are tested.

Only metallic copper was observed when the specimens were immersed in slurry containing 1 wt % alumina abrasive in DI water. This shows that oxidation of copper was almost negligible in this slurry. When samples were immersed in slurries without any hydrogen peroxide, but only 0.0078M and 0.5M citric acid + 1 wt % alumina abrasives, the surface showed formation of CuO and $Cu(OH)_2$ along with the presence of metallic copper. Fig. 2-7 shows the XPS spectra of copper immersed in the above slurries. Addition of 9 vol % hydrogen peroxide changes the scenario drastically. When added to the slurry containing lower citric acid, it promotes formation of CuO, $Cu(OH)_2$. The peak associated with metallic Cu disappeared. This enables us to ascertain that oxide film formed was rather thick.

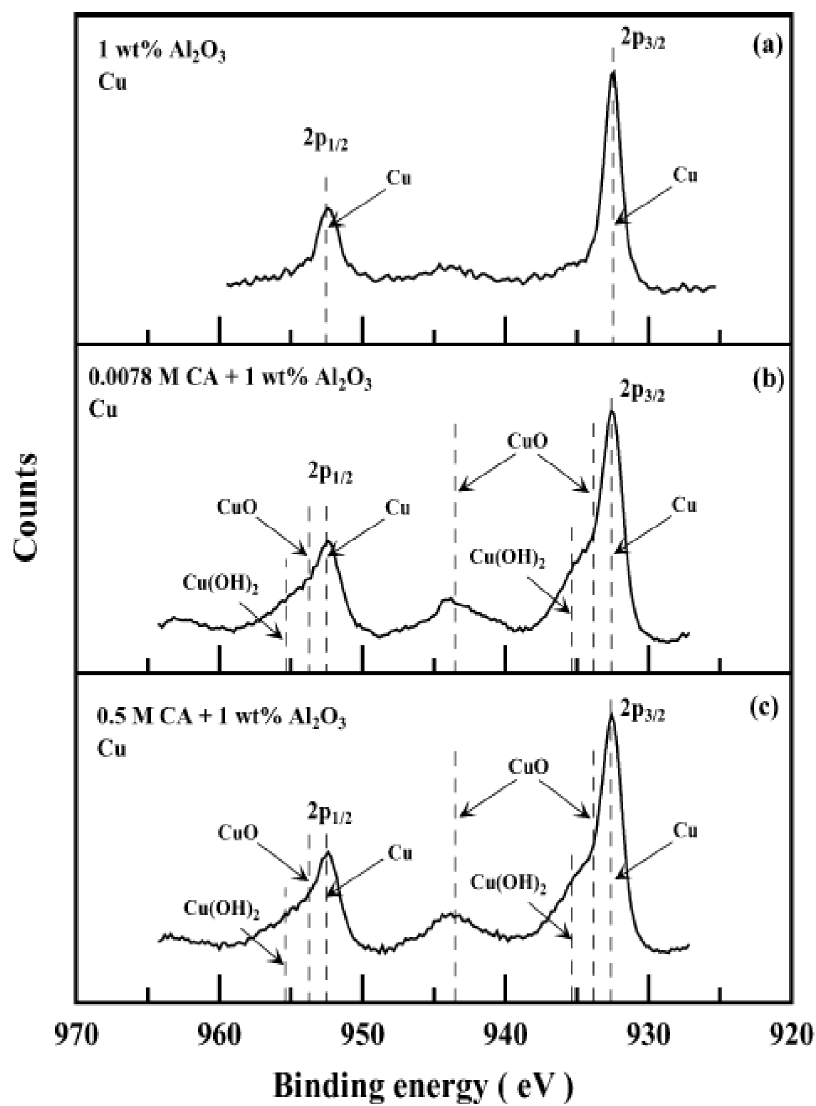

Fig. 2-7 : XPS spectra of Cu 2p3/2 and 2p1/2 after immersion in (a): 1 wt % alumina abrasive, (b): (a) + 0.0078M citric acid, (c): (a) + 0.5M citric acid [60].

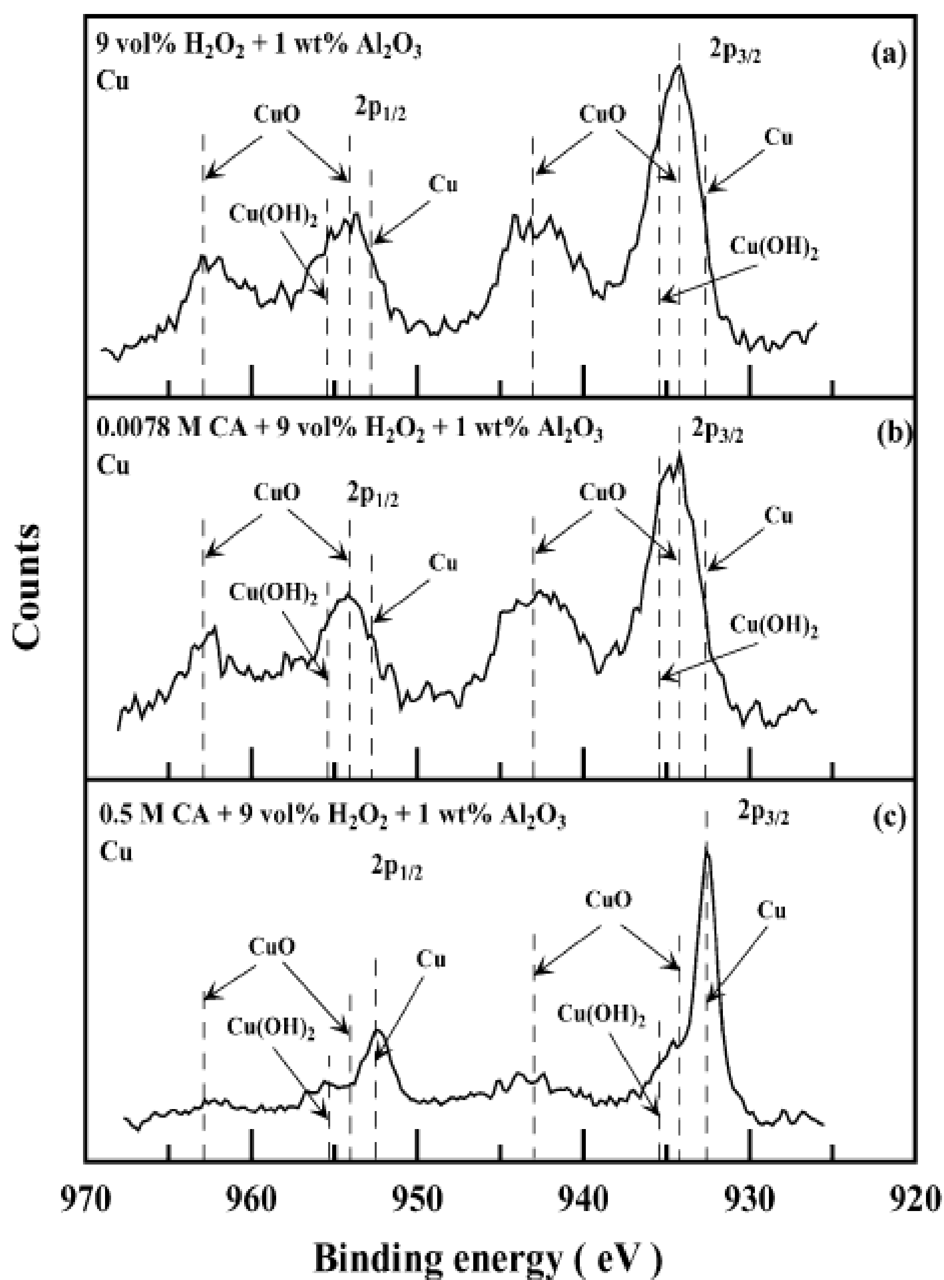

Fig. 2-8 : XPS spectra of Cu $2p_{3/2}$ and $2p_{1/2}$ for Cu after immersion for 60 min in different slurries, (a): 1 wt % alumina + 9 vol. % H_2O_2; (b): (a)+0.0078M Citric acid: (c): (a) + 0.5 M Citric acid [60].

On the other hand, adding hydrogen peroxide to the slurry containing higher citric acid reduces the intensity of the peak associated with CuO. As can be seen from Fig. 2-8, the peak associated with metallic copper reappears with a higher intensity. This indicates that citric acid retards oxide film formation, while addition of an oxidizing agent enhances the dissolution of copper into the slurry.

The presence of citric acid and hydrogen peroxide promotes the total copper removal rate in copper CMP. Addition of hydrogen peroxide in substantial amounts helps in the formation of passivation layer over bare copper at low citric acid concentrations. The addition of citric acid to the polishing slurry increases copper dissolution by complexing the copper ions dissolved in the slurry. The complexing action of citric acid increases with increase in the concentration of citric acid.

2.3 Effect of complexing agent content

Removal of oxides from the pad-wafer interface and thus preventing redeposition is key in ensuring a defect-free polishing process. To facilitate easy removal, complexing agents (citric acid or glycine) are added to the polishing slurry. The activity of these species is also a function of the value of the polishing slurry pH [55]. Eom *et al.* [56] studied the combined effect of hydrogen peroxide as an oxidizing agent with citric acid as a complexing agent during Cu-CMP [56]. Results

indicate that static etch rate decreases significantly with increase in pH at high oxidizing agent contents. This again corroborates with the fact that at high pH and high oxidizing agent content, the oxide film is passivating preventing direct dissolution of copper into the slurry. Addition of glycine changes the polishing conditions. Glycine and Cu^{2+} form Cu – glycine complex. This catalyzes the process of production of hydroxyl (*OH) radicals, which are more stronger oxidizers than peroxides [2].

The complexing action of the slurry is also a function of the slurry pH. Kummert *et al.* [55] have shown that in the pH range of 3–5, the dissociation of phthalic salt increases with pH. Hence, at high pH, the greater concentration of phthalic anions would allow enhanced complexation of Cu^{2+} ions. In high pH polishing slurries addition of an extra complexing agent is not required as complexing is achieved due to the action of the dissolved ammonia gas [2]. Complexing by ammonia gas occurs due to shielding of Cu ions by the ammonia ions in solution. Ammonia molecules thus effectively shield the charge of one copper ion from the other thereby reducing the activity of copper ions in solution and allowing more ions to be accommodated. This gives enhanced solubility of copper in the presence of ammonia gas [2].

Aksu *et al.* [61] studied the role of glycine as a complexing agent for copper polishing slurries using potentiodynamic techniques. The

effect on the behavior of copper at various pH values with and without glycine is carried out using a rotating disk electrode (RDE) configuration. Copper has a tendency to passivate in aqueous solutions at high pH, while at low pH, it dissolves actively [1, 47, 48, 62]. Addition of glycine to the above aqueous solutions changes the picture drastically. The passivation observed at a pH of 9 is no more observed and copper shows active behavior till a pH of 9 [61]. This is attributed to the fact that both zwitterionic and anionic forms of glycine exist at this pH, which indicates enhanced complexing action of dissolved copper ions in the slurry. The removal rate at low oxidizing agent contents at low pH is thus limited by the ability to form cupric complexes, since at low pH the cupric species can dissolve easily, while at high oxidizer contents, the removal rate is a function of the thickness of the cupric oxide (CuO) film formed on the surface.

The combined effect of oxidizing agent content and complexing agent content are investigated by Eom *et al.* [56]. They used potentiodynamic polarization curves to study the effect of variation in oxidizing agent content in citric acid based slurries at different pH values. Static etch rates were used as a measure to study the behavior of copper in slurries with variable oxidizing agent content slurries.

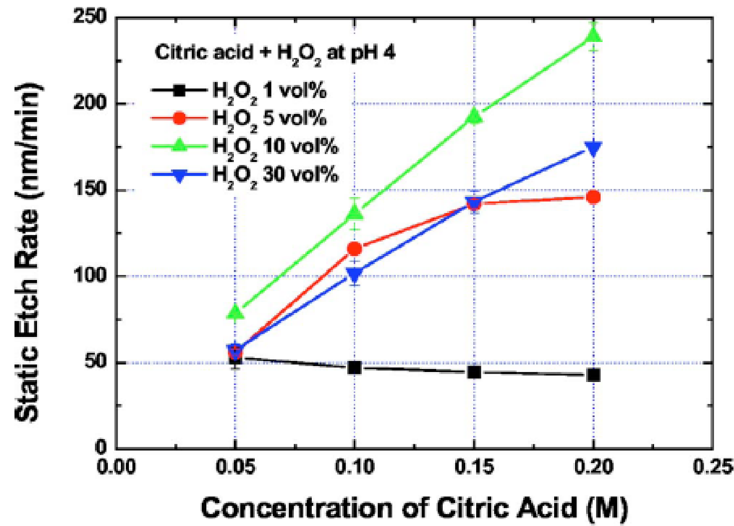

Fig. 2-9 : Static etch rate of copper as a function of citric acid concentration at pH 4 with varying oxidizing agent content [56].

Fig. 2-9 shows the static etch rate of copper in slurries with varying oxidizing agent content as a function of citric acid concentration at pH 4. For lower concentrations of hydrogen peroxide i.e. 1 vol %, the etch rate remained constant irrespective of the concentration of citric acid in the slurry. Increasing the hydrogen peroxide content up to 30 vol. % also does not show any signs of the removal rate reaching saturation. This indicates that at acidic pH values, active dissolution of copper in the slurry is favored than passivation. Increasing the pH to 6 changes the scenario rapidly as shown in Fig. 2-10. The etch rates at 1 vol % hydrogen peroxide is highest and increases linearly with increasing citric acid concentration, while the etch rates at 10 vol % and 30 vol % are significantly lower and remain constant for varying concentrations of citric acid.

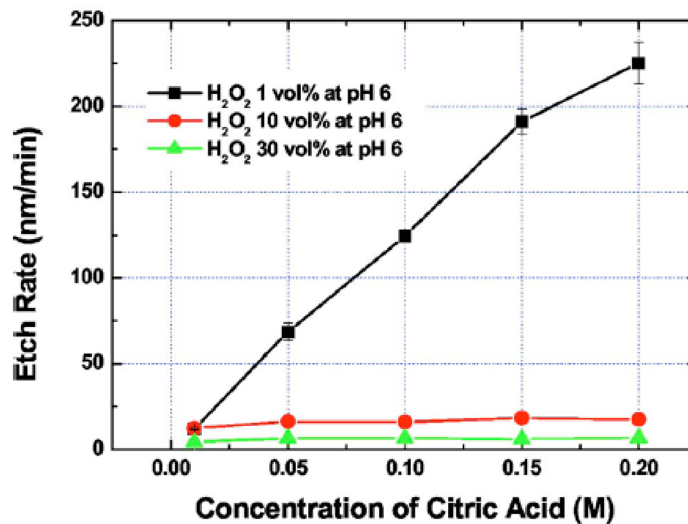

Fig. 2-10 : Static etch rate of copper in pH 6 slurry as a function of citric acid content and oxidizing agent content [56].

The trend observed under the above conditions is validated using potentiodynamic curves for each of the slurry combinations. It is seen that at both the pH values the corrosion potential shifted to a more positive value with increasing oxidizing agent content. Figs. 2-11(a) and (b) show potentiodynamic curves for the above conditions. These results also enabled reaffirming the passivating behavior of copper as the slurry pH is increased.

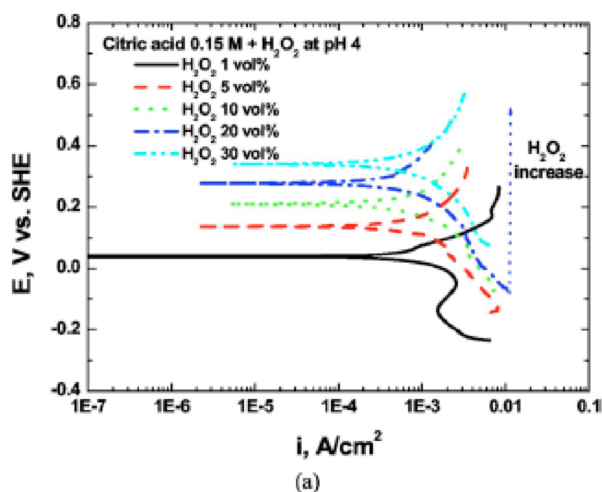

(a)

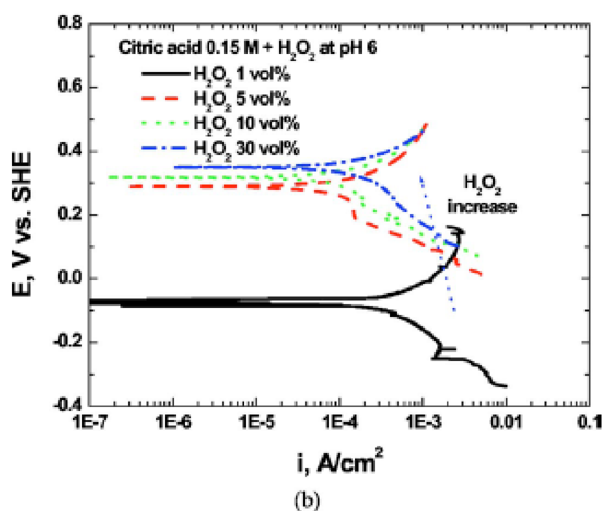

(b)

Fig. 2-11 : Potentiodynamic polarization curves for copper in Hydrogen peroxide and citric acid slurries at (a) pH 4, and (b) pH 6 [56].

The shift of corrosion potential to a more positive value means that the anodic reaction of copper will be inhibited and the dissolution of copper will be reduced due to formation of copper oxide passivation layer. Based on the results obtained from the above studies a mechanism for material removal under the conditions studied is proposed. Fig. 2-12 illustrates the mechanism of material removal for Cu-CMP under

conditions of low and high oxidizer concentrations with high and low pH polishing slurries.

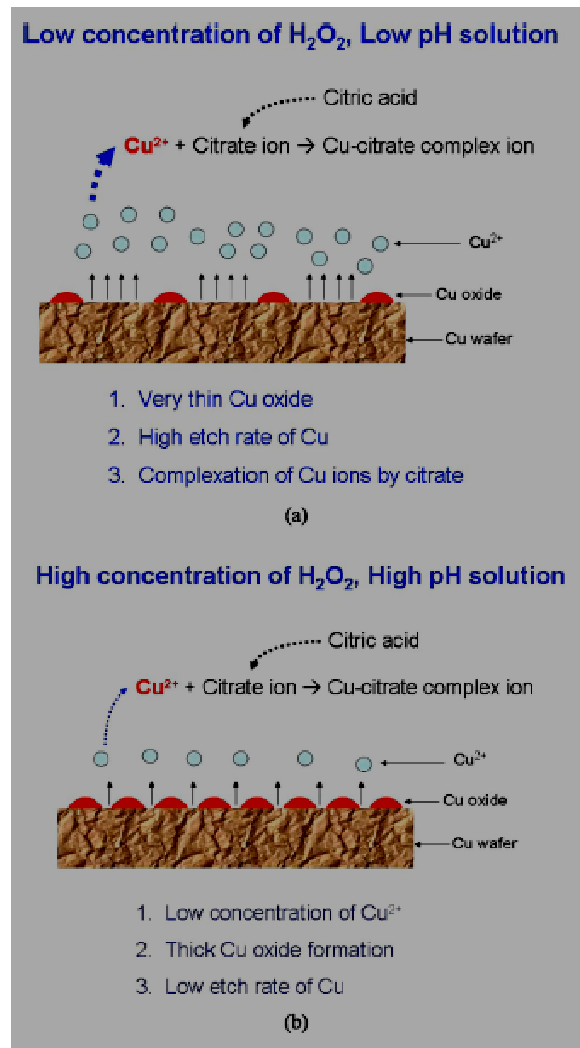

Fig. 2-12 : Schematic of the Mechanism of material removal at different polishing conditions of oxidizer content, slurry pH and complexing agent content [56].

Polishing in slurries with low oxidizing agent concentrations as well as low pH leads to the formation of Cu ions due to formation of thin oxide film. The film is hypothesized to be thin enough to be attacked by

other chemical ingredients in the slurry. These Cu ions can thus easily form Cu-citrate complexes with the citrate ions dissociated from citric acid in the slurry. This accelerates the etching of copper due to the availability of more space for Cu ions to be able to go into the slurry.

On the other hand polishing with slurries with high oxidizing agent contents and high pH leads to the formation of a thicker oxide film over bare copper surface. This reduces the amount of Cu ions that goes into the solution. This means a reduced complexing action of the complexing agent present in the slurry. The overall effect is that of reduced removal of copper from the substrate.

Aksu *et al.* [61] studied the role of glycine as a complexing agent in copper polishing slurries using potentiodynamic techniques. The effect on behavior of copper at various pH with and without glycine is carried out using a rotating disk electrode (RDE) configuration. Copper shows a tendency to passivate in aqueous solutions at high pH, while at lower pH it dissolves actively [1, 48].

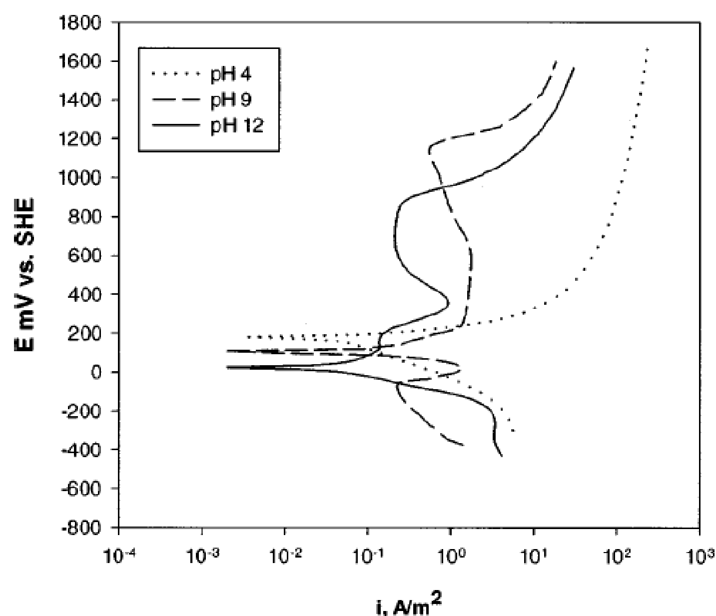

Fig. 2-13 : Effect of pH on polarization of copper in aqueous solutions at various pH [61].

As shown in Fig. 2-13, the anodic part of the curve shows clear passive regions at pH of 9 and 12 while at pH of 4 it is active with high anodic currents all through till the end of the scan. Addition of glycine to the above aqueous solutions changes the picture drastically. The passivation observed at a pH of 9 is no longer observed and copper shows active behavior till a pH of 9. This is attributed to the fact that both zwitterionic and anionic forms of glycine exist at this pH. It can be seen from Fig. 2-14, the corrosion current at pH 9 is higher than that at pH of 4. But, the anodic currents are higher at pH of 4 beyond the potential of 0.35 V. The general mechanism of complexation of copper by complexing agents such as glycine, ethylene diamine, ammonia requires

that dissolved oxygen be adsorped on the bare copper surface. This means that formation of a thin oxide layer is the first step in this process. Then complexing agents help dissolve the copper where the adsorption of copper has taken place. At higher pH values, formation of copper oxide competes with the dissolution of copper by complexing agent.

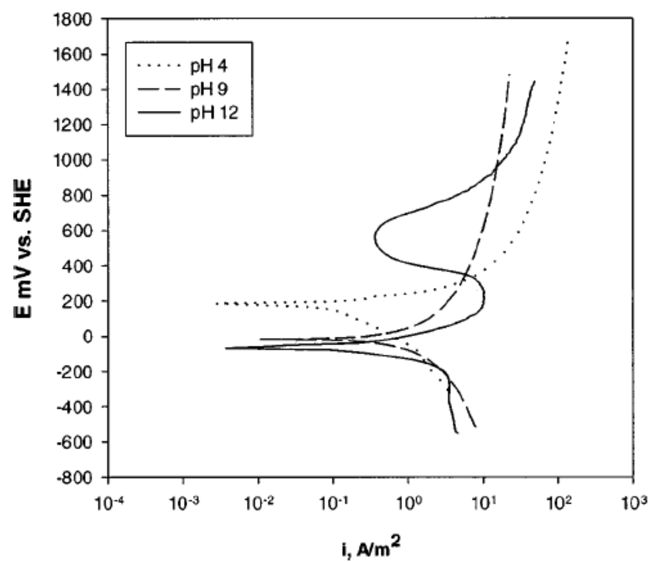

Fig. 2-14 : The Effect of addition of 0.01 M of glycine to aqueous polishing solutions on polarization behavior of copper [61].

The introduction of polishing pad and abrasive brings out some nuances of the process. Fig. 2-15 shows the polarization curves with no abrasion, polishing with only pad and polishing with pad with 5 wt % alumina abrasive.

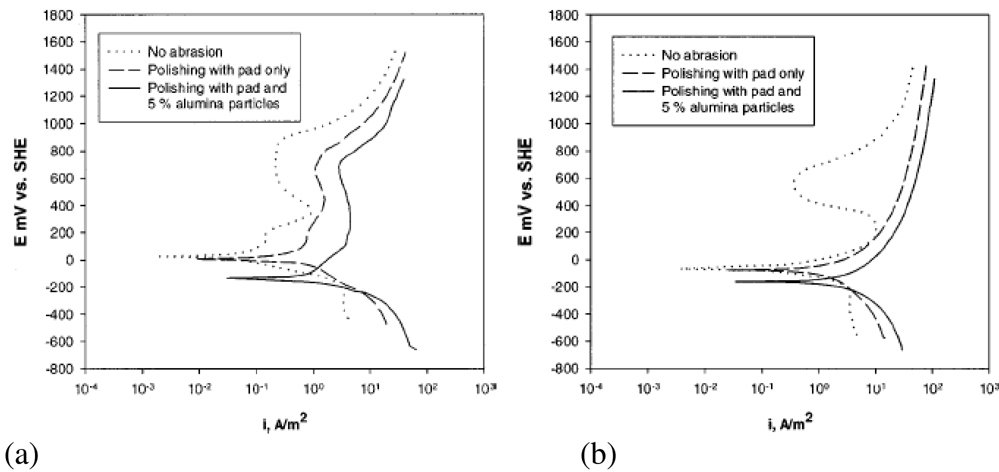

Fig. 2-15 : Polarization behavior of copper in aqueous solution at pH 12 (b) No Glycine and (b) 0.01 M Glycine : under no abrasion, polishing with pad and polishing with pad and 5 wt % abrasives [61].

The addition of abrasives seems to be preventing the formation of a passivating film. Comparing Fig. 2-15 (a) and (b) it is evident that a slurry at a pH of 12 with glycine promotes passivation to the low lying areas while at the same time enhances dissolution of the mechanically abraded region. This can be inferred from over two orders of magnitude difference in anodic dissolution in Fig. 2-15 (b) between with and without abrasion. This situation of high dissolution with abrasion and low dissolution without abrasion is ideal from the point of view of achieving planarity.

2.3 Effect of corrosion inhibiting agent content

The inherently reactive nature of low pH acidic slurries also presents the need to add a corrosion inhibitor (benzotriazole, BTA) to prevent static etching of low areas on the copper surface profile. Hence, the effect of the various slurry parameters on copper-CMP process is rather complex and inter dependant. BTA, however has its own drawbacks. For example, it is a weak acid and dissociates according to the following mechanism:

$$BTA \rightarrow BTA^{-} + H^{+}$$

The concentrations of BTA and BTA^{-} both depend on the overall concentration of BTA in the slurry and on the slurry pH. BTA^{-} is easily adsorbed on to the positively charged surface of the alumina abrasive at low pH. But the amount of BTA^{-} adsorbed is less as the dissociation itself is less due to low pH. Hence, the slurry even in the presence of BTA, remains stable at low pH. With increase in pH, the surface charge of the abrasive particles is negative and the dissociation of BTA^{-} is more. Since the surface charge is same, there is electrostatic repulsion and the slurry remains stable [53]. The amount of BTA in the slurry is critical, as excess BTA can reduce the MRR drastically. In conventional polishing slurries 0.01-0.05 wt % BTA effectively inhibits excessive static etching of Cu surface [42].

Luo *et al.* [53] investigated the effect of BTA on the slurry stability by performing settling rate tests. BTA is a preferred inhibitor incorporated in dissolution based Cu-CMP slurries to prevent excessive static etching of bare copper surface [1,48]. Zeta potential measurements were conducted to validate the results obtained from the settling rate tests. Fourier transformed infrared (FTIR) spectroscopy tests were also conducted subsequently for an insight into the adsorption of BTA on alumina abrasives. The effect of ferric nitrate on the stability of the slurry was also investigated. The effect of these parameters on the material removal rate (MRR) and selectivity of polishing between Cu and SiO_2 were also investigated.

A 50 ml vertical cylinder with a stopper was used to determine the settling rates of alumina particles under various BTA content conditions. The zeta potentials of the abrasive for different BTA content slurries were measured. The particles were naturally dried and kept in a desiccator for the FTIR measurements.

Fig. 2-16 shows the variation in zeta potential and its corresponding effect on settling rate of slurry as a function of BTA concentration in the slurry. At low concentration of BTA, the zeta potential of the abrasives is at the positive end of the range. As the concentration of BTA increases in the slurry, the zeta potential approaches the point of zero charge (PZC). At this point the settling rate

is very high, indicating that the slurry is very unstable and tendency of coagulation is very high.

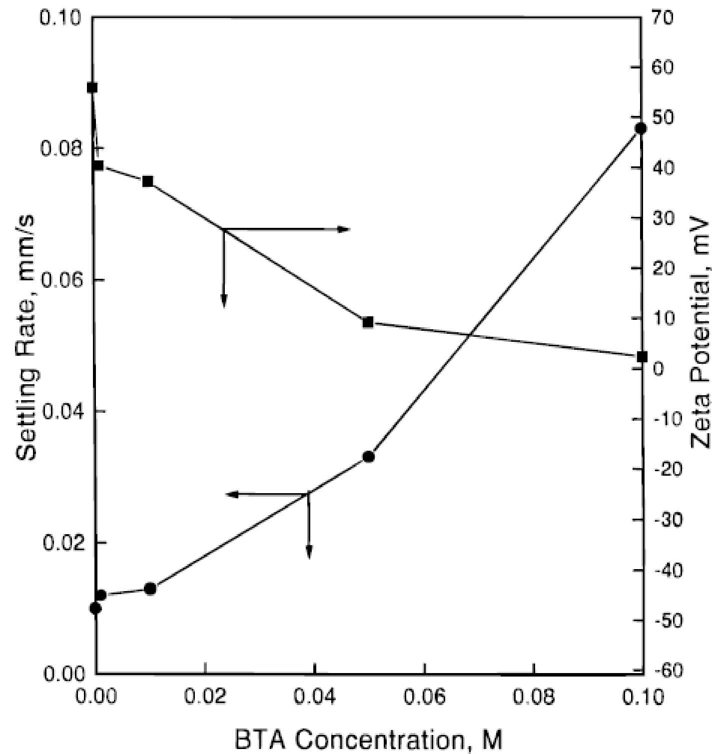

Fig. 2-16 : Effect of BTA concentration on the zeta potential and slurry stability measured by the slurry settling rate [53].

Fig. 2-17 shows a plot of adsorption isotherms of BTA on alumina abrasive particles at various pH values. The adsorption behavior of BTA on alumina abrasives is very highly pH dependant. At lower pH values the amount of pH adsorped is more than that at higher pH values. Since alumina particles are positively charged at low pH values, the adsorption of BTA^- is more. However as the pH increases, the abrasive particles become more negatively charged, which thus causes a reduction in the adsorption of BTA-. But surprisingly at pH of 5.5 the adsorption is the

maximum, which means that the adsorption is not just due to electrostatic forces but also due to chemical adsorption and/or hydrogen bonding.

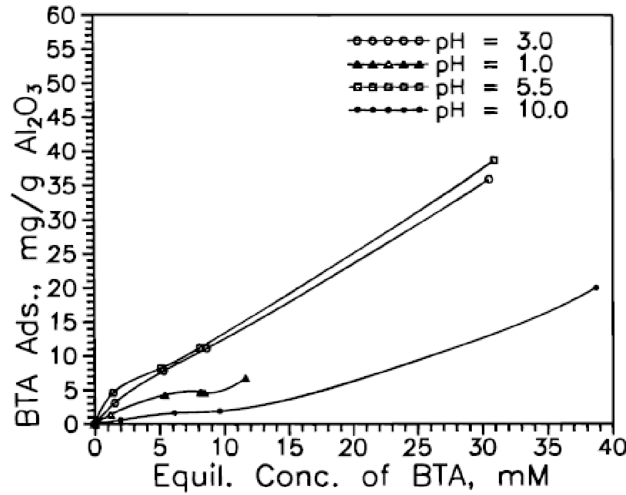

Fig. 2-17 : Adsorption isotherms of BTA on alumina abrasive particles [53].

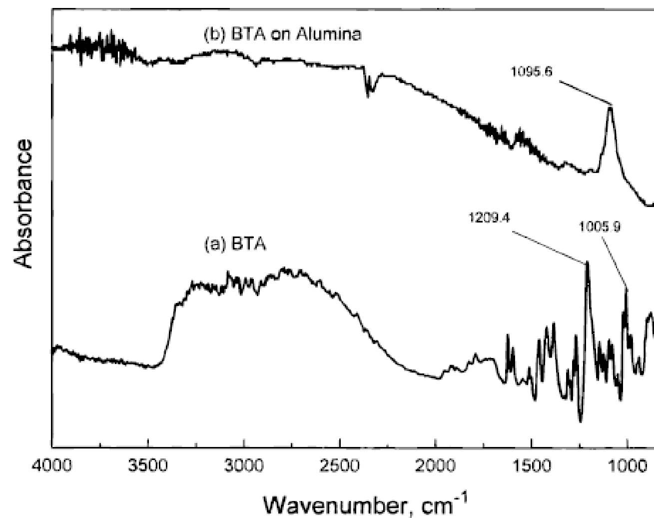

Fig. 2-18 : FTIR spectroscopy for (a) pure BTA, and (b) BTA adsorped on alumina abrasive particles [53].

Fig. 2-18 shows the FTIR spectroscopy for pure BTA and BTA adsorped on the alumina abrasive particle surface. The shift in the peak

from 1209 cm^{-1} observed in the spectroscopy for pure BTA to 1095 cm^{-1} in BTA adsorped on alumina indicates that Al on the surface of alumina particles is coordinated to unsaturated nitrogen ring forming a bidentate structure.

Other special additive to the Cu-CMP slurry includes a surfactant. The main purpose of a surfactant to the polishing slurry is to reduce pattern sensitive erosion of the interlayer dielectric layer. A 0.25 wt % cetyltrimethylammonium bromide (CTAB) is added as a surfactant to the polishing slurry [37]. Addition of stannate salts facilitates in increasing the slurry stability by preventing degradation of the oxidizing capabilities of the slurry. It exhibits affinity to trace metals to form complexes thereby preventing the ability of the trace metals to catalyze decomposition of the slurry itself. The stannate salts thus facilitate in preventing trace metal ions from reacting with the slurry oxidizer [44]. To prevent flocculation and settling of the slurry polymeric compounds are added to the slurry. Polyoxyalkylene ether is added in small quantities (~ 0.001 wt %) to achieve the desired steric stability [39].

Other enhancements like multiple abrasive slurries also have been suggested [38]. The use of ceria abrasive particles of 100 nm size alongwith smaller alumina abrasive of 50 nm size is proposed. The aim here is to reduce the overall abrasive size, thereby reducing the tendency of scratching yet achieving acceptable removal rates.

The use of coated abrasives has also been suggested to improve wettability, dispersability, and bonding. This again in a way helps in reducing scratching as well as agglomerate formation of individual abrasive particles [63].

To compensate for the variable hardness of materials to be polished on a substrate, use of softer abrasives which can polish copper overburden, while not damaging the barrier layer is also suggested [64]. More specifically, abrasives that are harder than copper, such as iron oxide, strontium titanate, apatite, diopase, fluorite, and hydrated iron oxide are used to polish copper over layer. They have hardness values less than the barrier layer. This, thus, protects the barrier layer from getting abraded during polishing.

To reduce the scratching probability and frictional heating buffering agents or caking agents are also added to the polishing slurries [32]. Potassium acetate is a common choice of buffering agent added to the slurry. Addition of potassium acetate is also known to facilitate in maintaining the slurry pH at desired level. It can be directly added to the slurry or generated *in-situ* in the slurry by the reaction of potassium hydroxide and acetic acid.

The oxidation energies associated with the conductive layer and the barrier layer demand the use of multiple slurry chemistries, more specifically with altered oxidizing capabilities [41]. Tungsten has an

oxidizing potential of 0.12V and that of Copper is 0.34V. This means that tungsten has a tendency to oxidize preferentially than copper. Care must be taken to completely eliminate this potential difference in oxidation or rather attempt to reduce it as much as possible.

It is thus evident that all the abovementioned slurry parameters have a strong interplay with each other and hence not only they individually affect the process performance but their interactions with each other also bear significant effect on process outputs. This scenario becomes even more complex when *in-situ* drifts occur in the initial set values of the above machine settings. For instance, as polishing progresses there is a gradual change in the slurry pH. To combat this, monitoring of the various process parameters such as the slurry pH, complexing agent content of the slurry, corrosion inhibitor content of the slurry should be effectuated.

Various sensor based monitoring approaches have been investigated for monitoring [49-51] and modeling [52] of chemical mechanical planarization of silicon as well as copper. A detail overview of the previous work in sensor-based techniques in process monitoring and modeling is presented in the next chapter.

Chapter 3: Sensors in CMP

Modeling silicon CMP by incorporating wired as well as vibration sensors is realized by the group of Bukkapatnam *et al.* [52]. These sensors were mounted on a polishing machine and the data acquired is analyzed offline. Pertinent features were extracted from the acquired sensor data in both the time and frequency domains. Once these features are extracted, a matrix comprising all these features is constructed. Then, principle component analysis (PCA) is performed on these candidate sensor features. The aim of performing PCA is to reduce the volume of data that needs to be handled as well as to normalize it. The MRR is then modeled using these extracted sensor features.

Numerous statistical tests and techniques were implemented to model the MRR in silicon CMP. In the first attempt, linear regression of MRR was performed with the machine settings as predictors. A modest regression coefficient of ~ 70% was achieved. In order to validate the

Effectiveness of sensors for process modeling, key sensor features were then incorporated in the model for MRR.

Some of the features extracted from the sensor signal data showed distinct variation with changes in the machine settings. For instance the signal skewness showed a sizeable drop upon increase in the polishing slurry pH. Fig. 3-1 shows the variation in signal skewness with variation in slurry pH.

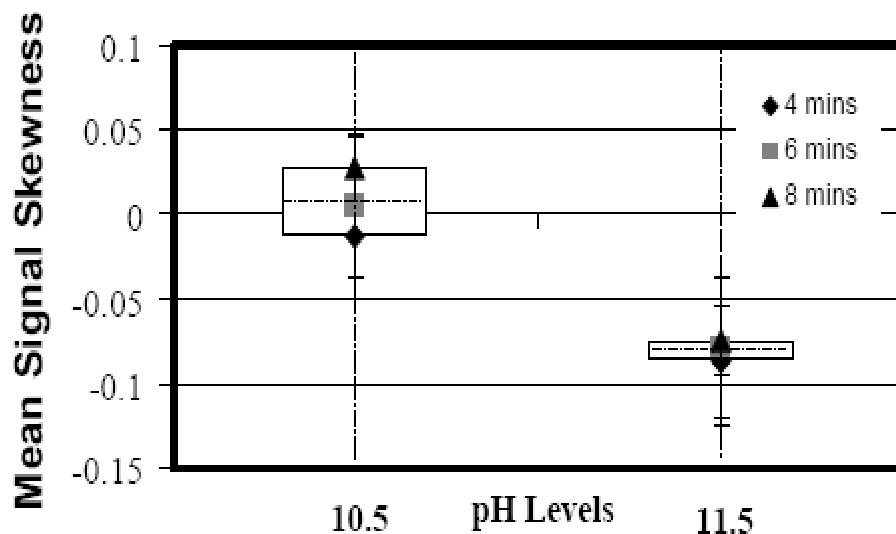

Fig. 3-1 : Variation of signal skewness for two slurry pH values [52].

An attempt was made to model the MRR with a main feature set, which is determined from the values of direction cosines obtained after performing PCA. But this does not help to improve the predictability of the MRR.

Hence it was concluded that linear modeling techniques do not help much in improving the predictability of the process. Hence, in a

second approach towards enhancing the predictability of the model, non linear techniques were implemented. Again in implementing non-linear techniques, a set of tests were carried out to determine the effectiveness of implementing non linear principles. These tests include determination of autocorrelation function, plotting the Poincaré section plots which help in determining inherent non-linearity in the process.

Various non-linear features, such as the Shannon entropy, maximum Lyapunov exponent, and Kaplan-Yorke dimension are extracted from the sensor data. In the subsequent analysis it is found that the maximum Lyapunov exponent effectively detects the variation in downforce levels and the Shannon entropy values capture changes in the levels of slurry flow rate. Inclusion of non-linear features in the model alongwith the machine setting gives an enhanced predictability of ~90%.

From a process monitoring standpoint, Tang et al. [65] suggest an acoustic emission based method for detection of the formation of scratches due to agglomeration of abrasives, or due to inherent contamination of the slurry, or in some cases due to a poor pad conditioning wheel. A conditioning wheel can leave diamond grit on the pad surface, which then can cause catastrophic scratches on the wafer. These scratches can lead to sites for electromigration defects and bear a significant effect on the successful production of the chip. Hence, prediction of occurrence of scratches, if effectuated, would help in

reducing catastrophic failure of an entire chip. Instead, the polishing process can be halted and necessary corrective actions initiated.

Use of acoustic emission sensors to detect microscratching in CMP has been reported by Tang *et al.* [65]. Two sets of tests were performed, one on a laboratory type polishing machine, and the other on an industrial grade machine. To detect the microscratching phenomenon, diamond abrasive grit of size 1μm is added to the slurry. Fig. 3-2 shows a typical AE rms signal for a normal polishing process taken on an industrial grade CMP machine. It has three distinct zones viz. the loading stage, the running in stage and the equilibrium stage. The point to notice here is that there are no significant periodic spikes observed in the signal. Primary tests are carried on a laboratory grade polisher. AE rms data was acquired for both before and after conditioning the pad with 250 μm grit diamond wheel. It is seen that in the signal before pad conditioning, the magnitude of signal (peak to peak) is significantly lower than that after pad conditioning is performed. Fig. 3-3 shows the signal before pad conditioning has been performed while Fig. 3-4 shows the signal after performing pad conditioning with a 250 μm grit diamond tool.

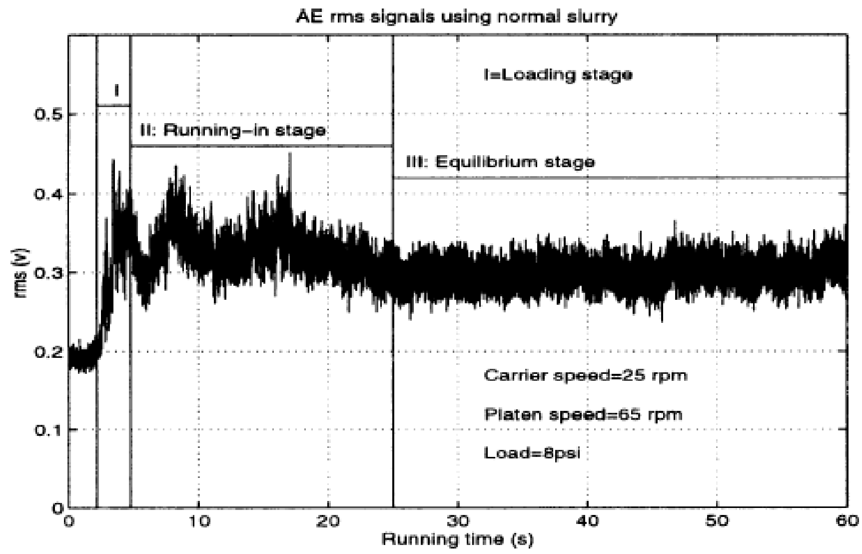

Fig. 3-2 : AE rms signal for a normal (unscratched) CMP run on an industrial grade machine [65].

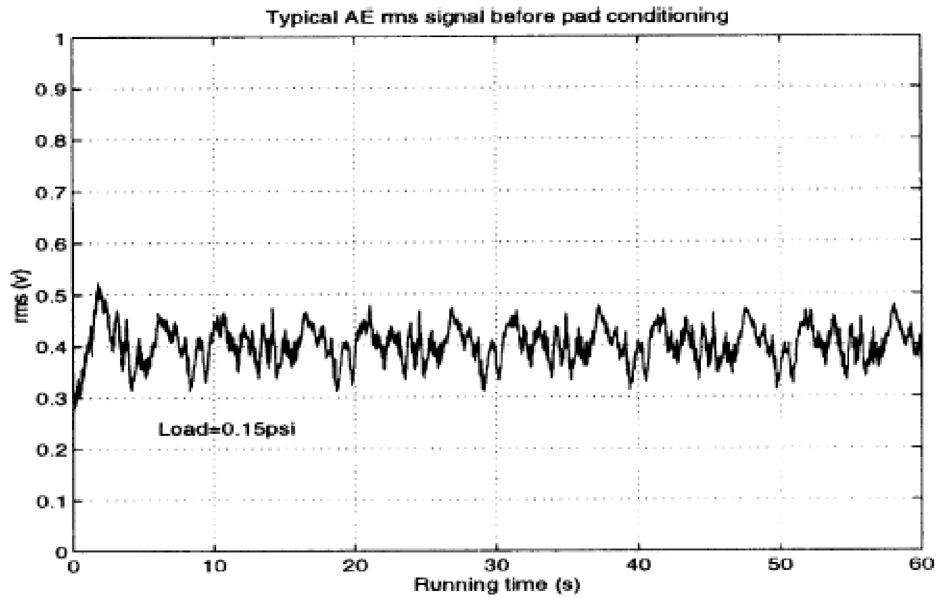

Fig. 3-3 : AE rms data on laboratory polishing machine before pad conditioning [65].

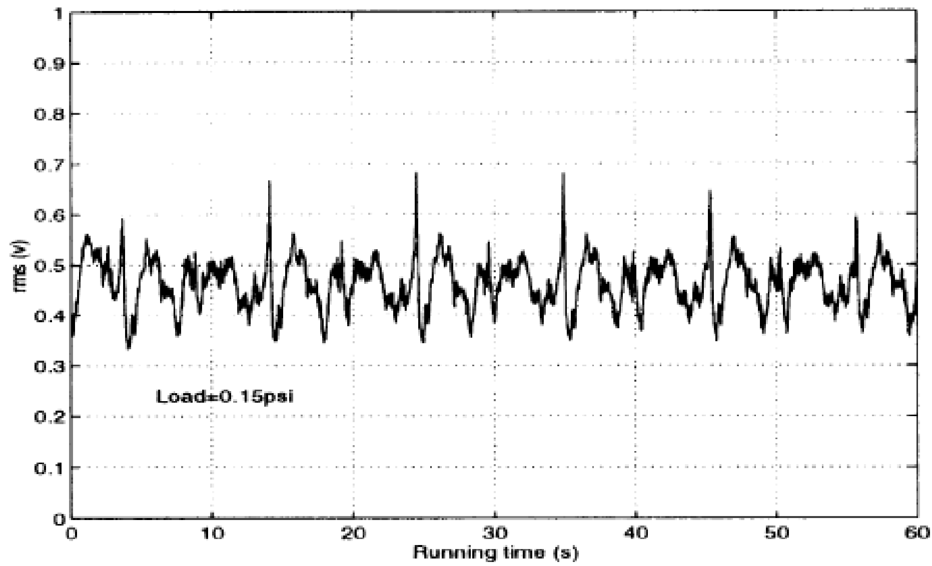

Fig. 3-4 : AE rms data on laboratory machine after pad conditioning with 250 μm diamond wheel [65].

As can be seen from the results obtained from the tests carried out on the laboratory grade polishing machine, have been extended to industrial grade machine.

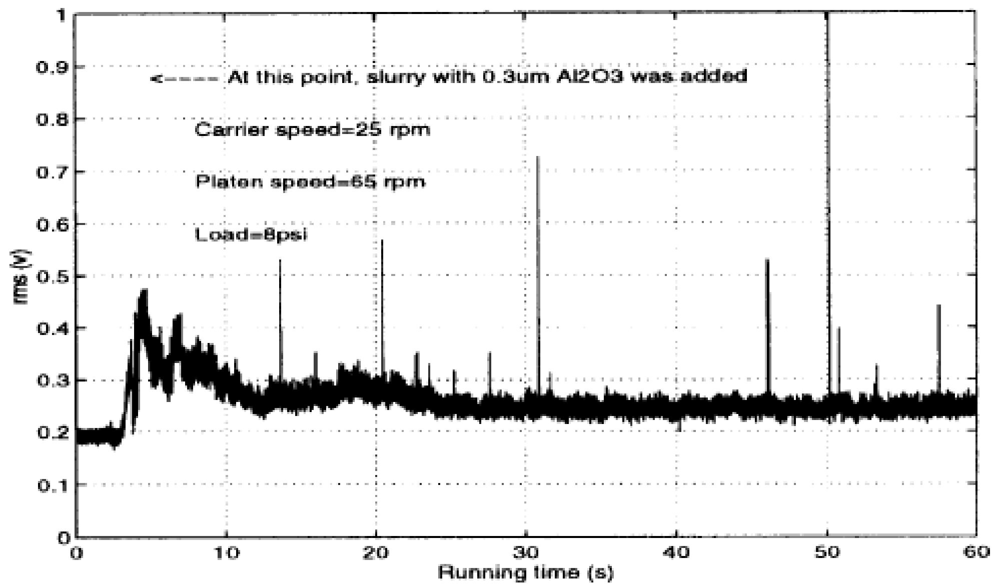

Fig. 3-5 : AE rms data taken on an industrial CMP machine after artificially adding hard and bigger alumina abrasives to the polishing slurry [65].

Fig. 3-2 shows the AE rms signal for an unconditioned pad while Fig. 3-5 shows the signal after 300 nm alumina particles were introduced in to the slurry. There is a significant presence of periodic spikes which are correlated to the scratching of the wafer due to hard and bigger alumina particles.

Based on the review of the literature, it affirms that multiple sensors can be implemented in monitoring as well as modeling of the CMP process. The incorporation of sensors in CMP process helps in achieving better process control as well as to improve the throughput by helping in reducing the damage caused due to wafer scrapping and rework.

Chapter 4: Problem Statement

As discussed in the literature review pertaining to the slurry chemistry effects in Cu-CMP process performance, the slurry chemistry and interactions between the individual slurry characteristics play a very important role in deciding the quality (surface finish, WIWNU) as well as quantity (MRR) of the process.

From a process control standpoint as well as process monitoring standpoint, it is important that the variability in the process performance associated with variations in input process parameters be quantified. Subsequent process control measures should also be established, thus developing a closed loop system.

A key step here is to quantify the variations in output with known variations in the input variables. This task is proposed to be achieved by conducting designed experiments. Subsequently, after knowing this variability, it is critical to be able to *in-situ* sense or track this variability in process variables, so that immediate corrective action can be initiated and process control is again established. In short, tracking the variations in input process variables should be accomplished so as to be able to control them, or fine tune them for maximized throughput.

To be able to track these variations, some indirect method has to be adopted, as the actual wafer pad interface is virtually inaccessible. In this investigation we incorporated multiple vibration sensors (Wired and Wireless) to investigate as to whether they can help in gathering insights into the process dynamics. The results of the experimental investigations as well as sensor-based modeling techniques shall be discussed in the later sections of the document.

To perform the experimental investigation of Cu-CMP, we use a Lapmaster 12 polishing machine instrumented with one wired and wireless vibration sensor. A two step modeling approach was incorporated, we first modeled the MRR using just the process variables and the interaction terms in between them as predictors. This helped in assessing the effect of each of the input process variables on the MRR. But as mentioned, from the process monitoring viewpoint, we then incorporated sensor features as predictors for the models. The models based on sensor features show improved estimation of the MRR as well help in tracking the variations in the input process parameters.

Chapter 5: Experimental Setup

5.1 Experimental Setup:

We present here, an investigation of implementing sensors on Cu-CMP machine. The process characteristics for Cu-CMP are entirely different than those for silicon or oxide CMP. Especially the slurry chemistry plays a pivotal role as copper is chemically more active and is prone to chemical damage, if faced with improper slurry chemistry selection.

In order to track the variations of various characteristics of Cu-CMP slurries and their effects on performance, to determine the average MRR of the copper-CMP process in real time, polishing studies have been carried out. Regression analysis is conducted based on the experiment data to investigate the relationship among process performance (MRR), machine settings, and sensor data.

Polishing tests are carried out on a LapMaster 12 bench top polishing machine instrumented with wired and wireless vibration sensors as shown in Fig. 5-1. Unpatterned copper wafers (1.25 mm thick and 100 mm diameter) are used. Different slurries of varying chemistry

are used and the effect of these variations on average MRR of Cu-CMP is investigated. Fig. 5-2 show the wafers used in this investigation.

The platen rotates at 60 rpm and the wafer is pressed face down against the rotating platen with a down pressure of 1 psi. The retaining

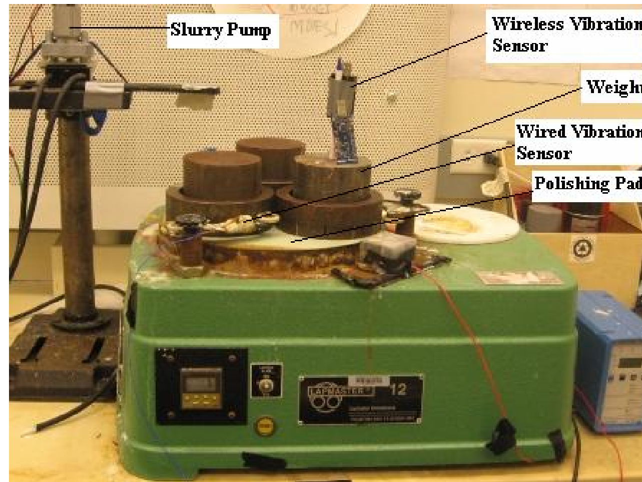

Fig. 5-1: Experimental setup used for conducting sensor based Cu-CMP investigation.

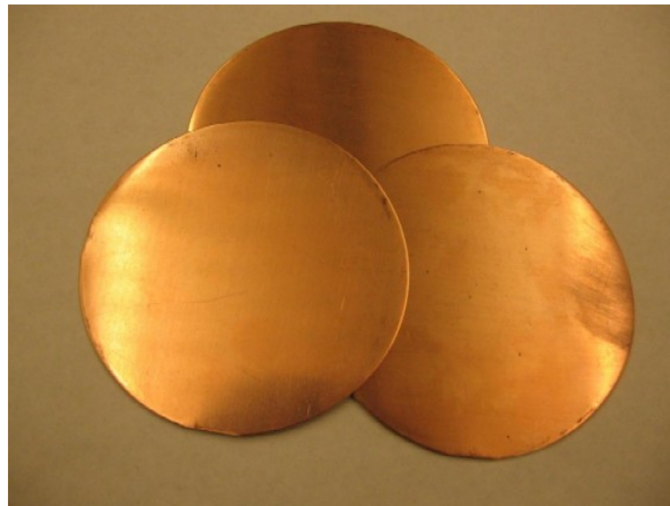

Fig. 5-2: Unpatterned copper wafer used in the sensor based Cu-CMP investigation.

rings keep the wafers in place during platen rotation. Use of a DC pump facilitates slurry delivery at the centre of the platen.

Two sensors namely, a wired accelerometer (KISTLER Model No. 8728A500, sampling at 5 KHz), and a single channel wireless accelerometer (MOTEiv, sampling at 500Hz) are mounted on the polishing machine at locations shown in Fig.5-1. Wired sensor signals are acquired through a charge amplifier (Kistler 5134A1) and digitized using NI PCI 6024 board, sampled at 5 KHz. The wireless sensor signals are acquired through a Universal Serial Bus (USB) receiver with the aid of a program designed in the Cygwin environment. Signals obtained from the wired and wireless vibration sensors are analyzed offline for monitoring the copper-CMP process.

Fig. 5-3: Wired vibration sensor (Kistler 8728A500) used for sensor based Cu-CMP investigation.

Table 5-1: Specifications of wired Kistler accelerometer used in the experimental investigation.

Technical Data Type		Units	8728A500
Acceleration Range		g	±500
Acceleration Limit		g_{pk}	±1000
Transverse Acceleration Limit		g	±1000
Threshold		g_{rms}	0.02
Sensitivity ±10%.		mV/g	10
Resonant Frequency mounted nom.,		kHz	76
Frequency Response	±5%	Hz	2 ...10000
	±10%	Hz	1 ...15000
Amplitude Non-linearity		%FSO	±1
Time Constant nom.		s	0.5
Transverse Sensitivity typ. (max.)		%	1.5 (3)
Base Strain Sensitivity @250 με, max.		g/με	0.03
Shock (1 ms pulse width) max.		g_{pk}	5000
Long Term-Stability		%	±1
Temperature Coefficient of Sensitivity		%/°F	-0.03
Temperature Range Operating (4mA supply current)		°F	–65 ... 250
Temperature Range Storage		°F	–105 ... 305
Output:			
Bias nom.		VDC	11
Impedance max.		Ω	100
Voltage F.S. nom.		V	±5
Current		mA	2

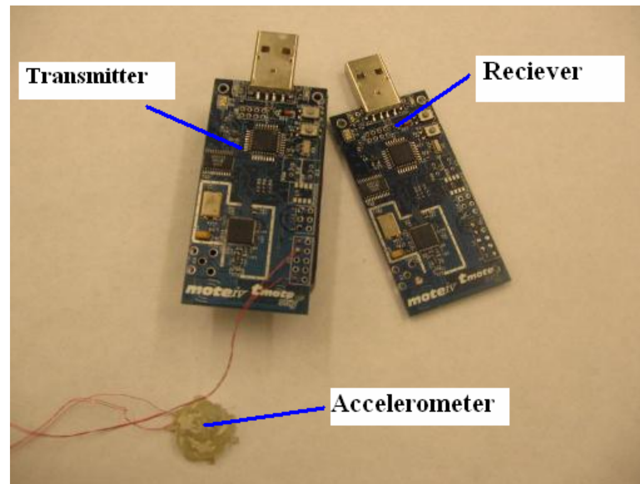

Fig. 5-4: Wireless vibration sensor unit used in sensor based Cu-CMP investigation.

Fig. 5-5: Sartorius manufactured precision digital weighing scale used to measure wafer weight after each polishing cycle.

Fig. 5-3 shows a wired vibration sensor used in this investigation. The technical specifications of which are given in Table 5-1. Fig 5-4 shows the wireless vibration sensor used.

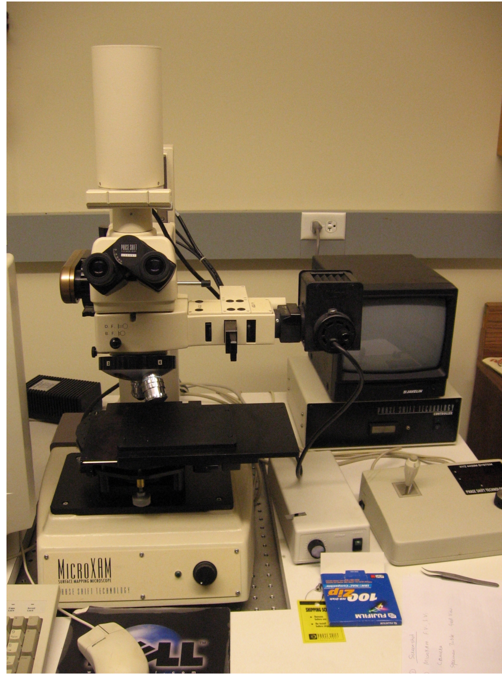

Fig. 5-6: ADE Phase Shift Technologies, MicroXAM, Laser interferometric microscope used for surface quality measurement during Cu-CMP experiments.

The material removal rate is measured using a high precision digital weighing scale (Sartorius Model 1712 MP8, resolution 0.1 mg) capable of measuring to the resolution of 0.1mg (Fig. 5-5). The specifications of this weighing scale are as follows:. Wafer weight measurements are taken at the end of every 20 second polishing cycle. Surface quality measurements are effectuated using a laser interferometric microscope (MicroXAM, ADE Phase shift Technologies).

The basic operating principle of interferometer is based on the classical Michelson interferometer. With an optical interferometer the physical distance between two objects can be measured in terms if

wavelengths of light. Fig. 5-6 shows the ADE Phase Shift Technologies, MicroXAM used in this investigation to qualitatively monitor the surface quality of the wafer during CMP.

5.2 Design of Experiments

Taguchi L12 array (see Table 5-2) was used to investigate the effect of various slurry ingredients (referred to as input variables) on the average MRR (henceforth, referred to as output variable) of the process. The resulting regression model is used to estimate the variation in slurry content and its effect on the average MRR from the sensor data acquired. As summarized in Table 5-3, the input variables (machine settings) include: (1) pH of the polishing slurry (range 3 to 5), (2) flow rate of the slurry (range 50 to 100 ml/min), (3) amount of complexing agent (range 0 to 20 gms/lit), and (4) amount of BTA (range 0 to 1 gm/lit).

Each polishing run at a given setting is comprised of multiple (4-6) 20 sec long polishing cycles. The average MRR is measured based on wafer weight differences over a polishing cycle measured using a precision weighing scale. The average MRR is given by:

$$MRR = (W_i - W_f) / (T_f - T_o)$$

where W_i is the wafer weight at the start of a polishing cycle (gms), W_f is the wafer weight at the end of a polishing cycle (gms), T_f is the time at the end of a polishing cycle (sec), and T_0 is the time at the start of a

polishing cycle (sec). The average MRR is an average of 3 wafers used simultaneously in each polishing run.

Table 5-2 : Taguchi L-12 Matrix implemented to study the slurry chemistry effects on MRR in Cu-CMP

	pH	**Down Force**	**Flow Rate**	**Complexing agent**	**BTA**
R1	L	H	L	L	L
R2	L	H	L	L	L
R3	L	H	H	H	H
R4	L	H	L	H	H
R5	L	H	H	L	H
R6	L	H	H	H	L
R7	H	H	H	H	L
R8	H	H	H	L	H
R9	H	H	L	H	H
R10	H	H	H	L	L
R11	H	H	L	H	L
R12	H	H	L	L	H

In the above table, 'H' denotes that for that particular treatment condition, the given machine setting is at the high setting, while 'L' denotes that it is at a low machine setting. The high and low values enable verifying whether the sensors are able to track variations in the machine settings.

Table 5-3 : High (H) and low (L) levels of machine settings given as per Experimental matrix defined in Table 5-1.

Machine Setting	**Low**	**High**
pH	3	5
Flow Rate, ml/min	50	100
Complexing Agent, gms	0	20
BTA, gms	0	1

Various chemicals and slurry ingredients used in the above investigation are as follows:

1. De-ionized water: A general vehicle for the polishing slurry compounds.
2. Hydrogen Peroxide (30%) (Reagent grade from Fisher Scientific): intended to facilitate formation of a passivation film over the virgin copper surface.
3. Nitric acid (Reagent grade, 98% pure): used to maintain acidic pH recommended for Cu-CMP.
4. Citric acid (Reagent grade): used as a complexing agent. It combines with abraded copper oxide species and removes them from the wafer surface thus preventing redeposition.

5. Abrasives: α-alumina (average diameter 50 nm, from Buehler) is used as an abrasive to facilitate mechanical abrasion and removal of material during CMP.
6. BTA (Benzotriazole) (Reagent grade from Aldrich): It is used to form a non-native film on the bare copper surface and protects the troughs on the surface profile from getting etched away by the slurry.

Chapter 6: Main Effects of various slurry chemistry parameters on average MRR

It is important to evaluate the effect of variation of each of the individual machine setting on the average MRR. This, although a simplistic test, can be used as a good indicator of the goodness of experiments. It also serves as a test that enables in determining the most significant machine parameter that affects the average MRR. The aim of these tests is to demonstrate the variations in average MRR with variation in the machine settings such as polishing slurry pH, complexing agent content, corrosion inhibiting agent content and slurry flow rate respectively.

Effect of slurry pH on average MRR

The variation in polishing slurry pH brings about a drastic variation in the average MRR in Cu-CMP. As stated in the literature review, copper has a tendency to dissolve actively at low acidic pH values. As the pH increases, the tendency to show passivation also is increased. This tendency of passivation causes a drop in MRR. Hence the experimental results agree well with the earlier research reported in the literature on

the effect of polishing slurry pH on MRR in Cu-CMP [46, 47]. The results of variation of MRR with polishing slurry pH are given in Fig. 6-1.

Effect of variation of complexing agent content on average MRR

The purpose of adding a complexing agent to the polishing slurry is to facilitate easy removal of abraded species. Complexing agent prevents redeposition of debris on the wafer surface. It also forms Cu-complexes and enhances the material removal capabilities of the polishing slurry.

Thus, addition of complexing agent should enhance the removal rate. The experimental results of effect of the variation of complexing agent content in the slurry on the MRR are shown in Fig. 6-1.

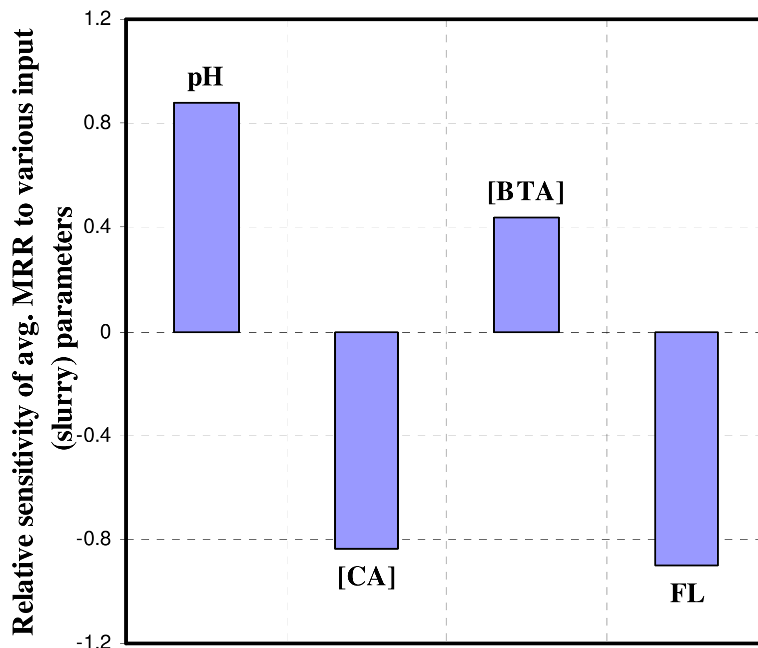

Fig. 6-1: Sensitivity of avg. MRR to various slurry chemistry parameters.

Effect of variation in the corrosion inhibiting agent content (BTA) on average MRR

When using low pH dissolution type slurries for Cu-CMP, it becomes very critical to protect the low areas of the wafer surface from being statically etched. This ensures achievement of planarity, else only material removal is achieved with no improvement or in many cases damaged profile is obtained.

As stated in the literature review, BTA is commonly used as a corrosion inhibiting agent in most Cu-CMP slurries. It forms a non-native inhibiting film which protects static etching of bare copper. This means that if BTA is added in excess than normally required, it will result in the formation of a thick inhibiting film causing an appreciable drop in the removal rate.

Theoretically, addition of BTA should reduce the MRR. The results illustrated in Fig. 6-1 show that addition of BTA does reduce the MRR cf copper during polishing.

Effect of variation of slurry flow rate variation on average MRR in Cu-CMP

Slurry flow rate is a key parameter when the transport mechanisms beneath the wafer are considered [26, 66]. Inadequate slurry flow rate might give rise to problems such as flash heating due to friction,

scratching due to lack of lubrication otherwise facilitated by the slurry flow. Overall, slurry flow causes flushing of abraded products from the wafer pad interface.

The removal rate of copper should increase with increase in the slurry flow rate, due to an increase in the flushing action of the slurry.

The effects of all the above slurry chemistry parameters on the average MRR are illustrated in Fig. 6-1. The y-axis is the difference in the values of average MRR for each of the slurry chemistry parameter.

Chapter 7: Sensor Signal Analysis and Feature Extraction

As detailed in the experimental section, we incorporated vibration sensors in the polishing machine to aid in process modeling and monitoring capabilities. The sensor data acquired is analyzed in the time and the frequency domain. Pertinent features are extracted from the sensor signal and used to model the process performance as well as track variations in the process parameters.

Fig. 7-1 shows a time series of the wired sensor signal and Fig. 7-2 shows the frequency domain representation of the wired sensor signal for treatment condition R 11 (see Table 5-1). Similar data is also acquired from the wireless vibration sensor. The only difference, as stated earlier, is that, the wireless sensor samples at a lower sampling frequency of 500 Hz. Fig. 7-3 shows a time series of data acquired from the wireless sensor signal and Fig. 7-4 shows the frequency domain representation of the wireless sensor data.

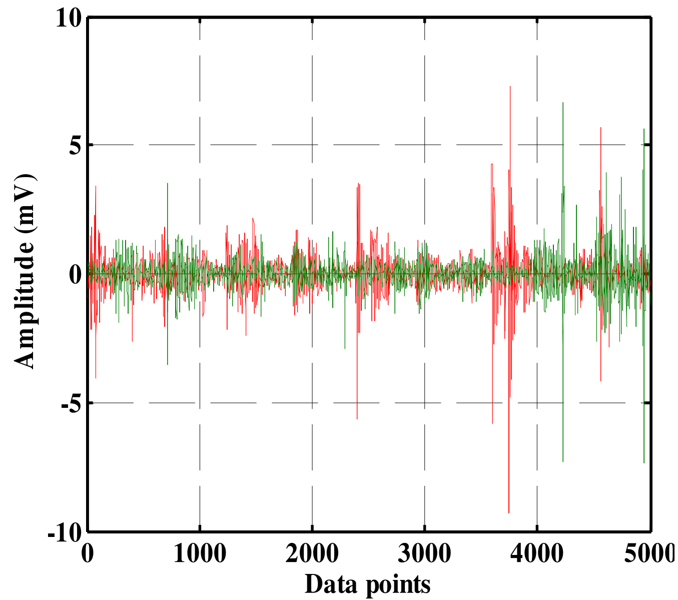

Fig. 7-1: Time series representation of wired sensor data for treatment condition R11 (pH = 5, down pressure = 1 psi, slurry flow rate = 50 ml/min, complexing agent content = 20 gms/lit. BTA content = 0 gm). Red: Polish start, Green: Polish end

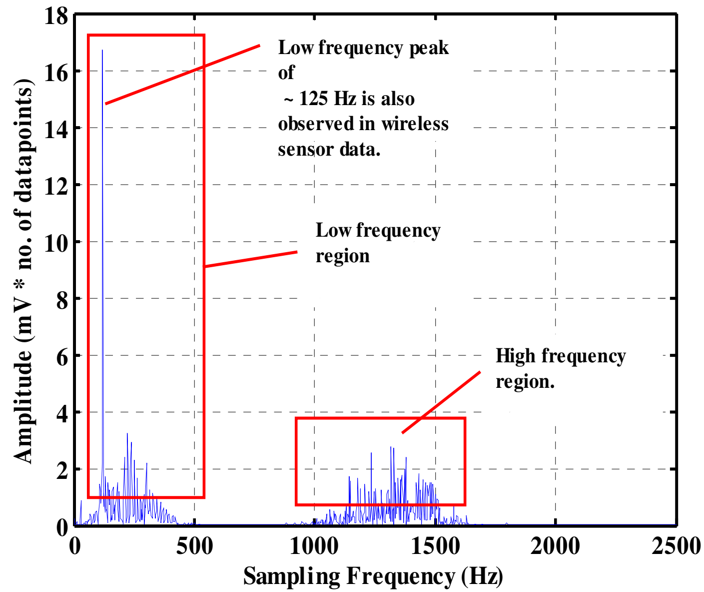

Fig. 7-2: Frequency domain representation of wired vibration sensor signal for treatment condition R 11.

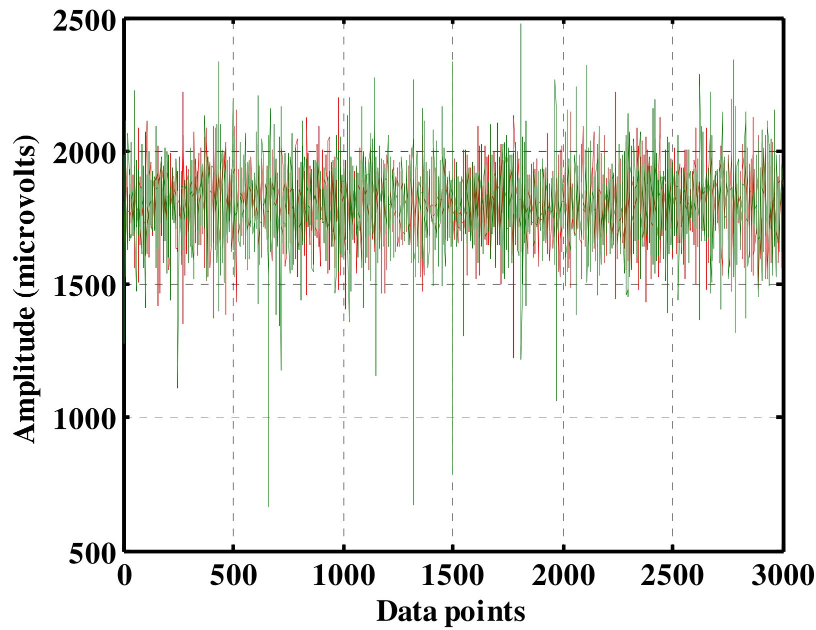

Fig. 7-3: Time series data from wireless vibration sensor signal for R 11 (Red: Polish start, Green: Polish end)

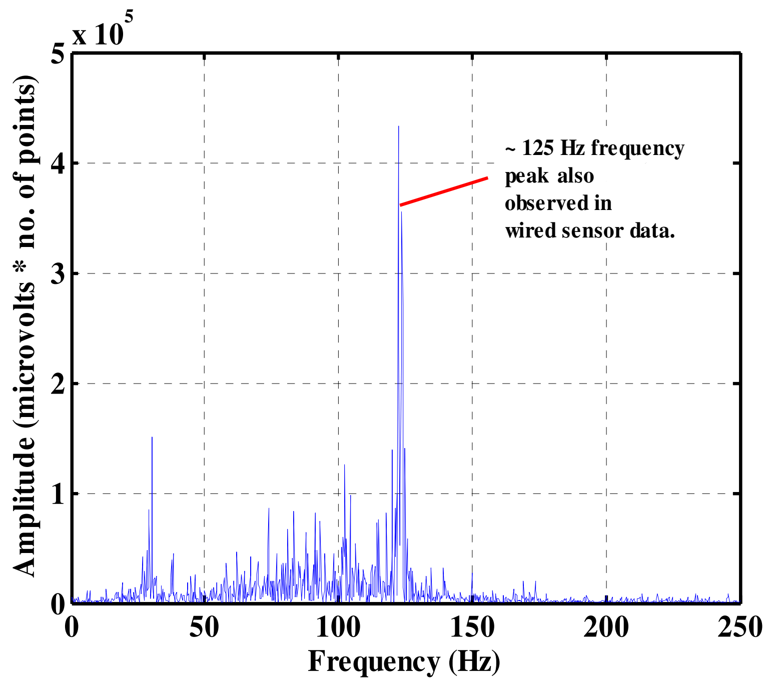

Fig. 7-4: Frequency domain representation of the wireless vibration sensor signal for treatment condition R 11.

Salient features are extracted from both wired and wireless sensor signals. Table 7-1 lists eight candidate features extracted from wired vibration sensor signal and Table 7-2 lists all the six candidate features extracted from the wireless vibration sensor signal. Some features listed in Tables 7-1 and 7-2 are extracted from the time series of the sensor signal while others are extracted from the frequency domain of the sensor signal.

Table 7-1 : Candidate feature matrix for wired sensor signal for treatment condition R 11

PTP (mV)	std dev	Freq 1 (Hz)	Energy in Freq 1 (mV^2)	Freq 2 (Hz)	Energy in Freq 2 (mV^2)	Skewness	Kurtosis
6.564	0.420	119.62	422.323	1343.50	44.768	-0.0504	9.763
15.475	1.023	328.57	96886.91	1413.57	626.218	-0.245	16.942
16.478	1.179	219.72	119087.23	1279.09	1063.954	-0.162	12.164
15.574	0.779	229.28	4511.189	1317.34	197.737	0.102	18.194

Polishing Time, (sec)	MRR, (mg/sec)
20	0.43
40	0.605
60	0.0245
80	0.02575

Table 7-2 : Candidate feature matrix for wireless sensor signal for treatment condition R 1

PTP (μV)	std.dev.	Freq 1 (Hz)	Energy in Freq 1 (μV^2)	Skewness	Kurtosis
1112.5	101.1529	123.41	1.0397E+12	-0.3201	2.097437
1994	103.6296	123.04	1.0114E+12	1.6820	20.0108
1209.5	100.5716	123.77	2.3009E+12	-0.0139	2.30975
853.5	87.35064	121.70	1.3463E+12	-0.0143	1.658281

Polishing Time (sec)	MRR, (mg/sec)
20	1.406
40	0.78
60	0.715
80	0.583

Machine settings for R1 are: pH = 3, down pressure = 1 psi, slurry flow rate = 50 ml/min, complexing agent content = 0 gms/lit. BTA content = 0 gm.

For example, the peak-to-peak amplitude (PTP) is extracted from the time domain analysis of the signal, while Freq1 (which refers to the first dominant frequency peak of the signal) is extracted from the frequency analysis of the sensor signal. The features extracted from the wired sensor are: PTP, standard deviation, first predominant frequency (Freq1), energy under Freq1, second predominant frequency (Freq2), energy under Freq2, signal skewness, and kurtosis. While the features extracted from the wireless vibration sensor are PTP, standard deviation, predominant frequency (Freq1), energy under Freq1, signal skewness and, kurtosis.

Chapter 8: Process Modeling using Response Surface Analysis

Based on the experimental and sensor data collected, three types of regression models are investigated. The response/predictor variables of these three models are as follows:

Model (1): Response variable is MRR and predictor variables are the process parameters (machine and slurry chemistry settings).

Model (2): Response variable is MRR and predictor variables are the sensor features.

Model (3): Response variables are the machine settings and predictor variables are the sensor features.

For model (1), the response surface analysis is conducted using the four original machine settings, namely, slurry pH, complexing agent content of the slurry, slurry flow rate, and BTA content as predictor variables. From the data analysis in Section 5, it can be seen that a total of 14 sensor features are extracted from the time series data recorded by the two sensors. If we directly apply the response surface methodology which takes the 14 sensor features as predictor variables, we may come up with a complex model with a large number of parameters. In order to

address this problem, the principal component regression (PCR) is used to fit a more compact model while still maintaining high predictability.

PCR is a technique used to combat multilinearity issue of the predictor matrix which is composed of a number of runs of predictor variables at different levels. This method uses the principal component analysis (PCA) [67] to transform the original predictor variables into a new set of orthogonal variables, called principal components. Subsequently, the new orthogonal variables are ranked in terms of their importance. After eliminating the least important principal components, a regression analysis of the response variable, based on reduced set of principal components is performed using ordinary least squares estimation. Details of PCR can be found in Ref. [68].

In order to apply PCR, PCA is carried out first on the predictor matrix which is composed of the original 14 sensor features obtained at different levels of process parameter settings. Thereafter, nine “key” features (principal components) remain which are significant (keeping 95% of the original variation) in capturing total variation. These key features are used to build a regression model for average MRR and formulate regression models to track variations in the machine settings, viz. pH of polishing slurry, complexing agent content, BTA content and slurry flow rate.

After conducting principal component analysis (PCA) on the data, the following nomenclature is used: (1) W_1 to W_4: the principal features extracted from the wired vibration sensor data, and (2) WL_1 to WL_5: the principal features extracted from the wireless vibration sensor data.

The model performance is evaluated using such methods as R^2, $R^2_{adjusted}$ and $R^2_{predicted}$. Here, R^2 is that statistic which gives information about the goodness of the fit of the regression model given by the equation:

$$R^2 = 1 - (SSE/SST)$$

Here, SSE is the sum of the squares of the differences of the predicted values and the grand mean. SST is the sum of the squares of the difference of the dependent variable and its grand mean. $R^2_{adjusted}$ is a modification of R^2 that adjusts for the number of predictor terms in a model. Unlike R^2, the $R^2_{adjusted}$ increases only if the new term improves the model more than would be expected by chance. The $R^2_{adjusted}$ can be negative, and will always be less than or equal to R^2. $R^2_{predicted}$ is used in regression analysis to indicate how well and accurate the model predicts responses for new observations. In contrast, R^2 indicates how well the model fits the given data. $R^2_{predicted}$ prevents over-fitting of the model and can be more useful than $R^2_{adjusted}$ for comparing models because it is calculated using observations not included in model estimation. A

detailed discussion of the results from the three aforementioned regression models is given in the following subsections.

8.1 Model 1: Modeling Average Material Removal Rate (MRR) with Process Parameters

Average Material Removal Rate (MRR) is fitted using response surface analysis against the process parameter settings, namely, pH of slurry, complexing agent content, BTA content, and slurry flow rate. Two way interactions between process parameters, which can be important in the prediction of MRR, are also incorporated in the model. For e.g., in Cu-CMP practice the interaction between the pH and the action of the complexing agent is important [55].

Table 8-1 : Regression model of MRR with machine settings with two way interactions (R^2 = 94.2%, $R^2_{adjusted.}$ = 92.2%m $R^2_{predicted}$ = 88.47%)

Predictors	p - val
constant	0
Time	0.224
pH	0
Flow Rate (Fl)	0.021
Complexing Agent (CA)	0

Predictors	p - val
BTA	0
Time*CA	0.003
Time*BTA	0
pH*CA	0.002
Fl*CA	0

Regression coefficients are given in Table 8-1. Fig. 8-1 shows the normal probability plot for the regression model of MRR with machine settings and key interactions between them. Although its direct influence

is minimal, as gathered from a large p-value, Flow rate term is retained in the model because it forms part of a significant interaction term.

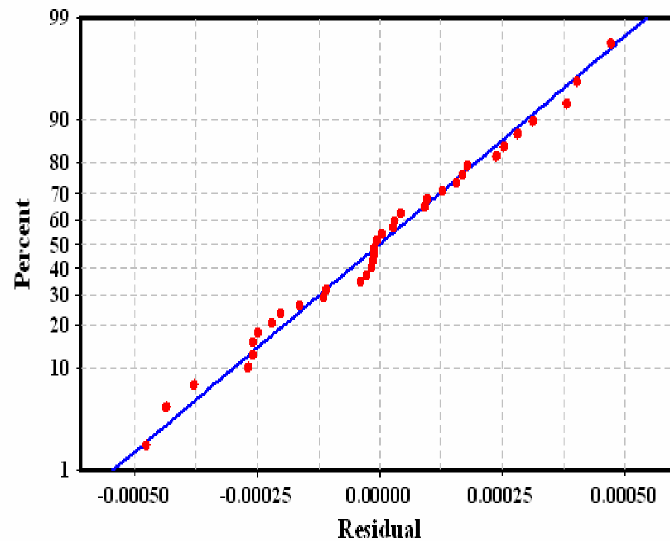

Fig. 8-1 : Normal probability plot of residuals for regression model of MRR against machine settings only namely, slurry pH, complexing agent content of slurry, BTA content and slurry flow rate.

It can be seen from Table 8-1 that a high predictability ca be achieved by response surface techniques. The model not only gives a high goodness of fit for the experimental data but also gives high predictability (~88%) for predicting average MRR for any given machine setting combination. The high $R^2_{predicted}$ value validates the fact that this model holds good for values of machine settings other than those tested in this investigation.

8.2 Model 2: Modeling average MRR with Key Sensor Features

Average MRR is fitted against key sensor features and their significant two way interactions. The aim here is to monitor the Cu-CMP process independent of the machine settings. The model though has a large (24) number of terms; it can be effectively used to monitor the MRR of the process. This also establishes the effectiveness of incorporating sensors in Cu-CMP process. Table 8-2 lists various terms and their p-values in the regression model with key sensor features.

Table 8-2 : Regression model of average MRR with key sensor features and two way interactions (R^2 = 97.7%, $R^2_{adjusted}$ = 92.66%, $R^2_{predicted}$ = 65.84%)

Predictor	Coefficient	p-val
Constant	0.000942	0.981
W1	-0.005502	0.003
W2	0.000979	0.028
W3	0.002464	0
W4	-0.002647	0.027
WL1	0.006323	0.009
WL2	0.002488	0.002
WL3	0.011006	0
WL4	-0.003465	0.017
WL5	0.007973	0.002
W1*W4	-0.009447	0
W1*WL1	0.010952	0.005
W1*WL3	0.018177	0.002

Predictor	Coefficient	p-val
W1*WL4	-0.008851	0.002
W1*WL5	0.01149	0.004
W2*WL3	-0.006772	0.002
W2*WL5	-0.001512	0.484
W3*WL4	0.002502	0.003
W4*WL4	-0.002401	0.004
WL1*WL2	-0.00131	0.337
WL1*WL4	-0.00626	0
WL1*WL5	0.005988	0
WL2*WL3	0.004771	0.012
WL2*WL5	0.007821	0
WL4*WL5	-0.000537	0.446

MRR=Constant-0.005502*W1+0.000979*W2+ …… -0.000537*WL4*WL5

The use of sensor signals for modeling the process performance, here MRR, has been proven effective. Good predictability is achieved from the model. Also this model turns out to be fairly predictive for data other than that tested in this investigation owing to the modest $R^2_{predicted}$ achieved from the model.

8.3 Model 3: Modeling the Variation in Machine Settings using the Sensor Data

As stated earlier, monitoring of the process variables is one of the objectives of this study. It is important to monitor these variations as small drifts can cause significant variation in the output or efficiency of the process. For instance, the etching behavior of copper can drastically change with decrease or increase in the pH of the polishing slurry [1, 48]. The dissolution rate of oxides also varies with pH [47]. In the pH range considered here, cupric oxide is less soluble than cuprous oxide [46]. The complexing action of citric acid also varies drastically with change in the pH value [55].

Non-native film formed due to addition of BTA also plays a pivotal role in how efficiently the planarity is achieved. The key to success for dissolution based slurries with an inhibitor lies in the fact how efficiently the film is formed and how thick and integral the film is. The dissociation of BTA in any solution is pH dependant. The point being that all the machine settings are highly interrelated [2].

8.3.1 Modeling variations in slurry pH using key sensor features

Table 8-3 shows various terms in the regression model and their respective p–values for slurry pH using key sensor features obtained after conducting PCA on the candidate features only.

Table 8-3 : Regression model of pH of Polishing slurry with key sensor features and two way interactions (R^2 = 99.8%, $R^2_{adjusted.}$ = 99.12%, $R^2_{predicted}$ = 72.81%)

Predictor	Coefficient	p-val
Constant	1.6558	0
W1	-2.1954	0
W2	-0.213	0.624
W3	-0.4661	0.023
W4	-7.1823	0
WL1	6.3187	0
WL2	-4.9894	0
WL3	-1.0112	0.055
WL4	-1.1548	0
WL5	-0.1724	0.692
W4*W4	-3.4289	0
WL5*WL5	-1.6145	0
W1*W2	-5.1139	0
W1*WL1	7.9113	0

Predictor	Coefficient	p-val
W2*W4	6.3849	0
W2*WL3	-7.1305	0
W2*WL4	-1.7246	0.002
W3*WL2	-3.4001	0
W3*WL5	1.554	0.001
W4*WL1	7.3523	0
W4*WL3	4.7544	0
W4*WL4	-1.1951	0.026
W4*WL5	-1.3933	0.047
WL1*WL2	5.9046	0
WL1*WL4	5.1372	0
WL1*WL5	-2.5463	0
WL2*WL3	-5.5969	0
WL2*WL4	5.8692	0

pH = Constant-2.1954*W1-0.213*W2 ……+5.8692*WL2*WL4

Although the number of terms in the model is high (27), it is useful in the context of simultaneous process monitoring, i.e., the same feature combination is effective in tracking other setting as discussed further.

The sensor data is very effective in tracking the variations in polishing slurry pH. Excellent goodness of fit is observed as seen from the very high regression coefficient. The model also has a good predictability, as seen by the modest $R^2_{predicted}$ (~72%) achieved from the model.

8.3.2 Modeling variations in complexing agent content using key sensor features

Variations in complexing agent content of the polishing slurry are linearly regressed with the sensor data only. Table 8-4 shows various terms and their respective p-values in the regression model. As is the case with the pH model, the number of terms is again high (28) but it can be very effectively used for *in-situ* monitoring of variations in the complexing agent content in the slurry.

As stated in the literature review, the concentration of complexing agent content in the polishing slurry drastically affects the MRR of copper. It also has a strong interdependence on the slurry pH and oxidizing agent content of the slurry. To the best of the author's knowledge, till date no commercial sensors are available which can effectively track the variation of complexing agent content in the slurry. From the model given in Table 8-4, the sensor data is very effective in

tracking the variation in the citric acid content of the polishing slurry. Citric acid is one of the most preferred complexing agent used in Cu-CMP slurries.

Table 8-4 : Regression model of complexing agent in polishing slurry with key sensor features and two way interactions in between them (R^2 = 99.96%, $R^2_{adjusted}$ = 99.78%, $R^2_{predicted}$ = 92.73%)

Predictor	Coefficient	p-val
Constant	-13.236	0
W1	62.081	0
W2	211.363	0
W3	-40.665	0
W4	-90.385	0
WL1	4.014	0.006
WL2	-45.381	0
WL3	128.896	0
WL4	37.233	0
WL5	37.824	0
W1*W1	137.628	0
W2*W2	-64.141	0
W4*W4	-50.246	0
WL2*WL2	-43.08	0
WL3*WL3	-34.454	0

Predictor	Coefficient	p-val
W1*W2	106.245	0
W1*W3	-62.212	0
W1*WL2	17.741	0.003
W1*WL3	133.496	0
W2*W3	82.338	0
W2*W4	88.929	0
W2*WL1	-38.387	0
W2*WL3	-159.726	0
W3*W4	-18.797	0
W3*WL3	-16.27	0.001
W4*WL1	48.553	0
W4*WL2	-50.13	0
W4*WL3	97.368	0
WL2*WL4	143.309	0

Complexing agent=Constant+62.081*W1+211.363*W2...

...+143.309*WL2*WL4

The model not only effectively tracks the variations in this investigation (as seen from an excellent regression coefficient of ~99%), but also has a very good predictability for the data which is beyond that examined in this investigation (which can be seen from the very high R^2predicted value of ~92%).

This model can be used a building block for constructing more dynamic models which can be used for predictive modeling of slurry chemistry drifts which can predict in-situ upcoming changes, hence helping in taking proactive actions to prevent the consequences arising from these drifts.

8.3.3 Modeling the BTA content using key sensor features

BTA content used in the slurry is on the order of milligrams per liter of the solution. Sensing and monitoring of the BTA content *in-situ* is a difficult task. It needs control, as small drifts or changes in the BTA content changes the film formation dynamics on the bare copper surface quite drastically. Along the same line as the models for pH and complexing agent, BTA content of the polishing slurry is linearly regressed against sensor features. This model provides a reasonable fit, R^2 = 90.21%, $R^2_{adjusted}$ = 81.97%.

Table 8-5 shows various terms and their respective p–values in the regression model. Although the number of terms in the model is

significantly high (16), the predictability achieved is appreciable, especially as there are no sensors known to track the variation in BTA content in the slurry.

Table 8-5 : Regression model of BTA against key sensor features and two way interactions in between them (R^2 = 90.21%, $R^2_{adjusted}$ = 81.97%, $R^2_{predicted}$ = 58.14%)

Predictor	Coefficient	p-val
Constant	-1.4326	0
W1	-1.4178	0
W2	-0.5938	0.071
W3	4.0635	0
W4	-2.6194	0
WL1	-0.1268	0.356
WL2	-0.4223	0.018
WL3	0.7584	0
WL4	-0.2186	0.048

Predictor	Coefficient	p-val
WL5	-0.5565	0
W2*W2	0.8727	0.001
W3*W3	1.0486	0.007
W1*W3	7.3137	0
W1*W4	-2.4383	0.001
W2*W3	-2.7303	0
W2*WL3	-1.0195	0.059
W3*WL1	0.6037	0.007

BTA = Constant-1.41*W1-0.5938*W2...+0.6037*W3*WL1

A change of few milligrams of BTA in the slurry can shift the performance of the process by a large value. The content of BTA in the slurry is even more critical as it directly affects the slurry stability, which in turn can be damaging considering the damage inflicted by agglomerate formation on the overall surface quality by means of scratched surface, damaged dielectric layer and so on so forth.

8.3.4 Modeling slurry flow rate variations using key sensor features

Slurry flow rate becomes an important factor when considering the tribology at the wafer-pad interface. It plays a significant role in determining the transport of reacting species uniformly beneath the wafer. This, in turn, determines the reactions that would take place and the removal of reaction products (or debris) from the reaction site [66, 69, 70].

Table 8-6 : Regression model of variation in slurry flow rate with key sensor features and two way interactions between them (R^2 = 86.31%, $R^2_{adjusted}$ = 78.22%, $R2_{predicted}$ = 64.65%)

Predictor	Coefficients	p-val
Constant	6.658	0.566
W1	-94.012	0
W2	-82.684	0
W3	-17.966	0.01
W4	-59.678	0
WL1	35.631	0.001
WL2	-11.127	0.231

Predictor	Coefficients	p-val
WL3	-30.659	0
WL4	21.325	0.007
WL5	31.515	0.001
W1*W2	-105.163	0
W4*WL1	97.572	0
WL3*WL4	-69.637	0
WL3*WL5	-76.796	0.001

Flow rate = Constant-94.012*W1-82.684*W2…-76.796*WL3*WL5

The variation in the flow rate is linearly regressed with sensor features only. Any change in the slurry flow rate is predicted with good

accuracy by the model. Table 8-6 gives regression model of the slurry flow rate with sensor features.

Chapter 9: Electrochemical Polishing of Copper

All machining processes that rely on chemistry and a DC power source for material removal work on the basic principles of the simple electrochemical cell and Faraday's law that governs the cell. A brief description of a simple electrochemical cell and pertinent definitions are given below. As a matter of fact electrochemical machining (ECM) is controlled and intentional corrosion of metal surfaces to get high quality surfaces as well as remove excess material from areas of interest.

When the oxide free surface of a metal becomes exposed to an oxidizing solution, positively charged metal ions tend to pass into the solution, leaving behind electrons behind in the metal.

$$M \rightarrow M^{n+} + ne^-$$

The accumulation of negative charge on the metal due to the residual electrons leads to an increase in the potential difference between the metal and the solution. This potential difference is called the electrode potential, which then becomes more negative. The change in the potential tends to retard the dissolution of metal ions and encourages the deposition of dissolved metal ions from the solution onto the metal. Continuation of the dissolution and deposition of metal ions would result in the metal reaching a stable potential such that the rate of dissolution

becomes equal to the rate of deposition. This potential is termed as reversible potential and its value depends on the concentration of dissolved metal ions and the standard reversible potential for unit activity of metal ions in the solution. This potential can be calculated using the Nernst equation for non unit concentrations of dissolved ions.

In practical corroding solutions the scenario is different. The potential of a metal in a solution does not often reach the reversible potential but remains more positive because electrons can be removed from the metal by alternative reactions i.e. the excess electrons generated due to dissolution of metal ions are taken away by "electron acceptors". In acid solutions, electrons can react with hydrogen ions adsorbed on the metal surface from the solution to produce hydrogen gas.

$$2H^+ + 2e^- \rightarrow H_2$$

The occurrence of the above reaction permits the continued passage of an equivalent quantity of metal ions into solution i.e. there is always a way for electrons generated on the metal surface to be accepted. This means that instead of metal depositing by reaction if metal ions from the solution and electrons on the metal surface, the metal ions just dissolve and electrons are taken away by the hydrogen evolution reaction. This, leads to corrosion of metal.

In neutral solutions, the concentration of hydrogen ions is too low for hydrogen evolution to take place, but electrons in the metal can react

with oxygen molecules adsorbed on the metal surface from air dissolved in the solution to produce hydroxyl ions.

In electrochemical terminology, an electrode at which an oxidation reaction occurs is called an anode. The process of oxidation involves loss of electrons by the reacting species. An electrode at which a reduction reaction occurs is called a cathode. Reduction involves a gain of electrons. The reduction of hydrogen ions and oxygen are known as reduction reactions.

Typically a simple electrochemical cell consists of an anode which donates electrons or oxidizes. These electrons are consumed by the cathode which accepts these electrons and undergoes reduction. This combination of corrosion process (anodic reaction) of the metal dissolving as ions generates some electrons, which are consumed by a secondary process (cathodic reaction). These two processes have to balance their charges. The sites hosting these two processes can be located close to each other on the metal's surface, or far apart depending on the circumstances [71].

The current semiconductor fabrication scenario enables industry to use conventional CMP techniques for polishing the overburden. But as the industry makes inroads into the 32 nm era, alongwith incorporation of low-k dielectrics for reduced time lags, the limitations of CMP become more evident. These constraints are as follows:

1. To reduce the time lag that is accompanied with miniaturization of circuitry, a possible alternative suggested is to use low-*k* dielectrics.
2. These dielectrics are inherently soft and porous. The mechanical strength associated with these materials is very low and the structural integrity is lost at much lower forces than the current materials being used.
3. Hence, the forces that are involved in conventional CMP process tend to damage the low-k dielectric materials being used.

This calls for a much more 'soft' approach for polishing than CMP. A possible method being suggested is electropolishing of copper in various chemical slurries. This method almost completely eliminates the mechanical aspect of the process. The fundamentals of this process are the same as electrochemical machining. It is controlled dissolution of a metal into reacting slurry facilitated by the application of anodic overpotential.

Concentrated phosphoric acid-based slurries have been used to realize electrochemical polishing of copper [72, 73]. Conventional electropolishing processes are realized beyond the current density where the dissolution is dependant on the rate of mass transfer of a reactant to or from the surface being polished. This mass transfer limiting rate is a function of viscosity of the electrolyte, the diffusion coefficient of the

reactant and the convection conditions present in the polishing bath. When performing electropolishing at this mass transfer limiting region, the peaks on the electrode surface are polished preferentially as they are more accessible to the bulk solution [74]. Formation of a diffusion layer above the surface to be polished is a key step in copper electrochemical planarization. In fact the ability to achieve planarity is almost in entirety depends upon the dynamics of formation of this boundary layer. The schematic shown in Fig. 9-1 depicts the mechanism by which planarity is achieved in copper electrochemical polishing. The peaks on the profile have easy access to the bulk slurry, and are reacted upon preferentially. Once the first peak is dissolved, the next highest regions on the profile get reacted upon. This way over a period of time planarity is achieved.

To elucidate the mechanism by which planarity is achieved in copper electrochemical polishing, consider the system analogous to a resistance path for the slurry reactants. The path of highest resistance will be removed the least, while the parts that have the least resistance shall be removed preferentially. The schematic of which is as shown in Fig. 9-2.

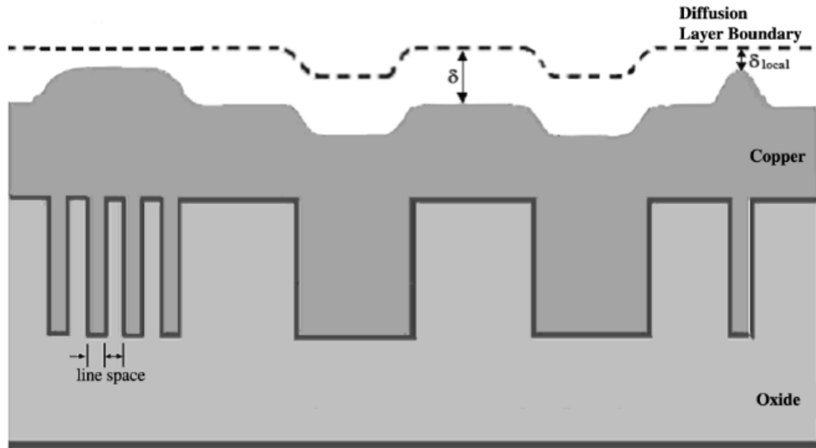

Fig. 9-1: Schematic of Copper overburden electropolishing [75].

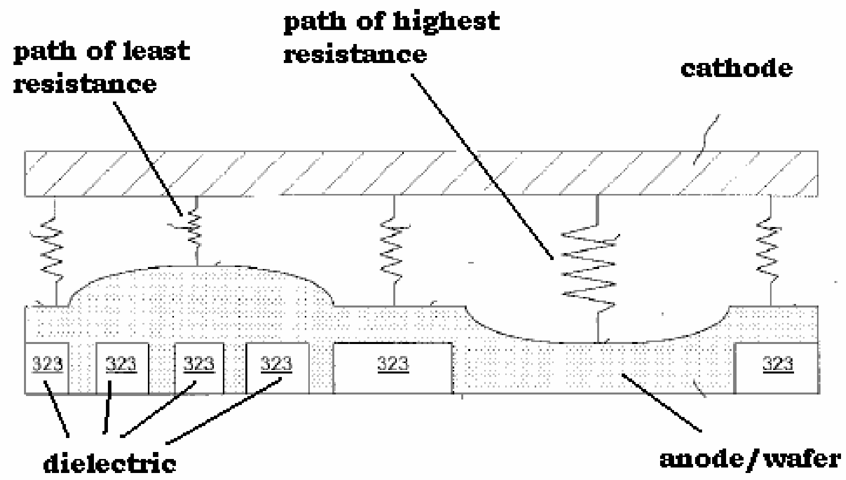

Fig. 9-2: Schematic illustrating the analogy behind achieving planarity during copper electrochemical polishing [76].

Fig. 9-3 illustrates the potentiodynamic behavior of copper in phosphoric acid slurry used in electrochemical polishing. In the initial stages (region A-B) as the anodic potential is increased, there is a rapid increase in the corrosion current flowing through the system. Further increase of anodic voltage (region B-C) gives rise to a reduction in the polishing currents. This indicates a start of the formation of a resistive film or layer over the surface to be polished. From the pattern of corrosion current the resistance of the film formed increases with further increase in anodic voltage. Inherently the corrosion current remains constant in this region (region C-D). This is the region of interest, and from the surface profile plots, it can be seen that the surface is highly bright and polished in this region than in any other region. Further increase in the voltage induces anodic reaction of oxygen evolution, this cause intense pitting on the surface of copper sample being polished. The damaged surface is portrayed in the last surface plot shown in Fig. 9-3.

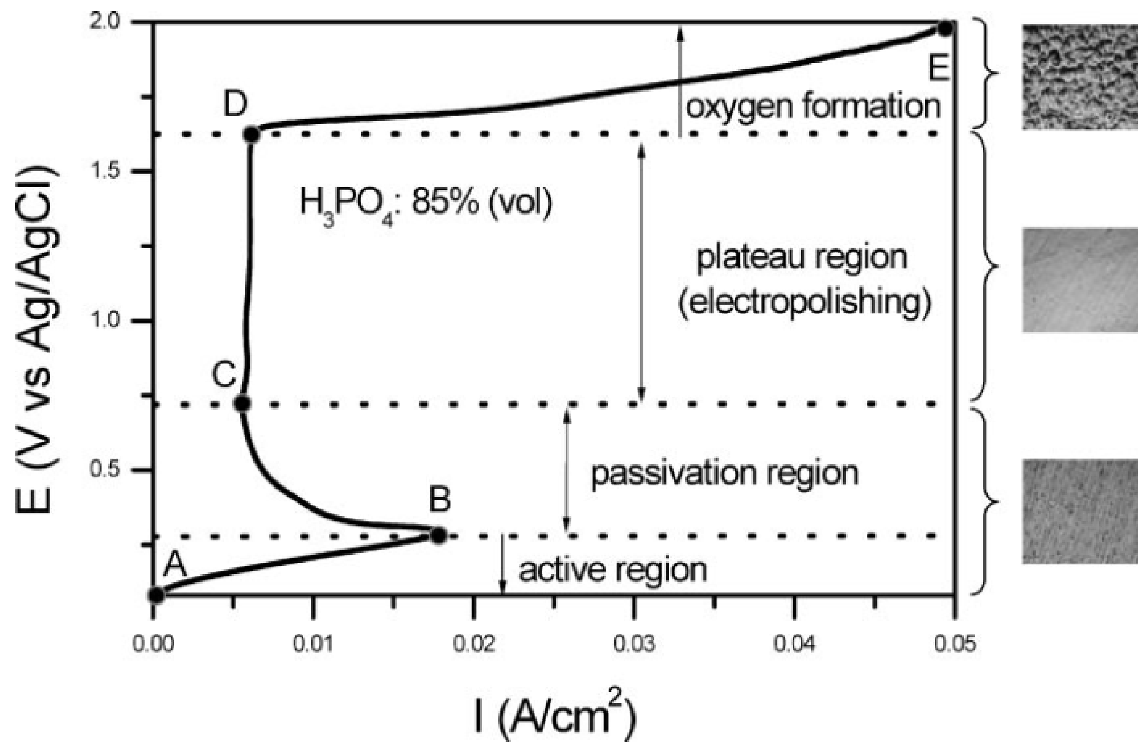

Fig. 9-3: Various regions of copper electropolishing; the constant current plateau is the region of interest where actual surface improvement is taking place [77].

Anodic polarization of metallic surfaces at low potentials causes dissolution at preferred crystallographic locations, such as grain boundaries. This results in etching and consequently dulling of the wafer surface. During etching, anodic current densities increase with increasing potential by an activation polarization relationship. If the anodic overpotential is increased beyond a certain threshold, the anodic current density stops increasing or becomes insensitive to the variations in the anodic potential. This threshold current density depends on various factors viz. solubility of dissolving species in the particular

electrolyte, the concentration, temperature, the diffusion coefficient, and fluid dynamics conditions prevalent. After this threshold is attained the dissolution of metal surface is controlled by mass transfer through the surface boundary layer. If the outer boundary layer were smooth, then the peak points on the metal surface would oxidize preferentially as they are more accessible to the bulk solution resulting in the generation of a smooth and shiny surface. If the potential is increased further, oxygen evolution reactions start and are marked with an increase in the current density.

Electropolishing of bulk copper is drastically different from planarization of thin copper films for ULSI applications. Here, the disparity in topography is significant in proportion to the thickness of the copper film. As stated above, electropolishing occurs only when a boundary layer is established over the virgin metal surface. Hence the amount of copper dissolution required to form this boundary layer dictates how effective electropolishing the surface would be [78].

Two mechanisms are proposed for the existence of the mass transport limited for the progress of the electropolishing process:

1. Salt film mechanism.
2. Acceptor mechanism.

A brief discussion of these two mechanisms is given in the following:

Salt Film Mechanism

Metallic ions accumulate near the electrode surface until the solubility of the salt is exceeded. At this instance a new phase nucleates and a salt film precipitates on the electrode surface. In the presence of this film the concentration of cationic and anionic components of the salt are determined by their solubility product, and the dissolution rate is subsequently dictated by mass transfer of the metallic ions from the film/electrolyte interface to the bulk solution. The schematic of the salt film mechanism is as shown in Fig. 9-4.

Iron polishing in sodium chloride solution is an ideal experimental validation of the salt film mechanism. During iron electropolishing the ferrous ions at the electrode surface increase until the solubility limit for ferrous chloride is exceeded. Once this limit is exceeded a salt film precipitates.

Acceptor Mechanism

A schematic of acceptor mechanism for the formation of diffusion limiting layer is as shown in Fig. 9-5. This mechanism is more suitable for the Cu/phosphoric acid polishing system [73]. In this mechanism, it is hypothesized that the metallic ions must be complexed (by water molecules in case of aqueous electrolytes) before they are transported away from the electrode surface. Thus, the dissolution of metal is limited by transport of the complexing agent to the electrode surface.

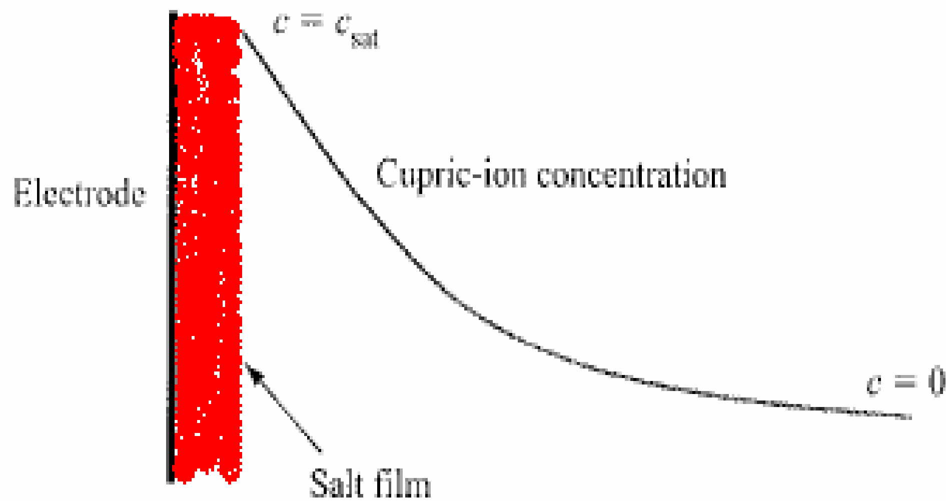

Fig. 9-4: Salt film Mechanism for formation of limiting current density plateau in copper electropolishing [79].

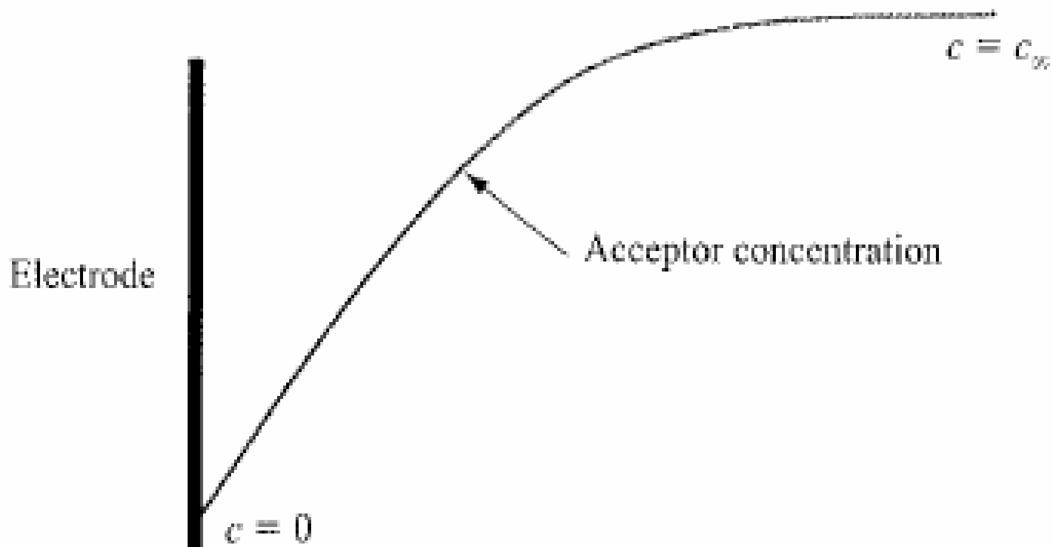

Fig. 9-5: Acceptor mechanism supporting the existence of limiting current density plateau during electropolishing [79].

Copper ECP has its own advantages and limitations. The key merit of this process is that of reduced post-process cleaning issues. As

compared to conventional CMP, where abrasive adhering to the substrate is a key issue which then brings along with it complicated cleaning methods.

Simplistically, average feature sizes at this technological node are 45 nm, while the average abrasive size of α-alumina abrasive particles used is ~50 nm. This means that even a single nano abrasive can cause a damaged feature on the chip. Previous research on post-CMP cleaning mechanisms showed that in non-contact type cleaning mode, removal of particles of sizes 100 nm and below are difficult. Using contact mode for cleaning shows that higher brush speeds are required to remove particulate contaminants remaining on the substrates after CMP [80]. This becomes more detrimental when using soft low-*k* dielectric materials on the microchip.

Another advantage when working with copper ECP is that of easy and effective end point detection. Copper ECP involves precise tuning of process parameters such as polishing voltage which gives a characteristic current waveform for different materials. This current waveform can be monitored to determine when polishing has to be stopped [81]. More specifically, the current density while polishing a copper overburden will be noticeably different than that when the slurry reactants make contact with the dielectric or barrier layer just beneath the copper layer. As soon as this change in current is observed it can be

confirmed that the copper layer has been polished successfully and completely.

Fig. 9-6 shows the logic of easy end-point detection, The sudden drop in polishing current with respect to polishing time is an indicator that copper layer has been polished and that polishing has reached its end.

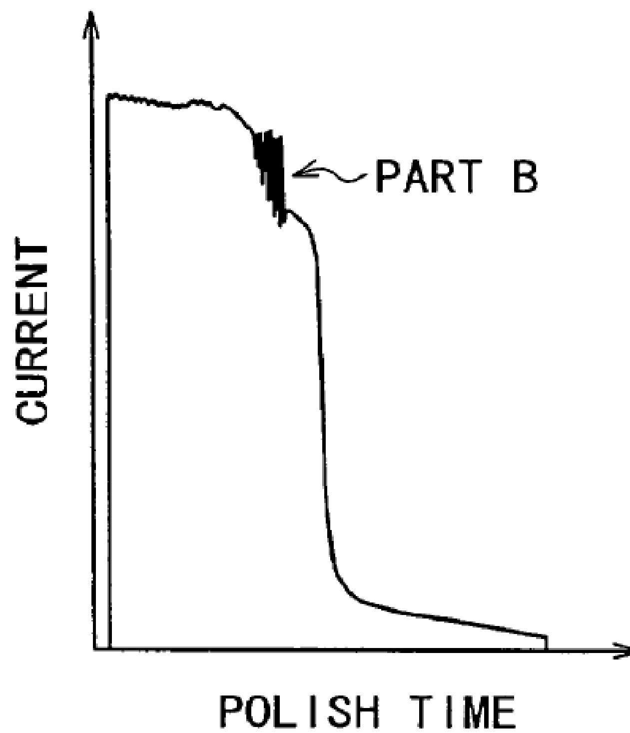

Fig. 9-6: End-point detection during copper ECP [81].

9.1 Effects of slurry chemistry on copper electrochemical polishing

Conventional electrochemical polishing slurry contains the following components:

1. Phosphoric acid.

2. DI water.
3. Ethylene glycol/Polyethylene glycol.
4. Acetic acid.

The concentrations of each of these additives plays a major role in deciding the Material Removal rate (MRR) as well as surface finish (Ra) of the copper wafer. Especially as the conductivity and slurry reactivity is affected drastically with small variation in concentrations. The effect of various slurry components is discussed in the following:

Effect of phosphoric acid content in the slurry

The phosphoric acid content of the slurry determines the conductivity of the slurry. This is a direct measure of the material removal capability of the slurry. The higher the phosphoric acid content of the slurry, the lesser the conductivity and hence lesser the removal rate capabilities [77]. Fig. 9-7 shows the trend of polishing currents with polishing time plotted for varying concentrations of phosphoric acids. It can be seen that for dilute phosphoric acid slurries, the conductivity is very high and hence the pattern of material removal is more on uncontrolled dissolution, hence the surface finish obtained is unacceptable. Severely roughened surface is obtained when polishing with dilute phosphoric acid slurries. But as the concentration of phosphoric acid content in the slurry is increased, the conductivity

drops, also reducing the material removal capability, but this shows a marked improvement in the surface quality produced from polishing.

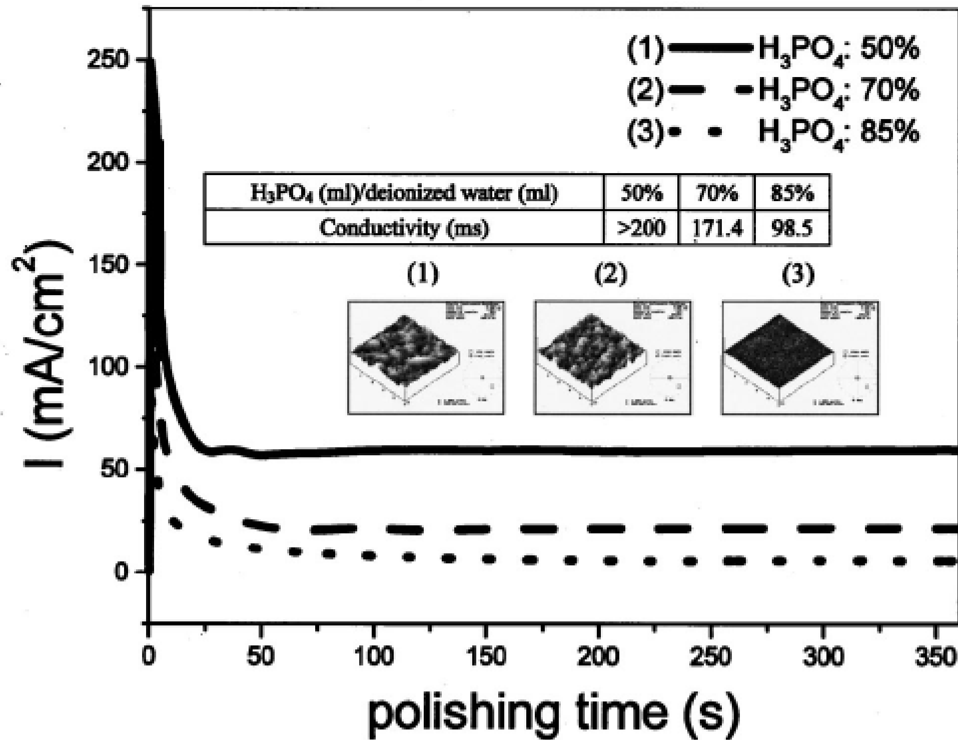

Fig. 9-7: Variation in conductivity of polishing slurries with variation in the content of phosphoric acid and its effect on the surface generated post polishing [22].

The approach suggested here relates to the use of dilute phosphoric acid slurries to facilitate fast material removal in the initial stages of polishing. The results obtained will be discussed in the following sections.

Effect of DI water content in the slurry

As discussed in the previous section of effect of phosphoric acid content of the slurry, DI water content directly affects the dissolution

behavior of copper in phosphoric acid based slurries. As shown in Fig. 9-7, dilution increases the conductivity of the slurry, thus increasing the removal rate of copper in any given slurry. However, excessive dilution might result in a severely pitted surface due to uncontrolled dissolution.

Effect of Ethylene glycol/Polyethylene glycol in the slurry

The most important factor in copper electrochemical polishing is that of tackling oxygen evolution reaction taking place at higher anodic potential. Huo *et al.* [82] show that addition of ethylene glycol results in drastic improvement in the attained surface roughness of the polished copper sample. The results presented in this investigation also agree with the findings of Huo *et al.* [82].

Effect of acetic acid in the slurry

Liu *et al.* [83] investigated the role of multiple additives on damascene copper electropolishing. Behavior of copper in organic acid accelerator and alcohol based phosphoric acid slurries were investigated. A mechanism governing improved planarizing efficiency was proposed. The additives perform the task of reducing the acidity as well as increase the resistance of troughs on the reacting surface. Both these actions inhibit Cu removal, hence improve the surface planarity.

Fig. 9-8 shows a schematic of a mechanism of acetic acid and alcohol based phosphoric acid slurries. These slurries show highest polishing efficiencies. This is especially critical when considering pattern

density and size effects during polishing. As seen from the above section, considerable efforts have been made to investigate the mechanisms and effect of various slurry chemistry effects on process performance.

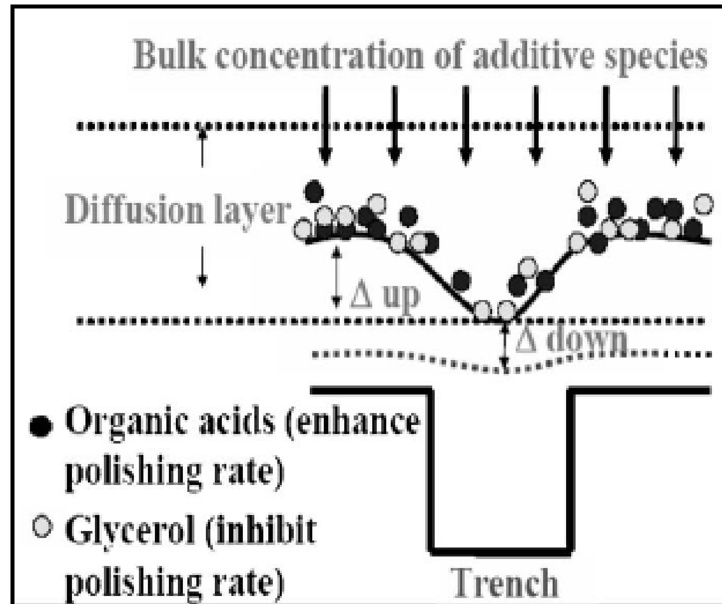

Fig. 9-8: Effect of addition of acetic acid and alcohol on copper electro chemical polishing [83].

But from the process control and process performance monitoring standpoint, no work has been yet performed. In this investigation we mount vibration sensors and analyzed the sensor signal to model the process performance as well as track the variations in the process parameters i.e. the slurry chemistry settings.

9.2 Experimental Apparatus and Design of Experiments

A Buehler Electromet III electropolisher was used to carry out the experiments. Copper samples of 4” diameter are used as samples. The area polished is a central circular region of diameter 1”. The polishing voltage during the experiments was set to a constant value of +1.1 V DC. The primary aim of this set of experiments is to validate the use of vibration sensors to monitor the process dynamics and to study and verify experimentally the effect of variations in the process output (MRR and Ra) with known variations in process inputs (slurry chemistry).

A wireless vibration sensor based on the MOTEiv technology sampling at 500 Hz is mounted on the back side of the wafer, thereby being very close to the actual process can sense even small changes in the process characteristics. Most of the vibrations associated with the ECP process are flow induced vibrations. They can be related to the formation of diffusion limiting layer over the substrate surface and also in some cases initiation of oxygen evolution reaction. We do not have experimental evidence which correlates exactly the vibration patterns to the abovementioned process characteristics. This investigation is aimed at investigating the effectiveness of vibration sensor signals in better estimating the process performance as well as tracking the changes in preset process parameter settings. MRR is arrived by measuring the disc weight after each 1-minute polishing runs. Surface roughness is

obtained by examining the wafer after such 1 minute polishing run under a ADE MicroXAM, a no contact type laser interferometric surface profiler. Surface roughness is analyzed at 6 locations after each 1 minute polishing cycle. Each experimental run consists of 3 such polishing runs. The vibration sensor and the weighing scale are the same as from the previous Cu-CMP experimental setup.

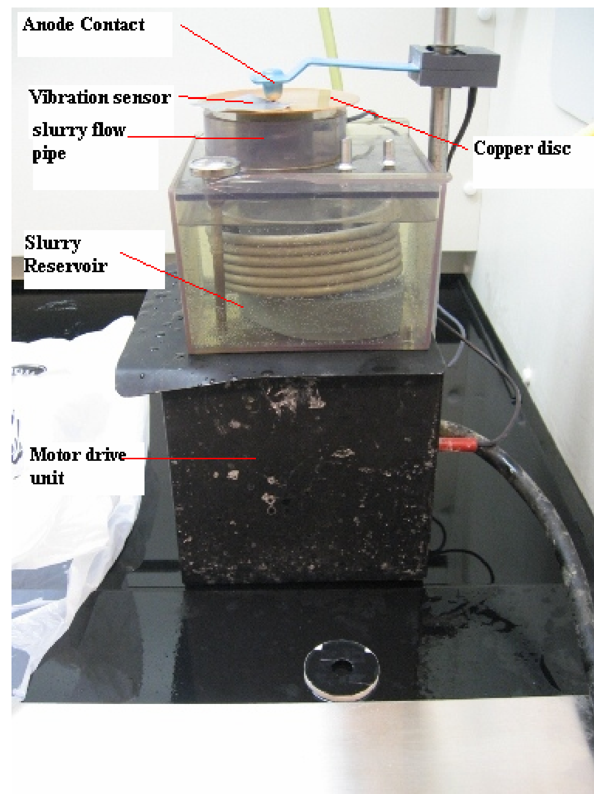

Fig. 9-9: Experimental apparatus used to conduct copper electro chemical polishing experiments.

Design of Experiments

A Taguchi L8 experimental matrix is leveraged to determine the effect of slurry chemistry effects on Material Removal Rate (MRR) and average surface roughness (Ra) during copper electro chemical polishing. The matrix has phosphoric acid, water content and salt content as the factors; the effect of which on MRR and Ra is to be determined. We implemented a L8 matrix here for the reason that we have 3 factors in the matrix and these factors are investigated at two levels i.e. high and low.

Table 9-1: Experimental matrix implemented in copper electropolishing experiments.

Run No.	**Phosphoric Acid**	**Water**	**Copper Sulfate**
R1	L	L	L
R2	L	L	H
R3	L	H	L
R4	L	H	H
R5	H	L	L
R6	H	L	H
R7	H	H	L
R8	H	H	H

Table 9-2: High and low levels of various factors investigated in Copper electrochemical polishing using phosphoric acid slurry chemistry.

Factor	**High**	**Low**
Phosphoric Acid	15 M	10 M
Water	15 M	10 M
Copper Sulfate	0.2 M	0 M

Table 9-1 lists the experimental matrix utilized to carry out the electropolishing experiments, and Table 9-2 lists the high and low values for the factors investigated in Table 9-1. Each polishing run consists of a total of 3 minutes of polishing divided into 3 polish steps of 1-minute duration each. This polishing slurry will be henceforth referred to as "phosphoric acid slurry chemistry".

As acetic acid and alcohol based slurries also showed enhanced polishing efficiencies, a second experimental matrix was formulated to test the effect of ethylene glycol content as well as acetic acid content on the behavior of copper during electrochemical polishing.

Table 9-3: Experimental matrix implemented to study the effect of ethylene glycol and acetic acid content in polishing slurry on copper electrochemical polishing.

Run No.	**Ethylene Glycol**	**Acetic acid**
R1	L	L
R2	L	H
R3	H	L
R4	H	H

Table 9-4: High and low levels of factors investigated in Copper electrochemical polishing using acetic acid slurry chemistry.

Factor	**High**	**Low**
Ethylene Glycol (EG)	300 ml	150 ml
Acetic acid (AA)	90 ml	50 ml

Table 9-3 illustrates the experimental matrix implemented, while Table 9-4 lists the high and low levels of slurry parameters used in the experimental study. The base composition for this slurry was kept constant at 800 ml of phosphoric acid and 100 ml of water. This slurry chemistry shall be henceforth referred to as “acetic acid slurry chemistry”.

Chapter 10: Surface profiles and MRR trends of Copper ECP

Chang *et al.* [77] have shown that with increasing water content in the polishing slurry the conductivity of the electrolyte is increased. This enhances the diffusion of dissolved ions into the bulk thus increasing the limiting current density. This means with higher water content slurries the limiting currents are going to be high thereby giving a high MRR. At high MRR values the planarization capability of the slurry is hampered significantly. Hence, it is recommended that concentrated phosphoric acid slurries are used to attain planarity as well as acceptable MRR values.

Fig. 10-1 shows the plot of average MRR for each treatment condition. Note that R1, R2, R5 and R6 are the conditions where the concentration of phosphoric acid is higher. It can be seen from the plot, that they yield significantly lower MRR than the runs where the phosphoric acid content is lower. These results agree with previous results reported in Ref [84]. Fig. 10-2 shows the surface profiles of an as-received copper disk and after 3 minutes of electropolish for experimental runs R3 and R7 respectively.

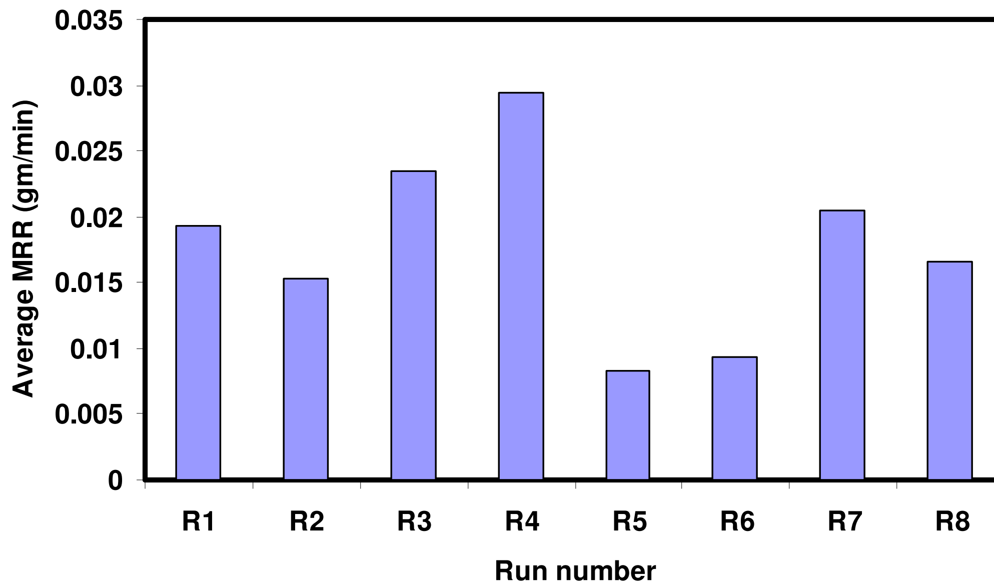

Fig. 10-1: Average MRR for Runs R1 to R8. For Runs with High water content (R3, R4, R7, R8) MRR is higher than that with the corresponding low water content treatment conditions.

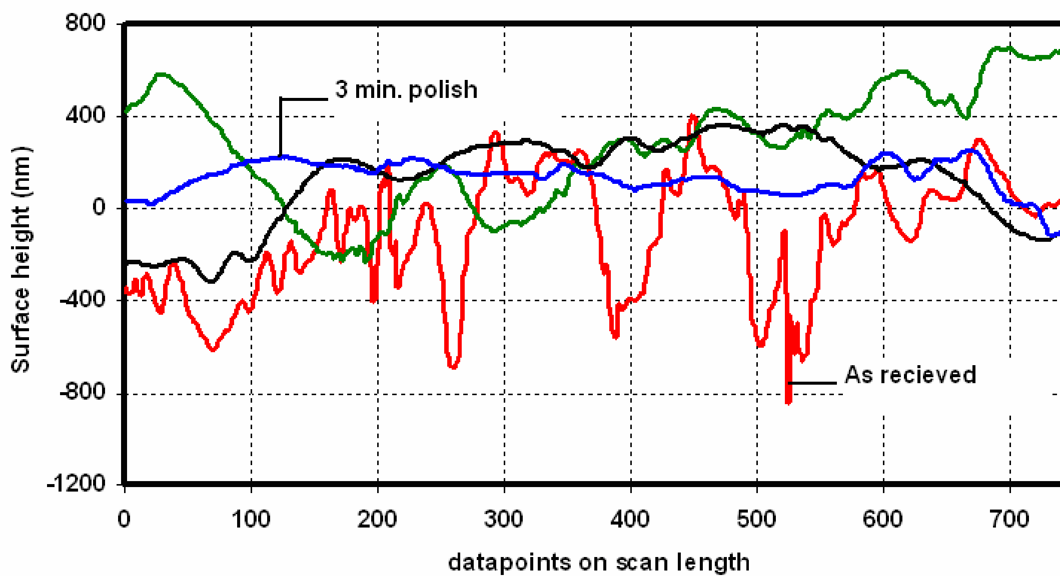

Fig. 10-2: Surface profile plots for treatment conditions R3, Red: As received profile, Green: surface profile after 1 min electropolish, Black: surface profile after 2 min electropolish, Blue: surface profile after 3 min electropolish.

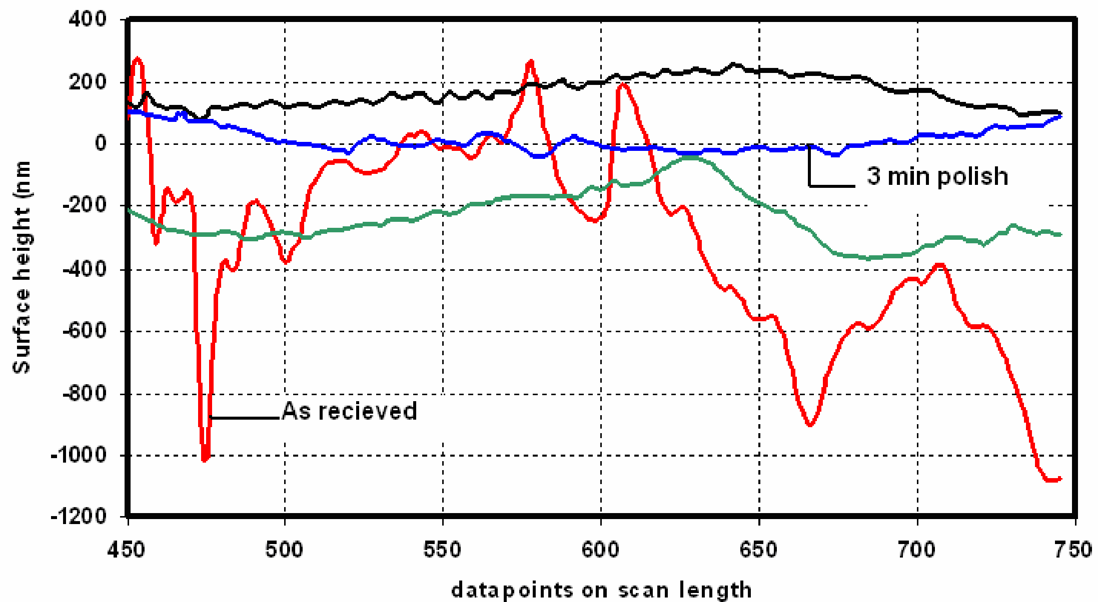

Fig. 10-3: Surface profile plot for treatment conditions R7, Red: As received profile, Green: surface profile after 1 min electropolish, Black: surface profile after 2 min electropolish, Blue: surface profile after 3 min electropolish.

A smoothening effect is visible as the surface asperities have become less pronounced in the surface profile after 3 minutes of polish. The average Ra of an as-received copper disc is ~220 nm while that of a 3 minute polished disc is ~ 60 nm.

The addition of acetic acid and ethylene glycol in the slurry, show improved surface finish with drastic reduction in pitting on the surface. This agrees with the work reported by Liu *et al.* [83].

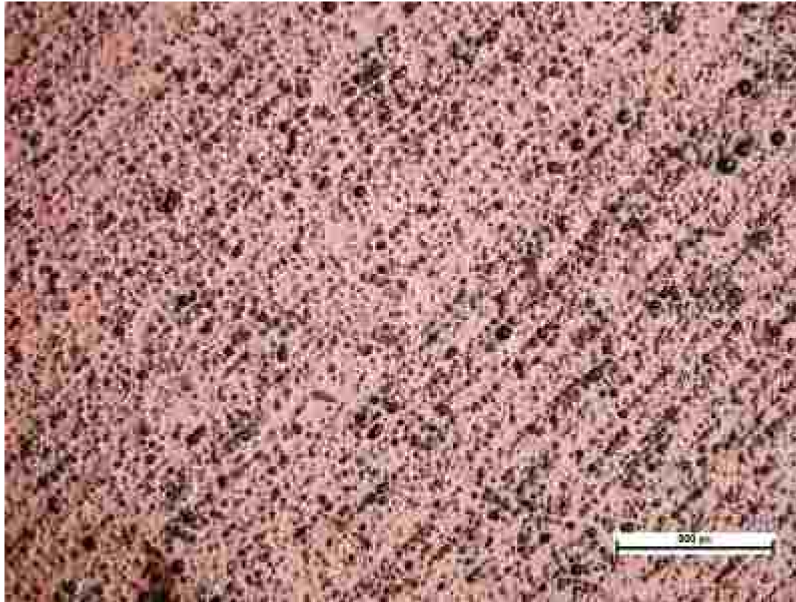

Fig. 10-4: Optical micrograph of 3 min polished copper surface in slurry with no acetic acid and ethylene glycol as additives for machine settings; Phosphoric acid = 10M, Water = 10M, Copper sulfate = 0.2M).

As shown in Figs. 10-4 and 10-5, noticeable improvement in the surface quality was observed when the copper specimen was polished with an acetic acid containing slurry. This makes us put forward a novel two step electrochemical polishing process for copper using different slurry chemistries for different stages of the process. The objective of the first stage of this process is to have material removal at a higher rate, and that of the second stage is surface quality improvement.

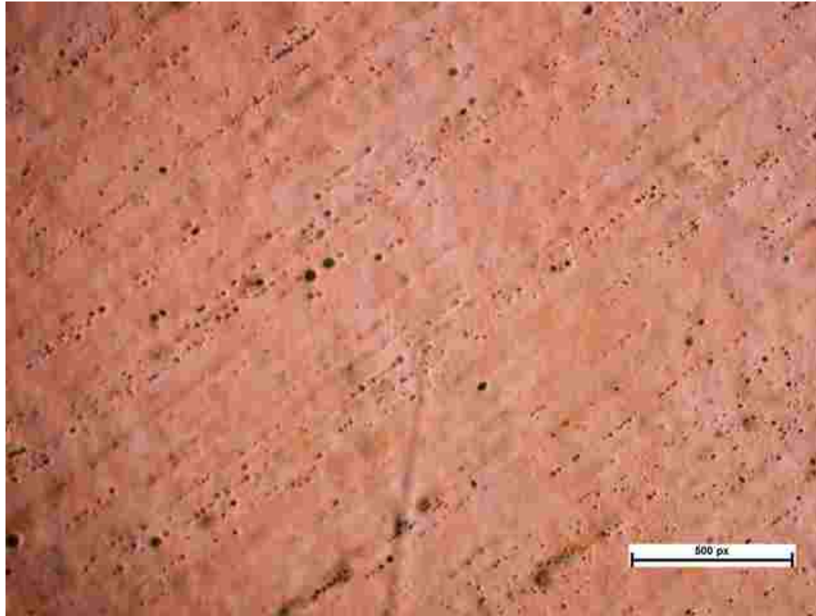

Fig. 10-5: Optical micrograph of copper surface after 3 min polishing in acetic acid and ethylene glycol added slurries with machine settings; Acetic acid = 90 ml, ethylene glycol = 300 ml.

Details of the two step process as well as the sensor based process modeling approach will be discussed in the next chapter.

Chapter 11: Sensor data, feature extraction and, process modeling

11.1 Vibration sensor data acquisition and processing

Vibration sensor data is continuously acquired on a personal computer and analyzed offline. A typical time series of the vibration data is shown in Fig. 11- 1. Pertinent features are extracted from the sensor data, some of which are extracted from the time series while others from the frequency analyses.

We extract 12 pertinent features from the time as well ad frequency domain representation of the sensor signals. These features are as shown in Table 11-1.

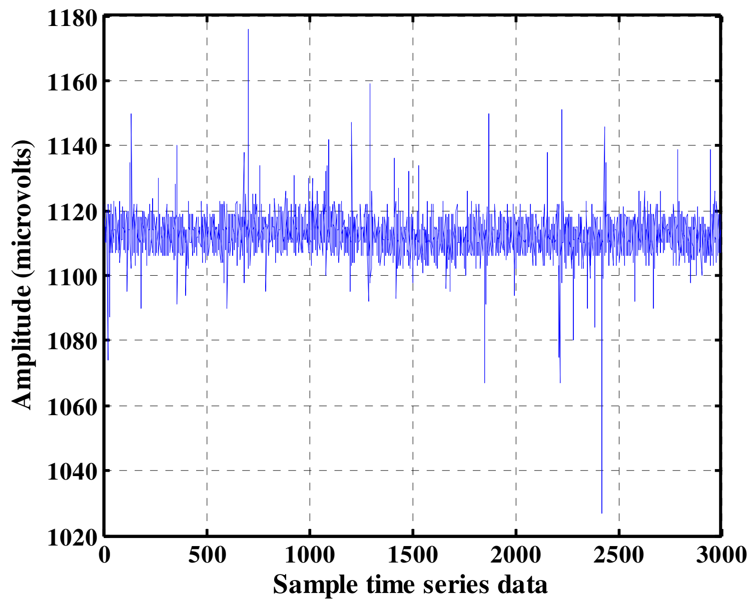

Fig. 11-1: Time series of wireless sensor data for treatment condition R1 (Phosphoric acid = 10 M, Water = 10 M, Copper sulfate = 0 M).

Table 11-1: Candidate feature matrix for R1

PTP	std dev	kurtosis	skewness	peak freq 1 (Hz)	amp freq 1 (µV)	peak freq 2 (Hz)	amp freq 2 (µV)	peak freq 3 (Hz)	amp freq 3 (µV)	peak freq 4 (Hz)	amp freq 4 (µV)
188.5	12.49	8.14	-0.335	43.13	6615.09	120.68	7715.3	183.06	5190.8	244.26	2580.02
243.1	43.37	4.88	0.572	38.49	11466.64	122.39	87491.1	184.57	26062.0	227.41	18282.9
137.8	6.43	20.83	-0.039	41.84	4342.83	121.53	195.289	185.10	1381.40	236.76	393.823

This data is then further reduced by performing principle component analysis (PCA). This helps in reducing the dimensions of the data to be analyzed. After doing PCA 8 principle features (named F1 – F8) remain which are used to perform response surface analysis.

11.2 Process Modeling

In this section various process models were considered. The details of which are given in the following:

1. Modeling process performance (MRR and Ra) with the input process parameters (Slurry chemistry parameters).
2. Modeling process performance (MRR and Ra) with sensor features.
3. Modeling variations in input process parameters (slurry chemistry parameters) with sensor features.

Modeling MRR with machine settings for phosphoric acid slurry chemistry

Using the phosphoric acid slurry chemistry parameters, we model the MRR using the slurry input parameters as inputs to the model. This enables in gathering of insights on parameters which have a significant bearing on the MRR during copper electrochemical polishing.

Table 11-2: Regression model of MRR with machine settings (R^2 = 69.3%, $R^2_{adj.}$ = 66.37%, $R^2_{predicted}$ = 59.9%)

Predictor	**p-val**
Phosphoric acid	0
Water	0

Table 11-2 gives the various slurry input parameters that have a significant effect on the MRR of copper during electrochemical polishing.

A modest regression coefficient of ~ 69% is achieved. This model shall help in providing conditions for maximizing MRR in the proposed first stage of a two step polishing process.

Modeling Ra with machine settings for phosphoric acid slurry chemistry

Table 11-3 gives the parameters for the regression model for predicting Ra with the machine settings only. The regression coefficient is very low (~ 29%). But one thing can be concluded that the amount of phosphoric acid in the slurry has a certain effect on the Ra that can be achieved from the given slurry.

Table 11-3: Regression model of average surface roughness with machine settings (R^2 = 29.23%, $R^2_{adj.}$ = 18.61%, $R^2_{predicted}$ = 0%)

Predictor	**p-val**
Phosphoric acid	0.133
sulfate	0.363
Phosphoric acid*Sulfate	0.038

The above two models indicate that there exists a need for a much better process modeling and process monitoring technique than just the process parameters. Hence, we incorporated sensors on to the polishing machine to aid in process modeling and process monitoring. Inclusion of time as a factor in all the above models showed marked improvements in

the overall predictability. But the polishing time is beyond the control of the operator and is mainly determined by the end point detection systems incorporated in the machine.

Modeling MRR with machine settings for acetic acid slurry chemistry

Table 11-4 gives the parameters for the regression model for avg. MRR with the machine settings and key interactions between them. The model is almost non existent. This again is an indication that more promising process modeling approaches are needed to be incorporated to effectively model the process.

Table 11-4: Regression model for avg. MRR with machine settings for acetic acid slurry chemistry (R^2 = 11.52%, $R^2_{adj.}$ = 0%, $R^2_{predicted}$ = 0%)

Predictor	p-val
(EG)	0.716
(AA)	0.415
(EG)*(AA)	0.699

Modeling Ra with machine settings for acetic acid slurry chemistry

Table 11-5 gives the parameters for the regression model for Ra with machine settings and key interactions in between them for acetic acid slurry chemistry. The model is very bad in predicting Ra, again

reiterating a need for a better way for process modeling and subsequent process monitoring.

Table 11-5: Regression model for Ra with machine settings for the acetic acid slurry chemistry (R^2 = 4.06%, $R^2_{adj.}$ = 0%, $R^2_{predicted}$ = 0%)

Predictor	**p-val**
(EG)	0.626
(AA)	0.651
(EG)*(AA)	0.84

Modeling the MRR and Ra with sensor features

Modeling MRR with sensor features for the phosphoric acid slurry chemistry

Incorporating sensors in the process have dual motives. Firstly they can be used to create static models which can be used to construct much more complex dynamic models and secondly they can be used for *in-situ* monitoring the process dynamics. Here we use sensor data to create static models for process performance (here MRR and Ra) and the process parameters (slurry chemistry parameters).

Table 11-6: Regression model of MRR for phosphoric acid slurry chemistry with sensor data only (R^2 = 93.92%, $R^2_{adj.}$ = 84.45%).

Predictor	Coef	p-val
Constant	0.04486	0
F1	0.027523	0
F2	-0.00321	0.561
F3	0.059572	0
F4	-0.06958	0
F5	-0.02857	0
F6	-0.03234	0
F7	0.016754	0

Predictor	Coef	p-val
F8	0.011622	0.014
F1*F2	0.081075	0
F1*F3	0.067556	0
F1*F7	0.043289	0.001
F1*F8	0.044434	0
F2*F5	-0.04029	0.001
F2*F6	-0.03348	0

MRR = Constant+0.027523*F1-0.00321*F2…-0.03348*F2*F6

As listed in the Table 11-6 above, sensor features are effectively incorporated to model the MRR in phosphoric acid chemistry. This shows implementation of a vibration sensor to model process performance of copper electrochemical polishing. Good regression coefficients are obtained for the model of MRR against sensor features. To illustrate the estimation capability of the model we plot the actual experimental MRR and the MRR predicted by the model. The comparison is as shown in Fig. 11-2.

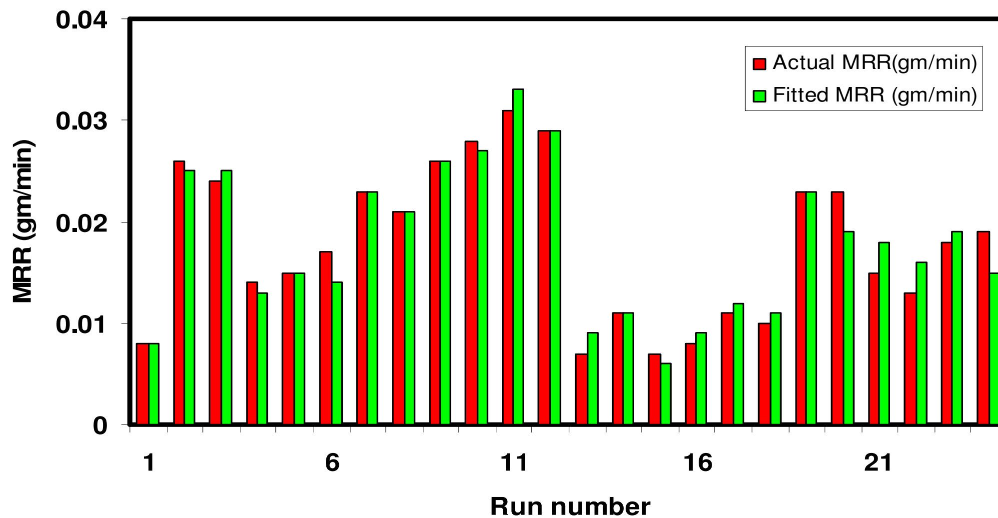

Fig. 11-2: Model performance of sensor based model for MRR for phosphoric acid based slurries.

Modeling Ra with sensor features for phosphoric acid based slurry chemistry

From the process monitoring standpoint, modeling the average surface roughness with sensor data becomes critical. This in its own importance is also crucial as it would help in reducing the damages caused due to excessive polishing. An excellent regression model is obtained for the Ra with sensor features.

Table 11-7: Regression model of average surface roughness with sensor data for phosphoric acid slurry chemistry (R^2 = 99.65%, $R^2_{adj.}$ = 98.40%)

Predictor	**Coef**	**p-val**
Constant	-154.2	0
F1	254.79	0
F2	-206.82	0
F3	162.57	0
F4	197.13	0
F5	187.51	0
F6	72.72	0.016
F7	139.29	0
F8	-93.19	0.001
F1*F1	535.7	0

Predictor	**Coef**	**p-val**
F2*F2	-171.85	0
F3*F3	-151.81	0
F2*F3	242.75	0
F2*F5	-548.64	0
F2*F6	-443.04	0
F2*F7	401.12	0
F4*F5	-662.91	0
F4*F6	-494.22	0
F4*F8	-239.63	0

Ra = Constant+254.79*F1-206.82*F2 ...-239.63*F4*F8

A regression coefficient of ~99% is obtained. This suggests that the Ra is in good correlation with the sensor data. Table 11-7 lists the various terms and their respective p-values in the regression model.

As illustrated for the MRR model for the phosphoric acid based slurries, we also plot the Ra as predicted by the model for the phosphoric acid chemistry. This again helps to get a quick snapshot of how the model performs in estimating the surface roughness based on the sensor signals. The comparison is as shown in Fig. 11-4.

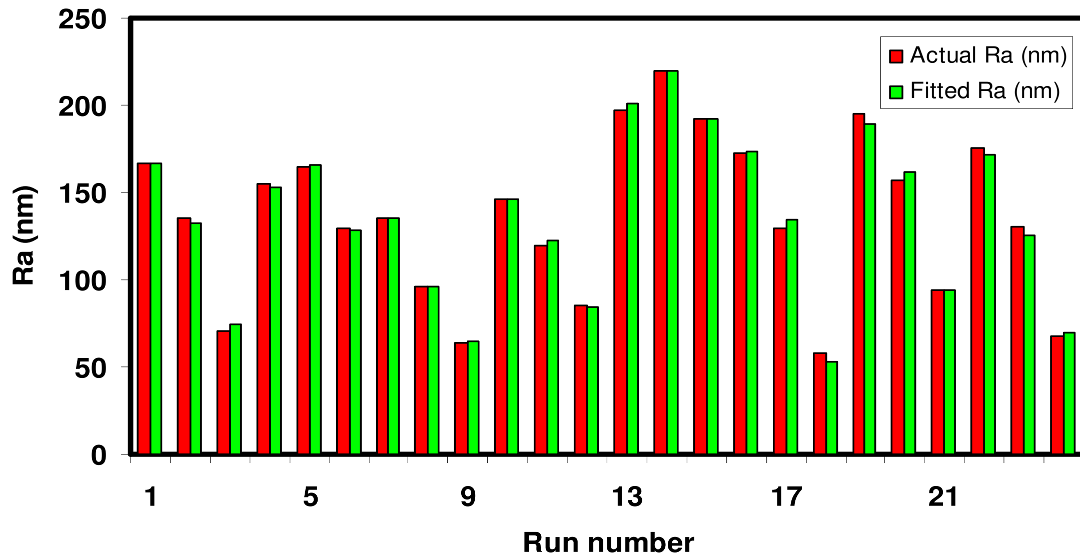

Fig. 11-3: Model performance of sensor based model for surface roughness of copper in phosphoric acid based slurries.

Modeling MRR with sensor features for acetic acid slurry chemistry

Table 11-8 illustrates the regression model for avg. MRR against the sensor features. The limitations of a poor model for avg. MRR based on machine settings is overcome with this model which gives a good regression coefficient. This model can be thus effectively used for further prediction and monitoring of process performance. Also such models make way for more dynamic models which can predict the process performance.

Table 11-8: Regression model for avg. MRR with sensor features for acetic acid slurry chemistry (R^2 = 98.64%, $R^2_{adj.}$ = 96.27%, $R^2_{predicted}$ = 73.59%)

Predictor	Coef	p-val
Constant	0.004759	0
F1	-0.0023	0.004
F2	-0.03068	0
F3	0.001114	0.043

Predictor	Coef	p-val
F4	0.002197	0.024
F2*F2	-0.03135	0
F3*F3	-0.00728	0.001
F4*F4	0.002221	0.058

MRR = Constant-0.0023*F1-0.03068*F2…+0.002221*F4*F4

Modeling Ra with sensor features for acetic acid slurry chemistry

Table 11-9: Regression model for Ra with sensor features for acetic acid slurry chemistry (R^2 = 96.45%, $R^2_{adj.}$ = 91.12%, $R^2_{predicted}$ = 62.39%)

Predictor	Coef	p-val
Constant	9.096	0.394
F1	-26.582	0.031
F2	-48.789	0.006
F3	-50.873	0.002
F4	-13.946	0.019

Predictor	Coef	p-val
F1*F1	40.187	0.007
F1*F2	-75.169	0.007
F1*F3	-51.618	0.001
F1*F4	-37.753	0
F2*F3	-42.467	0.002

Ra = Constant-26.582*F1-48.789*F2…-42.467*F2*F3

Table 11-9 illustrates the model for Ra with sensor features only for acetic acid slurry chemistry. The model shows a good fit for the surface roughness. This shows that wireless vibration sensors are able to capture excellent process performance dynamics.

Modeling the variations in slurry chemistry in Copper electrochemical polishing.

Modeling the variation in phosphoric acid content of the slurry

It is important from the *in-situ* process monitoring standpoint that the variations in the slurry chemistry are tracked efficiently by the sensor signals. Key sensor features are used to track the variations in the phosphoric acid content of the model.

Table 11-10: Regression model of variations in phosphoric acid content of slurry with sensor data.(R^2 = 96.17%, $R^2_{adj.}$ = 90.20%)

Predictor	Coef	p-val
Constant	-0.1242	0.647
F2	-1.7794	0
F3	2.7641	0
F4	2.7778	0
F5	3.3171	0
F6	-1.9062	0
F7	0.6346	0.018
F8	0.6387	0.072

Predictor	Coef	p-val
F2*F2	-1.4122	0.3855
F3*F3	-4.5686	0.5343
F2*F3	5.1875	0.6334
F2*F6	-4.3475	0.485
F2*F7	2.1084	0.4015
F4*F5	-8.1573	1.0659
F4*F8	-4.3682	0.8196

Phosphoric acid = Constant-1.7794*F2+2.7641*F3…-4.3682*F4*F8

A good fit is observed between the variations in phosphoric acid content and the sensor features; Table 11-10 lists all the terms and their

respective p-values for the regression model of phosphoric acid content with sensor data only.

Modeling the variations in the water content of the slurry

Again to effectively monitor the process *in-situ*, it is important that all the slurry chemistry parameters are monitored as accurately as possible. Water plays a major role in deciding the MRR of the process and in turn the surface finish that can be attained from a given slurry configuration [85].

Table 11-11: Regression model of variations in the water content of the slurry with sensor data only. (R^2 = 85.38%, $R^2_{adj.}$ = 75.99%)

Predictor	Coef	p-val
Constant	4.2378	0
F1	-0.7226	0.004
F2	3.478	0
F4	0.9288	0.015
F5	-1.0903	0

Predictor	Coef	p-val
F7	0.3631	0.168
F8	-1.3944	0
F1*F1	-4.8622	0
F7*F7	-1.5381	0.006
F8*F8	-0.9954	0.033

Water = Constant-0.7226*F1+3.478*F2...-0.9954*F8*F8

Modeling the variations in Ethylene Glycol content of the slurry

As a continuation of modeling the variations in the process parameters, we build a model that can effectively track the variations in the ethylene glycol content of the polishing slurry.

Table 11-12: Regression model for modeling variations in the Ethylene Glycol content of the slurry (R^2 = 95.08%, $R^2_{adj.}$ = 87.69%, $R^2_{predicted}$ = 69.91%)

Predictor	Coef	p-val
Constant	2.3756	0.001
F1	-0.2934	0.191
F2	1.3709	0.001
F3	3.7639	0
F4	2.3796	0.004

Predictor	Coef	p-val
F1*F1	-3.5373	0.001
F4*F4	1.0753	0.044
F1*F3	3.5285	0.002
F1*F4	2.0404	0.001
F2*F4	1.6886	0.065

Ethylene glycol = Constant - 0.2934* F1 + 1.3709 * F2 … + 1.6886 * F2 * F4

The importance of ethylene glycol content in the slurry has been proven to give good surface finish in copper electrochemical polishing [83].

Multi stage optimization of slurry chemistry for copper ECP

We suggest a two-step process for copper electrochemical polishing using concentrated phosphoric acid slurries. The first stage is designed to facilitate higher removal rates of copper while the second stage aims at giving enhanced surface finish. We suggest it as a composite process comprising of changing the slurry chemistry as the process switches regimes from high removal to a surface improvement. To verify the effectiveness of multistage optimization, single stage optimization was investigated first. But careful interpretation of Figs. 11-4 and 11-6 clearly demarcate two different regimes of polishing. Combining the results of

both the regimes of polishing has the effect of shadowing the output variables of interest.

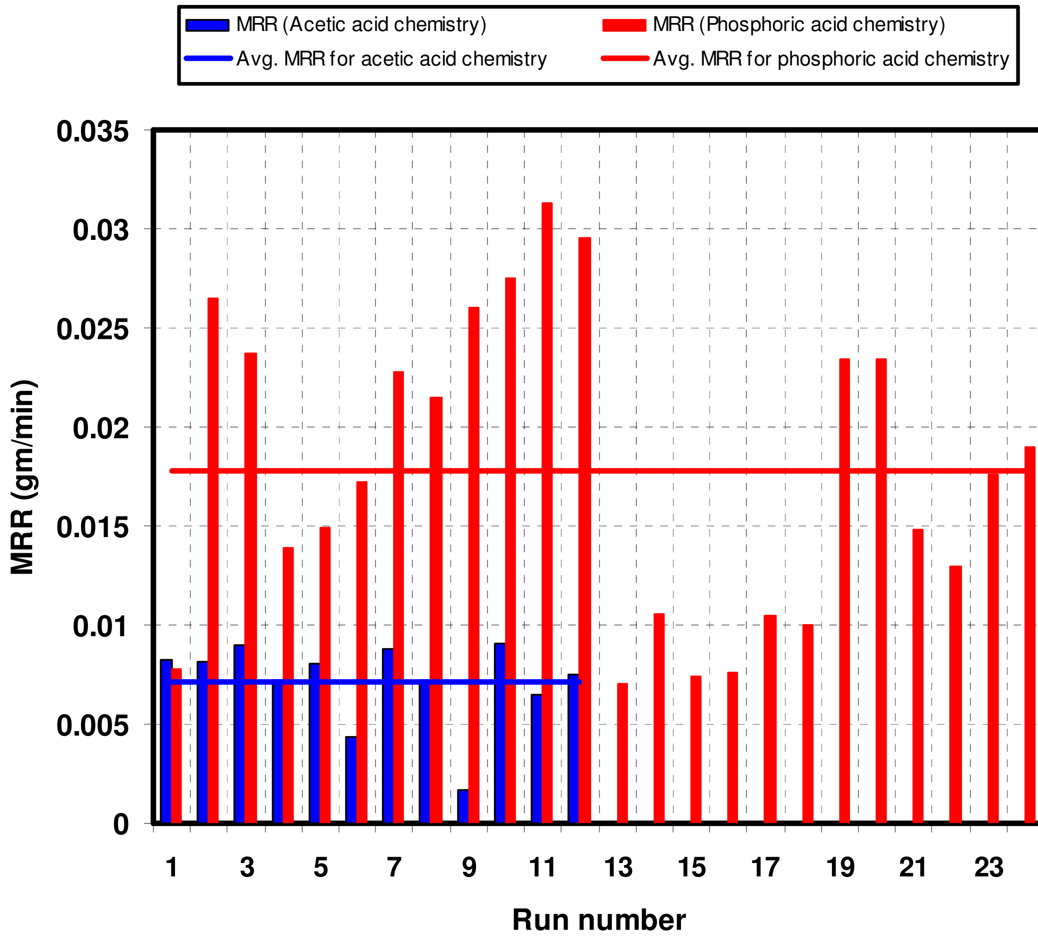

Fig. 11-4: Comparison of MRR for phosphoric acid based slurries (tall columns) and acetic acid based slurries (short columns).

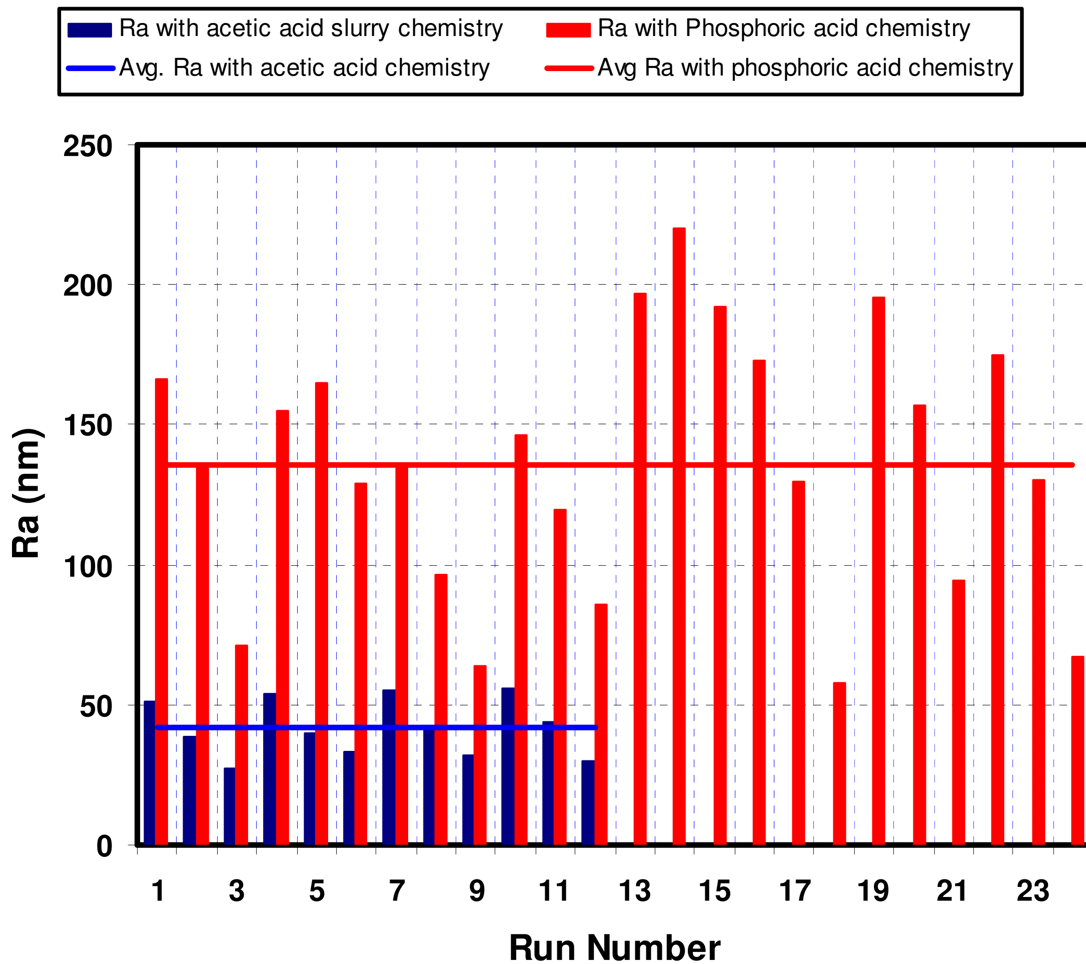

Fig. 11-5: Comparison of surface roughness achieved using phosphoric acid (tall columns) and acetic acid (short columns) based slurry chemistries.

More specifically, including surface roughness in the first stage optimization has the effect of reducing the optimization efficiency for MRR as it is clearly seen that, the input process variables that showed good surface roughness have a very low MRR value.

Fig. 11-5 shows that using phosphoric acid and water based slurries gives higher removal rates compared to acetic acid and ethylene

glycol based slurries. Hence, a ratio of 2/1 for phosphoric acid/water in the first stage of the process is suggested for achieving higher removal rates.

The second stage, improving the surface roughness is the primary concern rather than faster material removal. For this regime we propose adding ethylene glycol and acetic acid in a ratio of 3/1 to the base slurry would give better surface finish with minimal pitting on the surface.

Fig. 11-7 shows a flow chart of the two-stage process we propose from this investigation. In the first stage, introduce dilute phosphoric acid slurries which would yield higher removal rate and during the second stage, introduce the slurry with acetic acid and ethylene glycol to enhance the surface quality that can be achieved from the process.

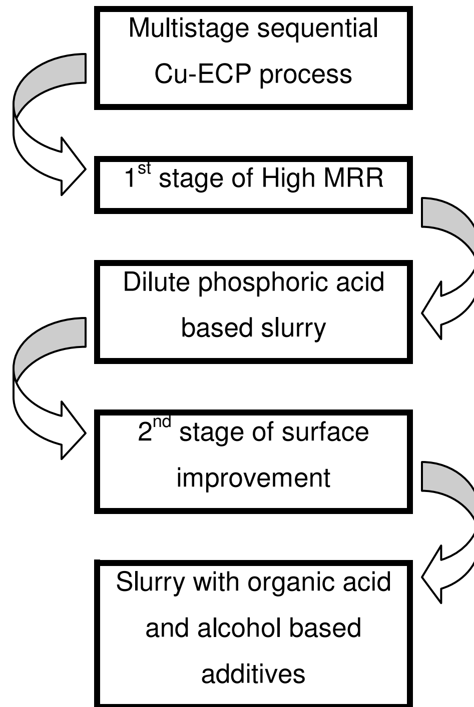

Fig. 11-6: Flow chart for two-stage process proposed for copper ECP.

Chapter 12: Conclusions and Future Work

From a process monitoring and control standpoint, it is important that a relationship between the process performance (here, MRR) and input process parameters (here, slurry chemistry) be established and quantified. This task was achieved in this investigation by conducting a Taguchi L12 set of experiments using a LapMaster 12 lapping machine. After establishing this relationship, to be able to *in-situ* sense the variations in input process parameters was important, so that necessary corrective action can be initiated and process control achieved.

To track these variations, an indirect method, such as the use of a vibration sensor, has to be adopted, as the actual wafer-pad interface is inaccessible. In this investigation we incorporated one wired and one wireless vibration sensor to gather information on the process dynamics. The vibration sensor signals have been analyzed and used to model the process performance as well variations in input process parameters. The results of the experimental investigation as well as sensor-based models will be enumerated below.

From the above investigation, primarily the effectiveness of sensors has been established in tracking the rather intractable variations in slurry chemistry parameters in Cu-CMP as well as Cu- Electrochemical

Polishing process. At this juncture the ability of the models proposed in this investigation to track changes in complexing agent content, corrosion inhibiting agent content are of prime importance and in a way novel. The details of each model for variation in slurry chemistry are as follows:

1. Sensor based model for tracking variations in polishing slurry pH; R^2 = 99.8%, $R^2_{adjusted}$. = 99.12%, $R^2_{predicted}$ = 72.81%.
2. Sensor based model for tracking variations in complexing agent content of polishing slurry; R^2 = 99.96%, $R^2_{adjusted}$ = 99.78%, $R^2_{predicted}$ = 92.73%.
3. Sensor based model for tracking variations in the corrosion inhibiting agent content of polishing slurry; R^2 = 90.21%, $R^2_{adjusted}$ = 81.97%, $R^2_{predicted}$ = 58.14%.
4. Sensor based model for tracking variations in the slurry flow rate; R^2 = 86.31%, $R^2_{adjusted}$ = 78.22%, $R^2_{predicted}$ = 64.65%.
5. Sensor based model for tracking variations in the phosphoric acid content of the slurry; R^2 = 96.17%, $R^2_{adjusted}$ = 90.20%.
6. Sensor based model for tracking variations in the water content of the slurry; R^2 = 85.38%, $R^2_{adjusted}$ = 75.99%.
7. Sensor based model for tracking the variation in ethylene glycol content of the slurry; R^2 = 95.08%, $R^2_{adjusted}$ = 87.69%, $R^2_{predicted}$ = 69.91%.

The process performance (here Material Removal Rate) is successfully modeled. The incorporation of multiple vibration sensors provides with a novel approach for process modeling and aids in formulating simple models which can be used for much more complex dynamic models. The model for MRR based on sensor data has the regression coefficients as follows; R^2 = 97.7%, $R^2_{adjusted}$ = 92.66%, $R^2_{predicted}$ = 65.84%.

Considering the process performance evaluation in Copper electrochemical polishing, following models are proposed:

1. Sensor based model for MRR in phosphoric acid based slurry chemistry; R^2 = 93.92%, $R^2_{adjusted}$ = 84.45%.
2. Sensor based model for Ra in phosphoric acid based slurry chemistry; R^2 = 99.65%, $R^2_{adjusted}$ = 98.40%.
3. Sensor based model for MRR in acetic acid based slurry chemistry; R^2 = 98.64%, $R2_{adjusted}$ = 96.27%, $R^2_{predicted}$ = 73.59%.
4. Sensor based model for Ra in acetic acid based slurry chemistry; R^2 = 96.45%, $R^2_{adjusted}$ = 91.12%, $R^2_{predicted}$ = 62.39%.

Thus as listed above, sensor signals and various features extracted from the signal are effectively used to model the Cu-CMP process performance as well as to track the variations in slurry chemistry settings.

A more sophisticated signal processing and filtering method can be incorporated which would help remove extraneous noise content much effectively, yielding better estimation efficiencies from the sensor based models.

From the models proposed here, investigations can be aimed at more dynamic modeling approaches. These models can actually aim at predicting the future state of the process from the models proposed in this investigation.

Modeling the surface planarity also is one of the key tasks that has to be accomplished by use of more sophisticated planarizing machines. Alongwith planarity monitoring, it also is a key to model global planarity or Within wafer non uniformity. In a nutshell, local as well as global planarity needs to be modeled.

Principles of electrochemistry such as monitoring the corrosion current to monitor the progress of surface being polished can be effectuated. It is known that corrosion current density is area dependant and that the corrosion currents are more for a rough surface, and a gradual drop should be seen in it if the surface being polished is actually polished. This concept can be effectively implemented to model as well as monitor the surface quality of the surface to be polished.

Chapter 13: Reference

1. Steigerwald, J.M., S.P. Murarka, R.J. Gutmann, and D.J. Duquette, "Chemical processes in the chemical mechanical polishing of copper," Materials Chemistry and Physics, 1995. Vol. 41, pp. 217-228.
2. J.M.Steigerwald, S.P.Murarka, and R.J.Gutmann, "Chemical mechanical planarization of microelectronic materials." 1997, New York: John Wiley & Sons Inc.
3. Srinivasa-Murthy, C., D. Wang, S.P. Beaudoin, T. Bibby, K. Holland, and T.S. Cale, "Stress distribution in chemical mechanical polishing," This Solid Films, 1997. Vol. 308-309, pp. 533-537.
4. Basim, G.B., J.J. Adler, U.Mahajan, R.K. Singh, and B.M. Moudgil, "Effect of particle size of chemical mechanical polishing slurries for enhanced polishing with minimal defects " Journal of the Electrochemical Society, 2000. Vol. 147 (9), pp. 3523-3528.
5. Borucki, L., L. Charns, and A. Philipossian, "Analysis of frictional heating of grooved and flat CMP polishing pads," Journal of the Electrochemical Society, 2004. Vol. 151 (12), pp. G809-G813.
6. Borucki, L., Z.Li, and A.Philipossian, "Experimental and theoretical investigation of heating and convection in copper polihsing," Journal of the Electrochemical Society, 2004. Vol. 151 (9), pp. G559-G563.

7. D.Castillo-Mejia, J.Kelchner, and S.Beaudoin, "Polishing pad surface morphology and chemical mechanical planarization " Journal of the Electrochemical Society, 2004. Vol. 151 (4), pp. G271-G278.

8. D.Rosales-Yeomans, T.Doi, M.Kinoshita, T.Suzuki, and A.Philipossian, "Effect of pad groove designs on the frictional and thermal rate characteristics of ILD CMP," Journal of the Electrochemical Society, 2005. Vol. 152 (1), pp. G62-G67.

9. Homma, Y., K. Fukushima, S. Kondo, and N. Sakuma, "Effects of mechanical parameters on CMP characteristics analyzed by two-dimensional frictional-force measurement," Journal of the Electrochemical Society, 2003. Vol. 150 (12), pp. G751-G757.

10. Jeng, Y.-R., P.-Y. Huang, and W.-C. Pan, "Tribological analysis of CMP with partial asperity contact," Journal of the Electrochemical Society, 2003. Vol. 150 (10), pp. G630-G637.

11. Li, Z., K.Ina, P.Leferve, I.Koshiyama, and A.Philipossian, "Determinig the effects of slurry surfactant, abrasive size and abrasive content on the tribology and kinetics of copper CMP," Journal of the Electrochemical Society, 2005. Vol. 152 (4), pp. G299-G304.

12. Li, Z., L.Borucki, I.Koshiyama, and A.Philipossian, "Effect of slurry flow rate on tribological,thermal,and removal rate attributes of copper CMP," Journal of the Electrochemical Society, 2004. Vol. 151 (7), pp. G482-G487.

13. Liang, H., F. Kaufman, R. Sevilla, and S. Anjur, "Wear phenomena in chemical mechanical polishing," Wear, 1997. Vol. 211 (2), pp. 271-279.

14. Philipossian, A. and S. Olsen, "Fundamental tribological and removal rate studies of Inter layer dielectric chemical mechanical planarization," Japanese Journal of Applied Physics, 2003. Vol. 42, pp. 6371-6379.

15. Runnels, S.R. and L.M. Eyman, "Tribology analysis of chemical mechanical polishing," Journal of the Electrochemical Society, 1994. Vol. 141 (6), pp. 1698-1701.

16. Chen, C.-Y., C.-C. Yu, S.-H. Shen, and M. Ho, "Operational aspects of chemical mechanical polishing polish pad profile optimization," Journal of the Electrochemical Society, 2000. Vol. 147 (10), pp. 3922-3930.

17. Mazaheri, A.R. and G. Ahmadi, "Modeling the effect of bumpy abrasive particles on chemical mechanical polishing," Journal of the Electrochemical Society, 2002. Vol. 149 (7), pp. G370-G375.

18. Runnels, S.R., "Feature - scale fluid based erosion modeling for chemical mechanical polishing," Journal of the Electrochemical Society, 1994. Vol. 141 (7), pp. 1900-1904.

19. Sorooshian, J., L. Borucki, D. Stein, R. Timon, D. Hetherington, and A. Philipossian, "Revisiting the removal rate model for oxide CMP," ASME Journal of Tribology, 2004. Vol. 127, pp. 639-651.

20. Sorooshian, J. and A. Philipossian, "Extending the flash heating removal rate model to various interlayer dielectric CMP consumables," Journal of the Electrochemical Society, 2005. Vol. 152 (12), pp. G933-G937.

21. Yao, C.-H., D.L. Feke, K. M.Robinson, and S. Meikle, "Modeling of chemical mechanical polishing processes using a discretized geometry approach," Journal of the Electrochemical Society, 2000. Vol. 147 (4), pp. 1502-1512.

22. Zhao, Y. and L.Chang, "A micro-contact wear model for chemical-mechanical polishing of silicon wafers," Wear, 2002. Vol. 252, pp. 220-226.

23. Homma, T., "Low dielectric constant materials and methods for interlayer dielectric films in ultralarge-scale integrated circuit multilevel interconnections," Materials Science and Engineering, 1998. Vol. R23, pp. 243-285.

24. Wang, Y.-L., C.Liu, M.-S.Feng, and W.-T.Tseng, "The Exothermic reaction and temperature measurement for tungsten CMP technology and its application on endpoint detection," Materials Chemistry and Physics, 1998. Vol. 52, pp. 17-22.

25. Sampurno, Y.A., L. Borucki, Y. Zhuang, D. Boning, and A. Philipossian, "A method for Direct Measurement of Substrate Temperature during Copper CMP," Journal of the Electrochemical Society, 2005. Vol. 152 (7), pp. G537-G541.

26. Zhuang, Y., Z.Li, J.Sorooshian, and A.Philipossian, "Tribological, thermal and kinetic attributes of copper and silicon dioxide CMP processes." 2004, American Institute of Chemical Engineers: New York.

27. Sundararjan, S., D.G. Thakurta, D.W. Schwendeman, S.P. Murarka, and W.N. Gill, "Two - Dimensional wafer-scale chemical mechanical planarization models based on lubrication theory and mass transport," Journal of the Electrochemical Society, 1999. Vol. 146 (2), pp. 761-766.

28. Vlassak, J.J., "A model for chemical mechanical polishing of a material surface based on contact mechanics," Journal of the Mechanics and Physics of Solids, 2003. Vol. 52 (4), pp. 847-873.

29. Yi, J., "On the wafer/pad friction of chemical-mechanical planarization (CMP) process - Part I : modeling and analysis," IEEE Transactions on Semiconductor Manufacturing, 2005. Vol. 18 (3), pp. 359-370.

30. Lloyd, J.R. and J.J. Clement, "Electromigration in copper conductors," Thin Solid Films, 1995. Vol. 262, pp. 135-141.

31. Cadien, K.C., "Slurries for chemical mechanical polishing." US patent no. 5340370 1994, Intel Corporation.

32. Cadien, K.C. and D.A. Feller, "Slurries for chemical mechanical polishing." US patent no. 5516346 1996, Intel Corporation.

33. Farkas, J., R. Jairath, M. Stell, and S.-M. Tzeng, "Method of using addictives with silica based slurries to enhance selectivity in metal CMP." US patent no. 5614444 1997, Sematech, Inc., Intel Corporation, National Semiconductor, Digital Equipment Corproration.

34. Hirabayashi, H. and M. Higuchi, "Copper-based metal polishing solution and method for manufacturing semiconductor device." US patent no. 5575885 1996, Kabushiki Kaisha Toshiba.

35. Lee, J.-D., B.-U. Yoon, and Y.-P. Han, "Chemical mechanical polishing slurry and chemical mechanical polishing method using the same." US patent no. 6887137 2005, Samsung Electronics Co., Ltd.

36. Lee, J.S. and K.S. Lee, "Metal CMP slurry compositions that favor mechanical removal of oxides with reduced susceptibility to microscratiching." US patent no. 6953389 2005, Chell Industries, Inc.

37. Miller, A.E., "Copper polish slurry for reduced interlayer dielectric erosion and method of using same." US patent no. 6852631 2005, Intel Corporation.

38. Minamihaba, G. and H. Yano, "CMP slurry and method for manufacturing a semiconductor device." US patent no. 6896590 2005, Kabushiki Kaisha Toshiba.

39. Neville, M., D.J. Fluck, C.-H. Hung, M.A. Lucarelli, and D.L. Scherber, "Chemical mechanical polishing slurry for metal layers." US patent no. 5527423 1996, Cabot Corporation.

40. Pryor, J., "Slurries of abrasive inorganic oxide particles and method for polishing copper containing surfaces." US patent no. 6447693 2002, W. R. Grace & Co.-Conn.

41. Sinha, N. and D. Chopra, "Slurry for use in polishing semiconductor device conductive structures that include copper and tungsten and polishing methods." US patent no. 6551935 2003, Micron Technology, Inc.

42. Tsuchiya, Y., T. Wake, T. Itakura, S. Sakurni, and K. Aoyagi, "Chemical mechanical polishing slurry." US patent no. 6585568 2003, NEC Electronics Corporation, Tokyo Magnetic Printing Co. Ltd.

43. Uchida, T., J. Matsuzawa, T. Hoshino, Y. Kamigata, H. Terazaki, Y. Honma, and S. Kondoh, "Abrasive liquid for metal and method for polishing." US patent no. 6899821 2005, Hitachi Chemical Company Ltd, Hitachi, Ltd.

44. Wang, Y., R. Bajaj, F.C. Redeker, and S. Li, "Chemical mechanical polishing composition and process." US patent no. 6872329 2005, Applied Materials, Inc.

45. Kaufman, F.B., D.B. Thompson, R.E. Broadie, M.A. Jaso, W.L. Guthrie, D.J. Pearson, and M.B. Small, "Chemical-mechanical polishing for fabricating patterned *W* metal features as chip interconnects," Journal of the Electrochemical Society, 1991. Vol. 138 (11), pp. 3460-3465.

46. Hernandez, J., P.Wrschka, and G.S.Oehrlein, "Surface chemistry studies of copper chemical mechanical planarization," Journal of the Electrochemical Society, 2001. Vol. 148 (7), pp. G389-G397.

47. Jindal, A. and S.V. Babu, "Effect of pH on CMP of copper and tantalum," Journal of the Electrochemical Society, 2004. Vol. 151 (10), pp. G709-G716.

48. Carpio, R., J. Farkas, and R. Jairath, "Initial study on copper CMP slurry chemistries," Thin Solid Films, 1995. Vol. 266 (2), pp. 238-244.

49. Dornfeld, D.A., Y. Lee, and A. Chang, "Monitoring of ultraprecision machining processes," International Journal of Advanced Manufacturing Technology, 2003. Vol. 21, pp. 571-578.

50. Dornfeld, D.A., "Process monitoring and control for precision manufacturing." 1999, University of California: Berkeley.

51. Hwang, E.I., "End-point detection in the CMP process: AE sensor." 2001, University of California: Berkeley.

52. Bukkapatnam, S., P. Rao, N. Chandrasekaran, and R. Komanduri, "Nonlinear stochastic dynamics and monitoring of chemical mechanical planarization process." 2006, Oklahoma State University.

53. Luo, Q., D.R.Campbell, and S.V.Babu, "Stabilization of alumina slurry for chemical - mechanical polishing of copper " Langmuir, 1996. Vol. 12 (15), pp. 3563-3566.

54. Choi, W., U. Mahajan, S.-M. Lee, J. Abiade, and R. K.Singh, "Effect of slurry ionic salts at dielectric silica CMP," Journal of the Electrochemical Society, 2004. Vol. 151 (3), pp. G185-G189.

55. Kummert, R. and W. Stumm, "The surface complexation of organic acids on hydrous gamma aluminum oxide," Journal of Colloid and Interface Science 1980. Vol. 75 (2), pp. 373-385.

56. Eom, D.-H., I.-K. Kim, J.-H. Han, and J.-G. Park, "The effect of hydrogen peroxide in a citric acid based copper slurry on Cu polishing " Journal of the Electrochemical Society, 2007. Vol. 154 (1), pp. D38-D44.

57. Lu, J., J.E. Garland, C.M. Pettit, S.V. Babu, and D. Roy, "Relative roles of hydrogen peroxide and glycine in CMP of copper studied with impedence spectroscopy," Journal of the Electrochemical Society, 2004. Vol. 151 (10), pp. G717-G722.

58. Booth, N.A., D.P. Woodruff, O. Schaff, T. Giebel, R. Lindsay, P. Baumgartel, and A.M. Bradshaw, "Determination of the local structure of glycine adsorbed on Cu(110)," Surface Science, 1998. Vol. 397, pp. 258-269.

59. Seal, S., S.C. Kuiry, and B. Heinmen, "Effect of glycine and hydrogen peroxide on chemical - mechanical planarization of copper," Thin Solid Films, 2003. Vol. 423 (2), pp. 243-251.

60. Chen, J.-C. and W.-T. Tsai, "Effects of hydrogen peroxide and alumina on surface characteristics of copper chemical-mechanical polishing in citric acid slurries," Materials Chemistry and Physics 2004. Vol. 87 (2-3), pp. 387-393.

61. Aksu, S. and F. M.Doyle, "The role of glycine in the chemical mechanical planarization of copper," Journal of the Electrochemical Society, 2002. Vol. 149 (6), pp. G352-G361.

62. Singh, R.K., S.-M. Lee, K.-S. Choi, G.B. Basim, W. Choi, Z. Chen, and B. M.Moudgil, "Fundamentals of slurry design for CMP of metal and dielectric materials," MRS bulletin, 2002. Vol. 27 (10), pp. 752-760.

63. Grunwald, J., "Abrasives for CMP applications." US patent no. 6896710 2005, J.G.Syatems, Inc.,.

64. Cadien, K.C. and A.D. Feller, "Abrasives for chemical mechanical polishing." US patent no. 6881674 2005, Intel Corporation.

65. Tang, J., D. Dornfeld, S.K. Pagrle, and A. Dangca, "In-process detection of microscratching during CMP using acoustic emission sensing technology," Journal of Electronic Materials, 1998. Vol. 27 (10), pp. 1099-1103.

66. Mudhivarthi, S., N. Gitis, S. Kuiry, M. Vinogradov, and A. Kumar, "Effects of slurry flow rate and pad conditioning temperature on dishing, erosion and metal loss during copper CMP," Journal of the Electrochemical Society, 2006. Vol. 153 (5), pp. G372-G378.

67. Johnson, R.A. and D.W. Wichern, "Applied multivariate statistical analysis," 5 ed. 2002, New Jersey: Prentice Hall.

68. Myers, R.H., "Classical and Modern Regression with Applications." 2000, Pacific Grove, CA: Duxbury Press.

69. Coppeta, J., C. Rogers, L. Racz, A. Philipossian, and F. B.Kaufman, "Investigating slurry transport beneath a wafer during chemical mechanical polishing processes," Journal of the Electrochemical Society, 2000. Vol. 147 (5), pp. 1903-1909.

70. Subramanian, R.S., L. Zhang, and S.V.Babu, "Transport phenomena in chemical mechanical polishing," Journal of the Electrochemical Society, 1999. Vol. 146 (11), pp. 4263-4272.

71. Jones, D.A., "Principles and Prevention of Corrosion," 2 ed. 1995: Prentice Hall.

72. Contolini, R.J., A.F. Bernhardt, and S.T. Mayer, "Electrochemical planarization for multilevel metallization," Journal of the Electrochemical Society, 1994. Vol. 141, pp. 2503-2510.

73. Vidal, R. and A.C. West, "Copper Electropolishing in Concentrated Phosphoric Acid," Journal of the Electrochemical Society, 1995. Vol. 142 (8), pp. 2689-2694.

74. Landolt, D., R.H. Muller, and C.W. Tobias, "Anode potentials in high rate dissolution of copper," Journal of the Electrochemical Society, 1971. Vol. 118 (36), pp. 40-46.

75. Suni, I.I. and B. Du, "Cu Planarization for ULSI processing by Electrochemical Methods: A Review," IEEE Transactions on Semiconductor Manufacturing, 2005. Vol. 18 (3), pp. 341-349.

76. Reid, J.D., "Method for Electrochemical Planarization of Metal Surface." USA patent no. 6653226 2003, Novellus Systems, Inc.

77. Chang, S.-C., J.-M. Shieh, C.-C. Huang, B.-T. Dai, Y.-H. Li, and M.-S. Feng, "Microleveling mechanisms and applications of electropolishing on planarization of copper metallization," Journal of Vaccum Science and Technology B, 2002. Vol. 20 (5), pp. 2149-2153.

78. Padhi, D., J. Yahalom, S. Gandhikota, and G. Dixit, "Planarization of Copper Thin Films by Electropolishing in Phosphoric Acid for ULSI Applications," Journal of the Electrochemical Society, 2003. Vol. 150 (1), pp. G10-G14.

79. West, A.C., H. Deligianni, and P.C.Andricacos, "Electrochemical planarization of interconnect metallization," IBM Journal of Research and Developement, 2005. Vol. 49 (1).

80. Busnaina, A.A., H. Lin, N. Moumen, J.-w. Feng, and J. Taylor, "Particle adhesion and removal mechanisms in post-CMP cleaning processes," IEEE Transactions on Semiconductor Manufacturing, 2002. Vol. 15 (4), pp. 374-382.

81. Sato, S., T. Kanagawa, Z. Yasuda, and M. Ishibara, "Polishing Method and Electropolishing Apparatus." USA patent no. 7156975 2007, Sony Corporation.

82. Huo, J., R. Solanki, and J. McAndrew, "Electrochemical planarization of patterned copper films for microelectronic application," Surface Engineering, 2004. Vol. 13 (4), pp. 413-420.

83. Liu, S.-H., J.-M. Shieh, C. Chen, K. Hensen, and S.-S. Cheng, "Roles of additives in damascene copper electropolishing," Journal of the Electrochemical Society, 2006. Vol. 153 (6), pp. C428-C433.

84. Chang, S.-C., J.-M. Shieh, C.-C. Huang, B.-T. Dai, and M.-S. Feng, "Pattern effects on planarization efficiency of Cu electropolishing," Japanese Journal of Applied Physics, 2002. Vol. 41 (12), pp. 7332-7337.

85. Huo, J., R. Solanki, and J. McAndrew, "Study of anodic layers and their effects on electropolishing of bulk and electroplated films of copper," Journal of Applied Electrochemistry, 2004. Vol. 34, pp. 305-314.

VITA

Upendra Milind Phatak

Candidate for the Degree of

Master of Science

Thesis: SENSOR BASED MODELING OF CHEMICAL MECHANICAL PLANARIZATION (CMP) OF COPPER FOR SEMICONDUCTOR APPLICATIONS

Major: Mechanical & Aerospace Engineering.

Education:

1. Completed the requirements for the Master of Science in Mechanical Engineering at Oklahoma State University, Stillwater, Oklahoma in May, 2008.
2. Bachelor's of Engineering (B.E.) in August 2005 from University of Pune, passed in distinction class.
3. Diploma in Mechanical Engineering (DME) in August 2002 from Maharashtra State Board of Technical Education, Mumbai with First class.

Achievements and Awards:

1. Awarded funding by MES College of Engineering, Pune, to conceptualize, design, manufacture, commission and calibrate a vibration test rig for automobile suspension testing. August 2004- June 2005.
2. First prize for research poster at 18th annual research symposium held at Oklahoma State University, 2006. Poster titled "Sensor based modeling of MRR in Cu-CMP for microelectronic applications". March 2006

Name: Upendra Phatak Date of Degree: May, 2008

Institution: Oklahoma State University Location: Stillwater, Oklahoma

Title of Study: SENSOR BASED MODELING OF CHEMICAL MECHANICAL PLANARIZATION (CMP) OF COPPER FOR SEMICONDUCTOR APPLICATIONS

Pages in Study: 144 Candidate for the Degree of Master of Science

Major Field: Mechanical Engineering

Scope and Method of Study: Material removal rate (MRR) and surface quality in copper CMP (Cu-CMP) process are highly sensitive to slurry chemistry parameters, namely, pH, and concentrations of complexing, corrosion inhibiting, and oxidizing agents. Capturing the effects of these slurry parameters on MRR and surface quality in real-time through the use of sensor signals is key to ensuring an efficient Cu-CMP process. In this investigation vibration sensor signals collected from the Cu-CMP experiments are used to capture the variations in various slurry parameters as well as their influence on the MRR.

Findings and Conclusions: The study has shown that features from wireless accelerometer signals sampled at 500Hz, and those from wired accelerometer signals sampled at 5 kHz can be used to estimate MRR more accurately than conventional static statistical regression models that relate the input (slurry) parameters to MRR. Here, the sensor features have been related to MRR using principal component regression (PCR) models. The improvement in the accuracy of estimation with sensor-based PCR models (R^2 of 97.7% compared to 89.8% with a conventional statistical regression model) is likely because the vibration sensor signal characteristics are not only sensitive to variations in MRR, but also to the relevant variations in the input (slurry) parameters during the operation. The in-process variations in the slurry parameters cannot be tracked in conventional (static) statistical regression models.

ADVISER'S APPROVAL: Dr.Ranga Komanduri .